

A.3 STRUCTURAL EVALUATION

A.3.1 Structural Design

Sections of this Chapter have been identified as “No change” due to the addition of 24PT4-DSC to the Advanced NUHOMS[®] system. For these sections, the description or analysis presented in the corresponding sections of the FSAR for the Advanced NUHOMS[®] system with the 24PT1-DSC is also applicable to the system with the 24PT4-DSC.

This chapter addresses the structural evaluation of the Advanced NUHOMS[®] System 24PT4-DSC. The AHSM structural analyses presented in Chapter 3 are applicable to the 24PT4-DSC because they are based on a conservative DSC weight of 85,000 lbs which bounds the weight of the 24PT4-DSC. On-site transfer of a loaded 24PT4-DSC is performed utilizing the NUHOMS[®] OS197H transfer cask (TC) described in the NUHOMS[®] FSAR [A3.8]. The FSAR analyses of the TC envelope the 24PT4-DSC configuration.

A.3.1.1 Discussion

The discussion presented in Section 3.1.1 applies to the 24PT4-DSC. The codes and standards used for the design, fabrication and construction of the 24PT1-DSC are also used for the 24PT4-DSC. In addition, for the 24PT4-DSC, ASME Code Case N-499-1 [A3.7] provides the basis for use of SA-533 Grade B Class 1 Carbon Steel material for fabrication of 24PT4-DSC spacer discs. Table A.3.1-1 summarizes the 24PT4-DSC design basis codes and standards.

A.3.1.1.1 General Description of the 24PT4-DSC

The principal characteristics of the 24PT4-DSC are described in Section A.1.2.1 and shown in Figure A.1.1-1. The drawings in Section A.1.5.2 provide the principal dimensions and design parameters of the 24PT4-DSC.

The 24PT4-DSC shell assembly, shown in Figure A.3.1-1, consists primarily of a cylindrical shell, the top and bottom cover plates and shield plug assemblies. The 24PT4-DSC shell, the inner cover plates of the top and bottom shield plug assemblies, the vent and siphon block, the vent and siphon cover plates, and the associated welds form the pressure retaining confinement boundary for the spent fuel (see Figure A.3.1-2). The outer top cover plate and associated welds to the shell functions as a redundant welded barrier for confining radioactive material within the 24PT4-DSC.

The remaining 24PT4-DSC shell assembly components include the outer top and bottom cover plates, the grapple ring assembly, support ring, and the lifting lugs. The lead shield plug assemblies provide biological shielding during fuel loading operations and storage of a loaded 24PT4-DSC. The grapple ring assembly is welded to the outer bottom cover plate for the purpose of inserting/extracting the 24PT4-DSC from the Advanced Horizontal Storage Module (AHSM). The support ring, welded to the cylindrical shell, supports the top shield plug assembly. Four lifting lugs are welded to the inside of the cylindrical shell and the support ring and are used to lift the unloaded 24PT4-DSC into the TC prior to fuel loading operations.

All pressure boundary components are constructed of Type 316 stainless steel. Non-pressure boundary components welded to the pressure boundary components are also constructed of Type 316 stainless steel. The lead shield plugs are made of ASTM B29 lead.

The 24PT4-DSC cylindrical shell and bottom end assembly including the bottom shield plug assembly, outer bottom cover plate, and the grapple ring assembly, and the internal basket assembly, are shop-fabricated components. The top shield plug assembly and the outer top cover plate are shop-fabricated and tested for fit-up but installed at the plant after the spent fuel assemblies have been loaded into the 24PT4-DSC internal basket.

The 24PT4-DSC shell assembly is designed, fabricated, examined and tested in accordance with the requirements of Subsection NB of the ASME Code including Code Case N-595-1 [A3.2] for closure welds. The circumferential and longitudinal shell plate weld seams are full penetration butt welds. The butt weld joints are fully radiographed and inspected according to the requirements of NB-5000 of the ASME Boiler and Pressure Vessel Code.

The 24PT4-DSC top closure is compliant with Code Case N-595-1 and NRC's ISG-15 [A3.3]. The inner cover plate of the top shield plug assembly is welded to the 24PT4-DSC shell to complete the pressure boundary as shown in Figure A.3.1-2. The top cover plate is sealed by a separate, redundant closure weld. All closure welds are multiple-layer welds and are examined by multi-level liquid penetrant methods to effectively eliminate leaks through welds.

The top end assembly of the 24PT4-DSC design incorporates a vent/siphon block, with two small-diameter penetrations into the 24PT4-DSC cavity for draining and filling operations. The vent port is terminated at the bottom of the shield plug assembly. The other port is attached to a siphon tube, which continues to the bottom of the 24PT4-DSC cavity. The ports include dog-leg type offsets to minimize radiation streaming. The vent and siphon ports terminate in normally closed quick-connect fittings.

During fabrication, leak tests of the 24PT4-DSC shell assembly are performed in accordance with ANSI N14.5-1997 [A3.4] to demonstrate that the shell is leaktight.

The 24PT4-DSC inner top closure welds, including the vent and siphon block subassembly welds, are leak tested after fuel loading to demonstrate that ANSI N14.5 [A3.4] leaktight criteria is met.

The stringent design and fabrication requirements described above ensure that the pressure retaining confinement function is maintained for the design life of the 24PT4-DSC. Pressure monitoring instrumentation is not used since penetration of the pressure boundary would be required. The penetration itself would then become a potential leakage path and, by its presence, compromise the leaktightness of the 24PT4-DSC design.

During draining, backfilling, and leak testing, a "Strongback Device" may be installed to minimize deformation of the top shield plug assembly during blowdown. The strongback is bolted to the top flange of the TC and provides support to the top shield plug assembly during those operations that may involve significant pressurization of the 24PT4-DSC cavity.

Transfer of the 24PT4-DSC from the TC into the AHSM is performed using a hydraulic ram that applies a load to the outer bottom cover plate, at the center of the 24PT4-DSC. During insertion of the 24PT4-DSC into the AHSM, the load is shared by the outer bottom cover plate and the inner bottom cover plate.

Frictional loads during 24PT4-DSC transfer are reduced by application of a dry film lubricant to the hardened nitronic surface of the AHSM support rails and the TC. The lubricant chosen for this application is a tightly adhering inorganic lubricant with an inorganic binder. The dry film lubricant provides a thin, clean, dry, layer of lubricating solids that is intended to reduce wear, and prevent galling in metals. It is applied as a thin sprayed coating, similar to paint, using a carefully controlled process. The lubricant is not affected by water and is designed to be highly resistant to aggressive chemicals. This product is designed for radiation service and has a low coefficient of sliding friction for stainless steel.

The internal basket assembly, shown in Figure A.3.1-3, provides structural support for and geometric separation of the SFAs. The basket assembly consists of 24 stainless steel guidesleeve assemblies, 28 carbon steel spacer discs, and four-support rod/spacer sleeve assemblies. The support rods and spacer sleeves are fabricated of precipitation hardened martensitic stainless steel.

The spacer disc details, shown in Figure A.3.1-4, identify the twenty-four cutouts for the SFAs and the four support rods. The spacer discs maintain cross-sectional spacing and support for the fuel assemblies and the guidesleeves when the 24PT4-DSC is in the horizontal position. When the 24PT4-DSC is in the vertical position, the spacer discs are held in place by the support rods and spacer sleeves; the rod assemblies maintain longitudinal separation between discs during all normal operating and postulated accident conditions. Fuel weight is transferred to the top or bottom cover plates by direct bearing.

Damaged fuel assemblies are stored in Failed Fuel Cans. The Failed Fuel Can is provided with a welded bottom closure and a removable top closure which allows lifting of the can with the enclosed fuel assembly. Failed Fuel Cans are provided with screens at the bottom and top to contain fuel debris and allow fill/drainage of water from the failed fuel can.

A.3.1.1.2 General Description of the AHSM

No change.

A.3.1.2 24PT4-DSC and AHSM Design Criteria

No change.

A.3.1.2.1 24PT4-DSC Design Criteria

A.3.1.2.1.1 Stress Criteria

No change.

The 24PT4-DSC is designed utilizing linear elastic and non-linear elastic-plastic analytical methods. ASME Code Service Level A and B allowables are used for normal and off-normal operating conditions, respectively. Service Level C and D allowables are used for accident conditions.

The 24PT4-DSC shell is designed by analysis to meet the criteria of the ASME Boiler and Pressure Vessel Code Section III, Division 1, Subsection NB, 1992 Edition through 1994 Addenda, supplemented by Code Case N-595-1 [A3.2] and ISG-15 [A3.3]. Stress criteria for pressure boundary components are summarized in Table 3.1-2. Stress criteria for (partial penetration) pressure boundary top closure welds are summarized in Table A.3.1-2.

The major internal basket components, spacer discs and guidesleeve assemblies, are designed to the criteria of ASME B&PV Code, Subsection NG as summarized in Table 3.1-4, supplemented by Code Case N-499-1 (for the spacer discs). The support rods and spacer sleeves are designed to the criteria of ASME B&PV Code, Subsection NF. The Boral[®] neutron absorbing material is non-Code and is not considered a load-carrying component.

A.3.1.2.1.2 Stability Criteria

No change.

A.3.1.2.1.3 Loads and Load Combinations

No change to the load combinations provided in Table 3.1-5. However, Note 3 is modified to reflect the pressure boundary for the 24PT4-DSC. For completeness, the load combinations for the 24PT4-DSC are summarized in Table A.3.1-3.

A.3.1.2.1.3.1 Deadweight

No change.

A.3.1.2.1.3.2 Internal and External Pressure

Internal pressure loads for the 24PT4-DSC are developed as described in Chapter A.4. The bounding normal, off-normal, and accident pressures used for the structural analyses of the 24PT4-DSC are given in Table A.3.1-4.

Load cases which include external pressures for the 24PT4-DSC are the same as those given in Table 3.1-7.

The internal basket components, such as the support rod assemblies, spacer discs, and guidesleeves, are not affected by pressure loads.

A.3.1.2.1.3.3 Thermal Loads

No change.

A.3.1.2.1.3.4 DSC Transfer/Handling Loads

No change.

A.3.1.2.1.3.5 Cask Drop

No change.

A.3.1.2.1.3.6 Seismic Loads

No change.

A.3.1.2.1.3.7 Flood Loads

No change.

A.3.1.2.2 AHSM Design Criteria

No change.

A.3.1.2.3 Exceptions to the ASME Code for the 24PT4-DSC

The ASME Code Exceptions summarized in Table 3.1-14 and Table 3.1-15 for the 24PT1-DSC, are shown in Table A.3.1-5 and Table A.3.1-6 for the 24PT4-DSC.

Code Case N-499-1 is applicable to the spacer disc material.

Table A.3.1-1
Codes and Standards for the Design, Fabrication and Construction of 24PT4-DSC
Principal Components

Component, Equipment, Structure	Code of Construction
24PT4-DSC	ASME Code, Section III, 1992 Edition through 1994 Addenda, supplemented by Code Case N-595-1, Code Case N-499-1, and ISG-15

**Table A.3.1-2
Stress Criteria for Partial Penetration Pressure Boundary Welds**

Service Level	Allowable Primary Stress	Primary and Secondary	Notes
Level A	$0.7 S_m$	$0.7 (3.0 S_m)$	Note 1
Level B	$0.7 S_m$	$0.7 (3.0 S_m)$	Note 1
Level C	greater of $0.7 (1.2 S_m)$ or $0.7 S_y$	N/A	Note 1
Level D Elastic	lesser of $0.7 (2.4 S_m)$ or $0.7 (0.7 S_u)$	N/A	Note 1
Level D Plastic	greater of $0.7 (0.7 S_u)$ or $0.7 (S_y + 1/3 (S_u - S_y))$	N/A	Note 1

Note:

1. These limits are based on Code Case N-595-1.

**Table A.3.1-3
24PT4-DSC Load Combinations and Service Levels**

Load Case		Normal Operating Conditions						Off-Normal Conditions				Accident Conditions						
		1	2	3	4	5	6	7	1	2	3	4	1	2	3	4	5	6
Dead Weight Load	Vertical/Horizontal DSC, Empty	X	X(10)															
	Vertical, DSC w/Fuel + Water			X(10)														
	Vertical, DSC w/Fuel				X(5)				X				X	X				
	Horizontal, DSC w/Fuel					X	X	X		X	X	X		X	X	X	X	X
Thermal Load	Inside HSM: 0° to 104°F							X	X									X
	Inside Cask: 0° to 120°F		X	X	X				X				X					
	Inside HSM: -40° to 117°F										X	X				X	X	
	Inside Cask 0° to 117°F (1)					X				X				X				
	Inside HSM: Blocked Vents; 117°F														X			
External Pressure			X	X					X				X				X	
Internal Pressure Load	Hydrostatic Pressure		X	X														
	Normal Pressure (4)				X	X	X	X										
	Off-Normal Pressure (4)									X	X	X	X(7)	X		X		X
	Accident Pressure (3)														X			
DSC Loading Operation Pressure (11)									X									
Handling/Transfer Loads	Handling Loads	X				X(8)												
	Normal DSC Transfer					X(8)		X										
	Off-Normal DSC Transfer									X		X						
	Accident DSC Transfer																	X
Cask Drop Load (side and corner drop)(9)														X				
Seismic Load																X		
Flooding Load																	X	
ASME Code Service Level		A	A	A	A	A	A	A	B	B	B	B	D	D	D	D	C	C
Analysis Load Cases in Section 3.6, Table 3.6-1		NO-3 NO-4	FL-1 FL-2 FL-3	FL-4 FL-5 FL-6	TL-1 TL-2 TL-3 TL-4	TR-1 to TR-8 LD-1 LD-2	HSM-1 HSM-2	UL-1 UL-2	DD-1 DD-2 DD-3 DD-4 DD-5	LD-3 LD-4	HSM-3 HSM-4 HSM-5 HSM-6	UL-3 UL-4	RF-1	TR-10 TR-11	HSM-11	HSM-9 HSM-10	HSM-12 HSM-13	UL-5

NOTES:

1. Outside fuel building, at temperatures over 100°F, a sunshade is required over the Transfer Cask. Temperatures for the 117°F with shade are enveloped by the 100°F without sunshade case.
2. **NOT USED.**
3. The 24PT4-DSC pressure boundary includes the inner bottom cover plate and the inner top plate that is structurally integral with the top shield plug.
4. The 24PT4-DSC normal and off-normal pressure is 20 psig.
5. 24PT4-DSC inside cask is horizontal for load cases TL-3, TL-4.
6. **NOT USED.**
7. Reflood pressure is 20 psig.
8. Handling loads apply to inertial TR-1 to TR-8. Transfer loads apply to LD-1 and LD-2.
9. Both horizontal and corner drop cases are considered.
10. Cask in vertical orientation only for those load cases.
11. Pressure varies from 0 psia (vacuum drying), to Hydrostatic + 20 psi (blowdown).

Table A.3.1-4
24PT4-DSC Internal Pressure Loads

Operating Condition	Internal Pressure	ASME Service Level
Normal Pressure	20 psig	A
Off-Normal Pressure	20 psig	B
Accident Pressure	100 psig	D
Design	20 psig @ 500°F	Design

**Table A.3.1-5
ASME Code Exceptions for the 24PT4-DSC (NB)**

Reference ASME Code Section/Article	Code Requirement	Exception, Justification & Compensatory Measures
NCA	All	Not compliant with NCA
NB-1100	Requirements for Code Stamping of Components	The 24PT4-DSC shell is designed & fabricated in accordance with the ASME Code, Section III, Subsection NB to the maximum extent practical. However, Code Stamping is not required. As Code Stamping is not required, the fabricator is not required to hold an ASME "N" or "NPT" stamp, or to be ASME Certified.
NB-2130 NB-4121	Material must be supplied by ASME approved material suppliers Material Certification by Certificate Holder	All materials designated as ASME on the FSAR drawings are obtained from ASME approved MO or MO supplier(s) with ASME CMTR's. Material is certified to meet all ASME Code criteria but is not eligible for certification or Code Stamping if a non-ASME fabricator is used. As the fabricator is not required to be ASME certified, material certification to NB-2130 is not possible. Material traceability & certification are maintained in accordance with TN's NRC approved QA program.
NB-6111	All completed pressure retaining systems shall be pressure tested	The shield plug, support ring, and vent and siphon block are not pressure tested due to the manufacturing sequence. The support ring is not a pressure-retaining item and the siphon block weld is helium leak tested after fuel is loaded and the inner top closure plate installed in accordance with Code Case N-595-1.
NB-7000	Overpressure Protection	No overpressure protection is provided for the 24PT4-DSC. The function of the 24PT4-DSC is to contain radioactive materials under normal, off-normal and hypothetical accident conditions postulated to occur during transportation and storage. The 24PT4-DSC is designed to withstand the maximum internal pressure considering 100% fuel rod failure at maximum accident temperature. The 24PT4-DSC is pressure tested to 120% of normal operating design pressure. An overpressure protection report is not prepared for the 24PT4-DSC.
NB-8000	Requirements for nameplates, stamping & reports per NCA-8000	The 24PT4-DSC nameplate provides the information required by 10CFR 71, 49CFR 173 and 10CFR 72 as appropriate. Code stamping is not required for the 24PT4-DSC. QA data packages are prepared in accordance with the requirements of 10CFR 71, 10CFR 72 and TN's approved QA program.

**Table A.3.1-6
ASME Code Exceptions for the 24PT4-DSC Basket (NG/NF)**

Reference ASME Code Section/Article	Code Requirement	Exception, Justification & Compensatory Measures
NCA	All	Not compliant with NCA
NG/NF-1100	Requirements for Code Stamping of Components	The 24PT4-DSC baskets are designed & fabricated in accordance with the ASME Code, Section III, Subsection NG/NF to the maximum extent practical as described in the FSAR, but Code Stamping is not required. As Code Stamping is not required, the fabricator is not required to hold an ASME N or NPT stamp or be ASME Certified.
NG/NF-2130 NG/NF-4121	Material must be supplied by ASME approved material suppliers Material Certification by Certificate Holder	All materials designated as ASME on the FSAR drawings are obtained from ASME approved MO or MO supplier with ASME CMTR's. Material is certified to meet all ASME Code criteria but is not eligible for certification or Code Stamping if a non-ASME fabricator is used. As the fabricator is not required to be ASME certified, material certification to NG/NF-2130 is not possible. Material traceability & certification are maintained in accordance with TN's NRC approved QA program.
Table NG-3352-1	Permissible Joint Efficiency Factors	Joint efficiency (quality) factor of 1 is assumed for the guidesleeve longitudinal weld. Table NG-3352-1 permits a quality factor of 0.5 for full penetration weld with visual inspection. Inspection of both faces provides $n=(2*0.5)=1$. This is justified by this gauge of material (0.125 inch) with visual examination of both surfaces which ensures that any significant deficiencies would be observed and corrected.
NG/NF-8000	Requirements for nameplates, stamping & reports per NCA-8000	The 24PT4-DSC nameplate provides the information required by 10CFR 71, 49CFR 173 and 10CFR 72 as appropriate. Code stamping is not required for the 24PT4-DSC. QA data packages are prepared in accordance with the requirements of 10CFR 71, 10CFR 72 and TN's approved QA program.
N/A	N/A	Oversleeve to guidesleeve welds are non-code weld which meet the requirements of AWS D1.3-98, Structural Welding Code-Sheet Steel.

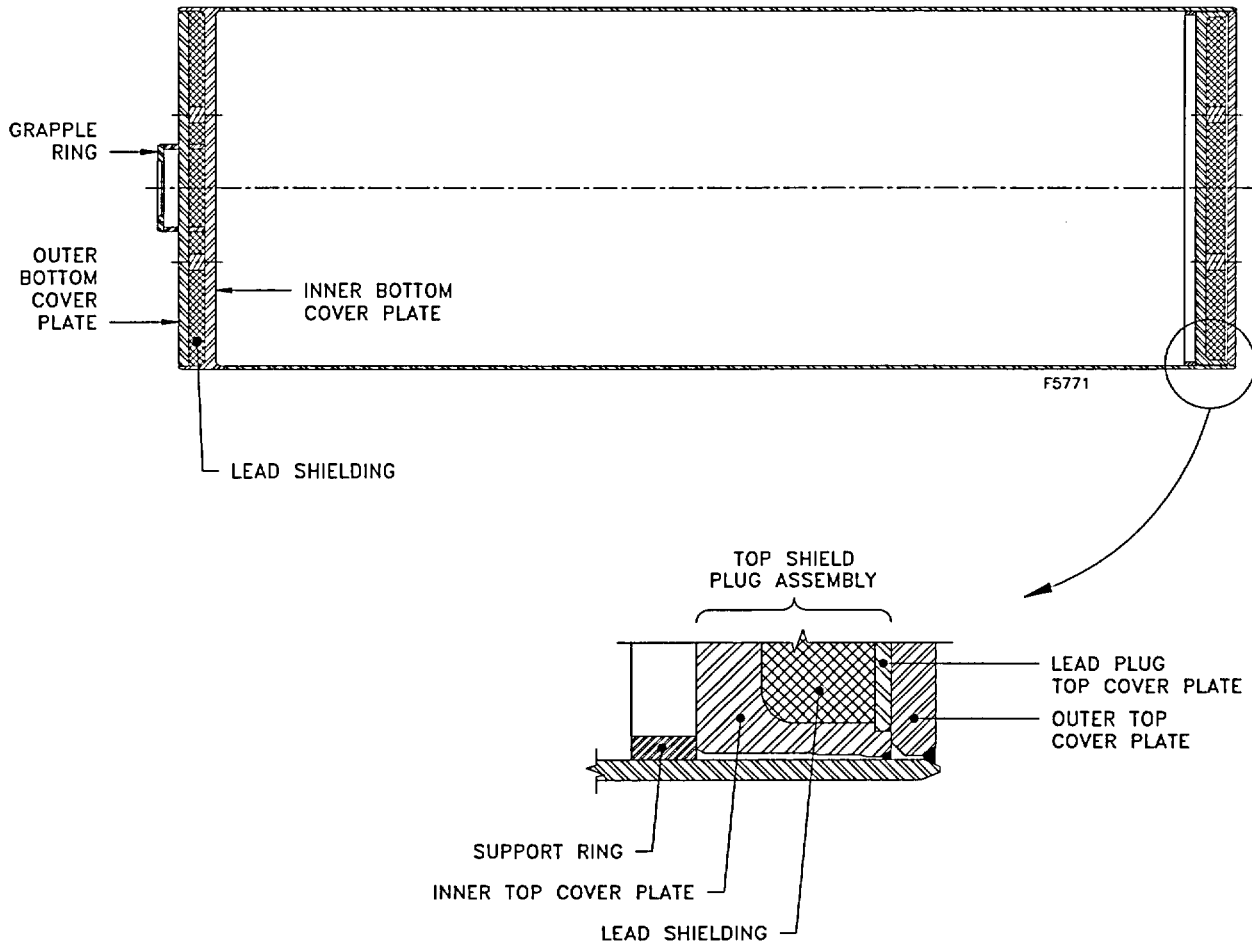
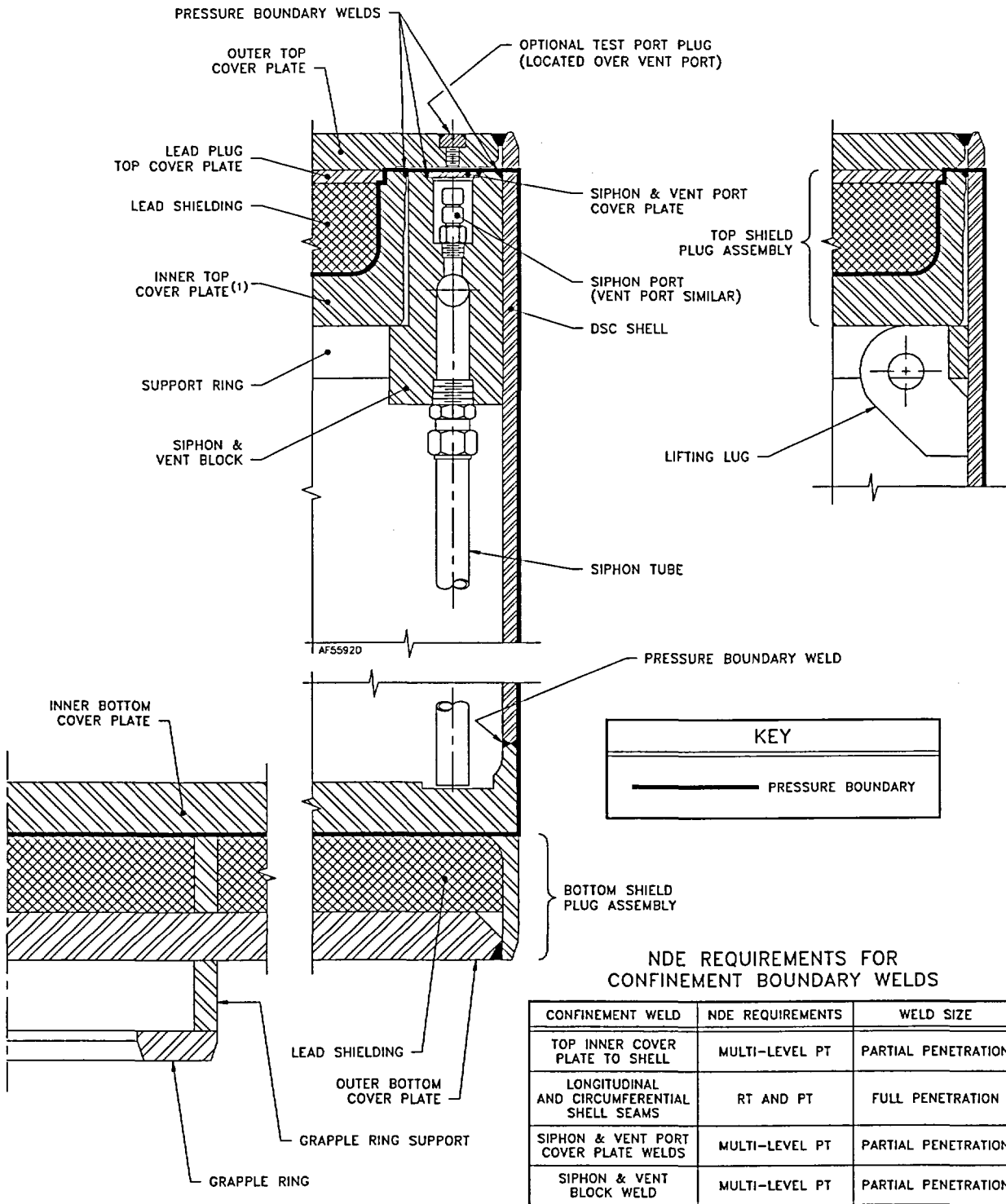


Figure A.3.1-1
Advanced NUHOMS® System 24PT4-DSC Canister Shell Assembly



(1) FORGING CONFIGURATION IS SHOWN. MAY BE FABRICATED FROM SEPARATE INNER TOP COVER AND SIDE CASING PLATES.

Figure A.3.1-2
Advanced NUHOMS® System 24PT4-DSC Pressure Boundary Location

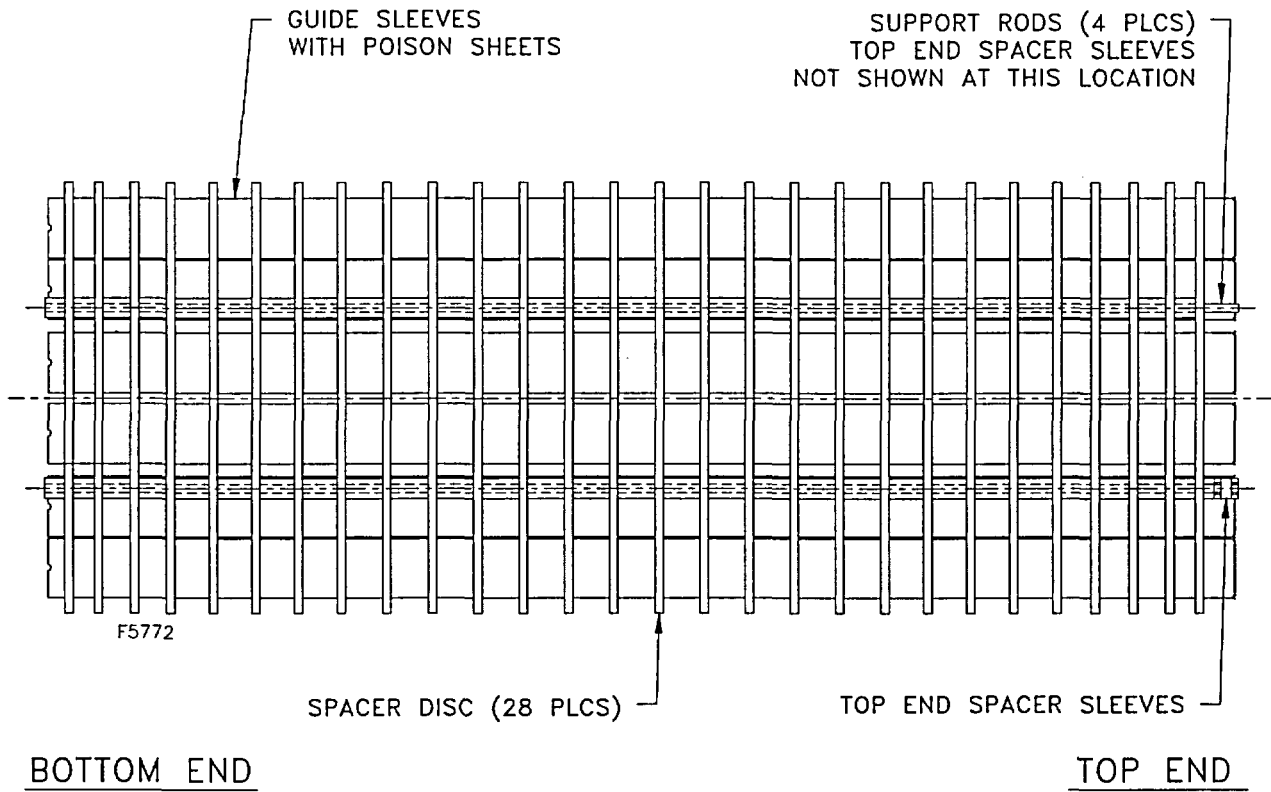


Figure A.3.1-3
Advanced NUHOMS® System 24PT4-DSC Canister Basket (Side View)

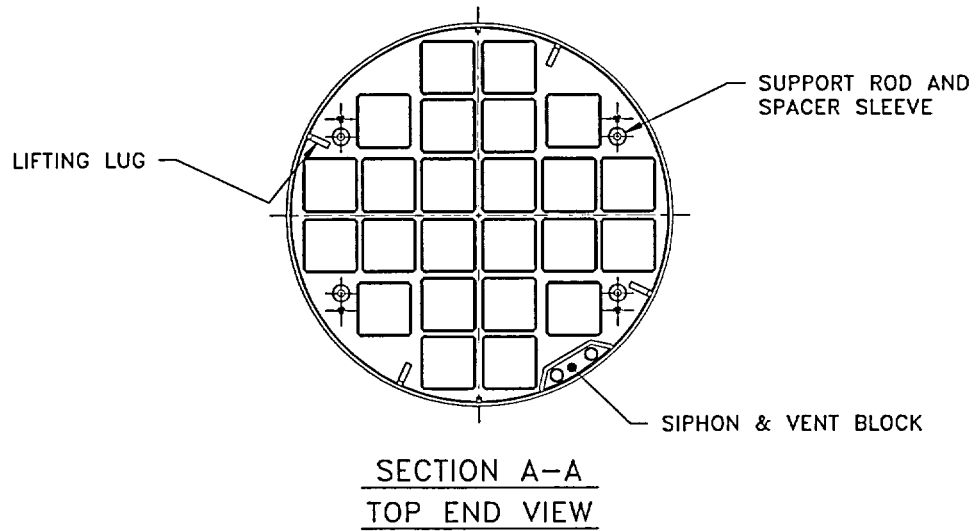
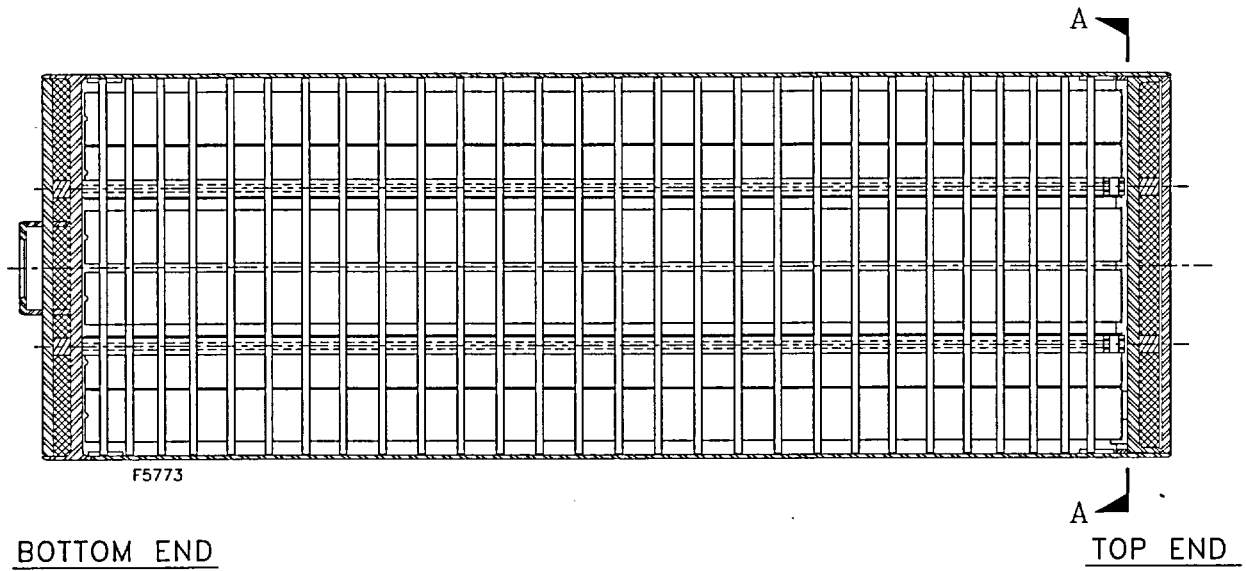


Figure A.3.1-4
Advanced NUHOMS® System 24PT4-DSC Canister Basket & Shell
(Side and Top End View)

A.3.2 Weights and Centers of Gravity

The weight and center of gravity of a 24PT4-DSC loaded with Westinghouse-CENP, Combustion Engineering 16x16 fuel, is listed in Table A.3.2-1. The radial center of gravity is on the axis of the 24PT4-DSC.

The total weight of the 24PT4-DSC includes the shell assembly, the internal basket assembly and the fuel.

Table A.3.2-1 also gives an upper (loaded AHSM) and lower (unloaded AHSM) bound weight and center of gravity for the AHSM. For the upper bound weight, the AHSM is assumed to be loaded with a 24PT4-DSC that weighs 85,000 lbs, and for the lower bound weight the AHSM is assumed to be unloaded.

**Table A.3.2-1
Weights and Centers of Gravity of the 24PT4-DSC**

	Component	Weight ⁽⁵⁾ (lbs)
24PT4-DSC Canister ⁽³⁾	Shell Assembly	15,500 ⁽¹⁾
	Basket Assembly	23,100 ⁽⁶⁾
	Top Shield Plug Assembly	7,350
	Outer Top Cover Plate	1,250
	Westinghouse-CENP, Combustion Engineering 16x16 Fuel	37,400
	TOTAL	84,600
	Center of Gravity	94.7 inches ⁽¹⁾
Loaded AHSM ⁽⁴⁾	Weight	403,300
	Center of Gravity	121.1 inches ⁽²⁾
Unloaded AHSM	Weight	318,300
	Center of Gravity	126.1 inches ⁽²⁾

NOTES:

- (1) See Figure A.3.2-1 for the location of the center of gravity relative to the outside edge of the outer bottom cover plate of the 24PT4-DSC.
- (2) See Figure A.3.2-2 for the location of the center of gravity relative to the bottom of the AHSM.
- (3) The total 24PT4-DSC weight includes Westinghouse-CENP, Combustion Engineering 16x16 Fuel.
- (4) The total loaded weight of a loaded AHSM includes a loaded 24PT4-DSC that weighs 85,000 lbs. The center of gravity (cg) for the loaded AHSMs with the 24PT1-DSC is bounding.
- (5) The weight values are rounded to the nearest 50 lbs.
- (6) Weight includes weight of failed fuel can top and bottom lids on 12 cans.

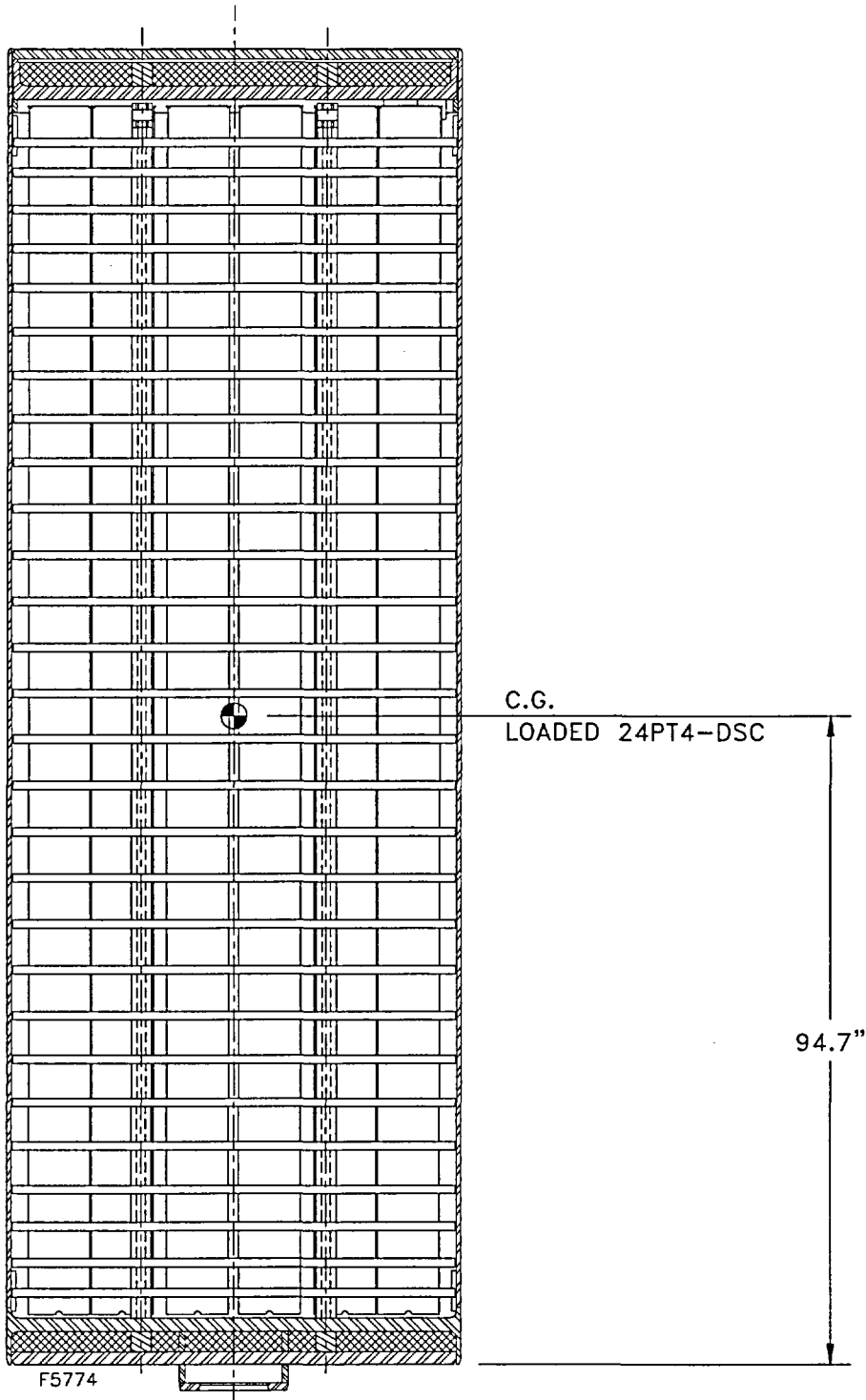


Figure A.3.2-1
Schematic Location of Center of Gravity of the 24PT4-DSC

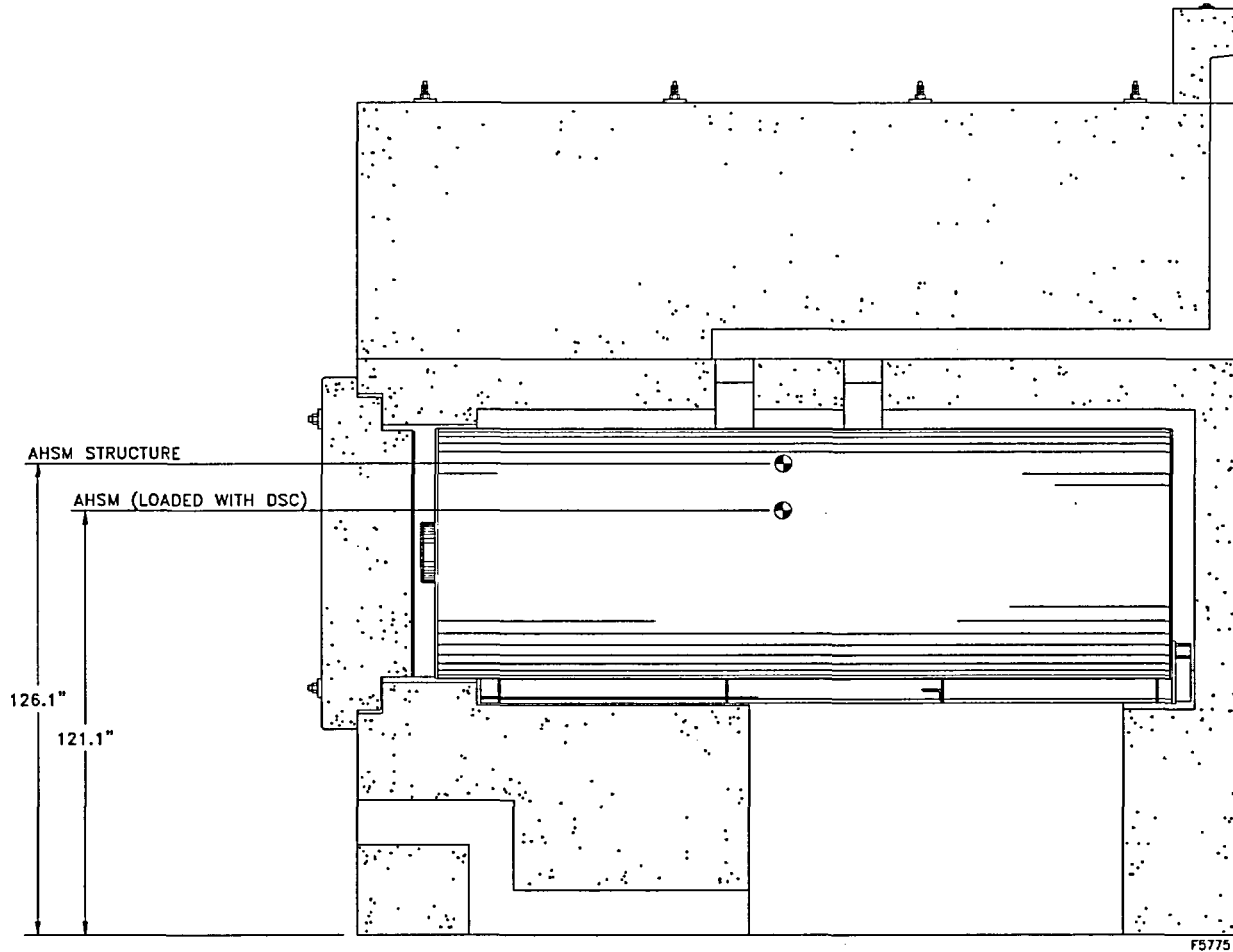


Figure A.3.2-2
Schematic Location of Center of Gravity of the 24PT4-DSC in the AHSM

A.3.3 Mechanical Properties of Materials

A.3.3.1 24PT4-DSC Material Properties

The materials used for fabrication of the 24PT4-DSC are the same as those presented in Section 3.3.1 with the following exceptions/clarifications:

- The 24PT4-DSC shell assembly's top and bottom ends include stainless steel forgings (material specification SA-182 Type F316) and/or Type 316 stainless steel plates that encase the lead (ASTM B29) shield plugs. Properties of the forging material are the same as the Type 316 plate material used for fabrication of the 24PT1-DSC. Properties for the ASTM B29 lead are shown in Table A.3.3-1.
- SA-533 Grade B Class 1 carbon steel material is used for fabrication of the 24PT4-DSC basket assembly spacer discs, instead of the SA-537, Class 2 used for the 24PT1-DSC spacer discs. ASME Code Case N-499-1 [A3.7] allows limited elevated temperature service up to 1000°F for SA-533 Grade B Class 1 carbon steel, compared to SA-537 Class 2 carbon steel, limited to 700°F [A3.2]. The properties of SA-533 Grade B Class 1 material are shown in Table A.3.3-2.
- Table A.3.3-3 provides the support rod material properties, SA-564 Type 630 Steel.

All other materials for the shell and basket assemblies are the same as the 24PT1-DSC.

A.3.3.1.1 Radiation Effects on 24PT4-DSC Materials

No change.

A.3.3.1.2 Weld Material

No change.

A.3.3.1.3 Brittle Fracture

Brittle fracture is not a concern for the stainless steel components. For the SA-533, Grade B, Class 1 carbon steel spacer discs, the fracture toughness requirements of NG-2300 are met.

A.3.3.2 AHSM Material Properties

No change.

A.3.3.2.1 Radiation Effects on AHSM Concrete

No change.

A.3.3.3 Materials Durability

No change.

Table A.3.3-1
Static Mechanical Properties for ASTM B29 Lead

Temp (°F)	Static Stress Properties (ksi) ⁽¹⁾			Elastic Modulus (10 ⁶ psi)	Coef. of Thermal Exp (10 ⁻⁶ in/in/°F)
	YIELD (S _y)		ULTIMATE (S _u)		
	Tension	Compression	Tension		
-99	-	-	-	2.50	15.28
70	-	-	-	2.34	16.07
100	0.584	0.490	1.570	2.30	16.21
175	0.509	0.428	1.162	2.20	16.58
250	0.498	0.391	0.844	2.09	16.95
325	0.311	0.320	0.642	1.96	17.54
440	-	-	-	1.74	18.50
620	-	-	-	1.36	20.39

Note:

(1) Reference [A3.6].

**Table A.3.3-2
ASME Code Material Properties for SA-533 Grade B Class 1 Carbon Steel**

SA-533 Grade B Class 1 (Mn-½Mo-½Ni)

Temperature ⁽¹⁾ (°F)	S _m ⁽²⁾ (ksi)	S _y ⁽²⁾ (ksi)	S _u ⁽²⁾ (ksi)	E (x 10 ⁶ psi) ⁽²⁾	α _{Inst} (x 10 ⁻⁶ °F ⁻¹) ⁽²⁾	α _{Avg.} (x 10 ⁻⁶ °F ⁻¹) ⁽²⁾	K $\left(\frac{BTU}{hr \cdot ft \cdot °F}\right)$
75	26.7	50.0	80.0	29.2 ⁽³⁾	7.0 ⁽³⁾		22.3 ⁽³⁾
100	26.7	50.0	80.0	--	7.1	7.1	22.6
150	--		--	--	7.3	7.2	23.1
200	26.7	47.5	80.0	28.5	7.5	7.3	23.4
250	--		--	--	7.6	7.3	23.7
300	26.7	46.1	80.0	28.0	7.7	7.4	23.8
350	--	--	--	--	7.9	7.5	23.8
400	26.7	45.1	80.0	27.4	8.0	7.6	23.8
450	--	--	--	--	8.1	7.6	23.7
500	26.7	44.5	80.0	27.0	8.3	7.7	23.5
550	--	--	--	--	8.4	7.8	23.2
600	26.7	43.8	80.0	26.4	8.5	7.8	23.0
650	--	43.5	80.0	--	8.6	7.9	22.7
700	26.7	43.1	80.0	25.3	8.6	7.9	22.3
750	26.7	42.3	80.0	--	8.7	8.0	22.0
800	26.7	41.6	80.0	23.9	8.8	8.1	21.7
850	25.5	40.6	76.6	--	8.8	8.1	21.3
900	24.3	39.4	72.7	22.2	8.9	8.1	20.9
950	22.5	37.8	67.3	--	9.0	8.2	20.5
1000	20.7	35.9	62.2	20.1	9.0	8.2	20.1
Reference Code Case N-595-1	Table 3	Table 3	Table 3	Table 5	Table 6	Table 7	(4)

Notes:

- (1) Per Code Case N-499-1 [A3.7], Maximum permitted metal temperature for Level A events is 700°F. Metal temperatures exceeding 700°F are permitted for Service Level B, C and D events. See Code Case N-499-1 for additional information and restrictions.
- (2) These material properties listed are from Code Case N-499-1 tables.
- (3) At 70°F
- (4) From ASME Section II, Table TCD for Mn-½ Mo-½ Ni

**Table A.3.3-3
ASME Code Material Properties for SA-564 Type 630 Steel**

SA-564 Type 630 Precipitation Hardened Martensitic Stainless Steel (17Cr-4Ni-4Cu)

Temp. °F	ASME Code Material Properties ^(1,2)						
	S _m (ksi)	S _y (ksi)	S _u (ksi)	E ⁽³⁾ (x 10 ⁶ psi)	α _{inst} °F ⁻¹	α _{avg} °F ⁻¹	k BTU/hr-ft-°F
-100	--	--	--	29.4	--	--	--
-20	46.7	115.0	140.0	--	--	--	--
70	--	--	--	28.5	5.9	--	9.9
100	46.7	115.0	140.0	--	5.9	5.9	10.1
150	--	--	--	--	5.9	5.9	10.4
200	46.7	106.3	140.0	27.8	5.9	5.9	10.6
250	--	--	--	--	5.9	5.9	10.9
300	46.7	101.9	140.0	27.2	5.9	5.9	11.2
350	--	--	--	--	5.9	5.9	11.4
400	45.5	98.3	136.3	26.6	5.9	5.9	11.7
450	--	--	--	--	5.9	5.9	12.0
500	44.4	95.2	133.2	26.1	5.9	5.9	12.2
550	--	--	--	--	5.9	5.9	12.5
600	43.8	92.8	131.4	25.5	6.0	5.9	12.7
650	43.5	91.5	--	25.2	6.0	5.9	13.0
700	not permitted at temperatures above 650°F						
750	--	--	--	--	--	--	--
800	--	--	--	--	--	--	--
Reference (ASME II)	Table 2A	Table Y-1	Table U	Table TM-1	Table TE-1		Table TCD
	(17Cr-4Ni-4Cu)						

Notes:

1. This material has reduced toughness at room temperature after exposure for about 5000 hrs at 600°F and after shorter exposure above 650°F. (See Note B1(3) of Table Y-1, Note B1(2) of Table U and Note B1(12) of Table 2A.)
2. These values apply to material which has been age hardened at 1100°F. (See Note B1(6) of Table 2A, Note B1(5) of Table Y-1 and Note B1(5) of Table U.)
3. Per Table TM-1, S17400 (see Note 11 of Table TM-1), 1998 Edition with 1999 Addenda. This data is used since specific data for this material is available in the 1998/1999 Edition code. The data available in the 1992/1994 code year is grouped together for all 17Cr materials. The 1998/1999 Edition provides the 17Cr values and, in addition, provides values for S17400 (17Cr, Type 630). Use of the 1998/1999 code year, therefore, provides more specific material properties for this material than is available in the 1992/1994 code year.

A.3.4 General Standards for 24PT4-DSC and AHSM

A.3.4.1 Chemical and Galvanic Reactions

The review for chemical and galvanic reactions presented in Section 3.4.1 for the 24PT1-DSC is applicable to the 24PT4-DSC, since fuel loading, unloading, handling and storage processes and environments are similar for both the 24PT1 and the 24PT4-DSCs. The following applies specifically to the 24PT4-DSC:

- Materials used for the 24PT4-DSC are shown in the Parts List of Drawing ANUH-01-4001 in Section A.1.5.2.
- From a chemical and galvanic reaction standpoint, the only differences between the 24PT4-DSC and the 24PT1-DSC designs are the shell assembly top and bottom ends which include stainless steel-encased and sealed lead in the shield plugs. The lead is not exposed to the external environment and is thus not subject to any chemical reactions. Both the 24PT1-DSC spacer discs and the 24PT4-DSC spacer discs are fabricated from Carbon Steel and plated with electroless nickel.

A.3.4.1.1 Behavior of Austenitic Stainless Steel in Borated Water

No change.

A.3.4.1.2 Behavior of Boral[®] in Borated Water

No change.

A.3.4.1.3 Electroless Nickel Plated Carbon Steel

No change.

A.3.4.1.4 Hydrogen Generation

No change.

A.3.4.1.5 Effect of Galvanic Reactions on the Performance of the System

No change.

A.3.4.2 Positive Closure

Positive closure is provided by the redundant closure welds consisting of the inner top cover plate of the shield plug assembly-to-shell weld, the outer top cover plate-to-shell weld, and the leaktight (tested per ANSI N14.5 [A3.4]) 24PT4-DSC shell assembly.

A.3.4.3 Lifting Devices

There are no permanent lifting devices used for lifting a loaded 24PT4-DSC, the loaded 24PT4-DSC is always inside a transfer/transportation cask during handling.

The evaluation of lifting devices is performed in the transfer system, see References [A3.8].

A.3.4.4 Heat

A.3.4.4.1 Summary of Pressures and Temperatures

Temperatures and pressures for the 24PT4-DSC are described in Chapter A.4. Section A.4.4, Section A.4.5, and Section A.4.6 describe the thermal evaluations performed for normal, off-normal, and accident conditions, respectively. Section A.4.7 describes the thermal evaluations during fuel loading/unloading operations. Maximum temperatures for the various components of the Advanced NUHOMS[®] System for normal, off-normal, and accident conditions are summarized in Table A.4.4-1 and Table A.4.4-2 for shell and basket assemblies, respectively. These temperatures are used for the structural evaluations documented in Section A.3.6. Stress allowables for the cask components are a function of component temperature. The temperatures used to perform the structural analysis are based on actual calculated temperatures or conservatively selected higher temperatures.

Table A.4.4-6 provides a summary of the maximum 24PT4-DSC pressures for normal, off-normal and accident conditions. The pressures used in the 24PT4-DSC stress analyses, are summarized in Table A.3.1-4 and bound those shown in Table A.4.4-6.

A.3.4.4.2 Differential Thermal Expansion

Potential interferences due to differential thermal expansion between the 24PT4-DSC shell assembly and the basket assembly components is evaluated in the longitudinal and radial directions of the 24PT4-DSC.

In the radial direction, the gaps between the spacer discs and the inside of the 24PT4-DSC shell are evaluated for possible interference due to differential thermal expansion of the materials because of the differences in their coefficients of thermal expansion. The analyses show that for the worst case statistical stack up of tolerances, the radial gap between the spacer disc and the inside of the shell will close, but will not impose significant stresses in the 24PT4-DSC shell or the spacer disc.

For the following interfaces, design clearances are established to ensure that there are no thermal interferences.

- Guidesleeve/Failed Fuel Can to 24PT4-DSC Cavity (Length)
- Guidesleeve/Failed Fuel Can to Spacer Disc Fuel Cutout
- Neutron Absorber (Boral[®]) to Oversleeve

- Support Rod Assembly to 24PT4-DSC Cavity (Length)
- SFA's to 24PT4-DSC Cavity (Length)
- Distance between AHSM rail stops to 24PT4-DSC overall length

The coefficient of thermal expansion of the spacer disc material is slightly greater than the coefficient of thermal expansion of the support rod/spacer sleeve material. Thus, as the basket temperature increases, the spacer disc(s) will tend to expand faster than the rod assembly. This will increase tension in the support rod and increase compression in the spacer sleeves (similar to increasing the initial preload in the rod assembly). However, this effect is offset by a reduction in stiffness at elevated temperatures such that the net result is a slight loss in rod preload at elevated temperatures. These stresses are included in the analysis of the rod assembly.

Poison rodlets used for criticality control are designed to remain contained within the fuel assembly. Fabrication of these rodlets from borated stainless steel or stainless steel encased B₄C ensures that thermal growth is bounded by the thermal growth of the longer stainless steel guidesleeves.

A.3.4.4.3 Stress Calculations

The stress analyses have been performed using the acceptance criteria and load combinations presented in Section A.3.1.2. The structural analyses for the 24PT4-DSC are summarized in Section A.3.6.1. The AHSM structural analyses with the 24PT4-DSC presented in Section 3.6.2 are also applicable to the 24PT4-DSC.

The stress analyses results for the 24PT4-DSC are summarized in Section A.3.6.1.1 for the shell assembly and Section A.3.6.1.2 for the basket assembly components. Table A.3.6-1 lists the detailed load combinations considered for the 24PT4-DSC. Finite element models of the shell assembly and the spacer discs have been developed, and detailed computer analyses performed using the ANSYS [A3.9] computer program. The guidesleeves, support rods and Failed Fuel Cans have been analyzed using a combination of ANSYS finite element models and hand calculations.

A.3.4.4.3.1 24PT4-DSC Shell Assembly

Table A.3.6-4 summarizes the calculated maximum stress intensities in the 24PT4-DSC shell assembly components for the controlling load combinations for normal and off-normal operating conditions (ASME Service Levels A and B). Similarly, Table A.3.6-5 and Table A.3.6-6 summarize the calculated maximum stress intensities in the 24PT4-DSC shell assembly components for the controlling accident conditions load combinations. All calculated stresses in the 24PT4-DSC confinement boundary assembly meet code allowables and are acceptable.

A.3.4.4.3.2 Basket Assembly

The stress analyses results for the basket assembly are summarized in Table A.3.6-7, Table A.3.6-8 and Table A.3.6-9. Table A.3.6-7 presents a summary of the calculated maximum stress intensities obtained for the spacer discs for the controlling load combinations.

Table A.3.6-8 presents a summary of the maximum stress intensities for the guidesleeves.

Table A.3.6-9 presents a summary of the highest interaction ratios for the support rod assemblies. The support rod preload is specified as 40 ± 15 kips. For conservatism the calculations were performed for a preload of 65 kips using elevated temperature material properties. For these very conservative assumptions the maximum interaction ratio is calculated to be 0.96. For axial end drops the load cancels the pre-stress and therefore, the maximum stress for accident conditions is 0.62 for the support rods and 0.63 for the spacer sleeves.

The analyses presented in Section A.3.6 demonstrate that even in the extremely unlikely hypothetical accident scenarios, there is sufficient margin to ensure that the basket components perform their intended function.

A.3.4.4.3.3 AHSM

There is no change to the AHSM results presented in Section 3.4.4.3.3 since the calculations are based on an enveloping weight of 85,000 lbs. which bounds the loaded weight of the 24PT4-DSC.

A.3.4.4.4 Comparison with Allowable Stresses

The stresses for each of the major components of the 24PT4-DSC are compared to their allowables in Table A.3.6-4 through Table A.3.6-9.

A.3.4.5 Cold

The AHSM and 24PT4-DSC have been designed for operation at daily average ambient temperatures as low as -40°F . The permanent AHSM and DSC shielding materials are all solids, so there is no concern over freezing.

The SA-240 Type 316 stainless steel is not subject to brittle fracture for the range of operating temperatures of the 24PT4-DSC.

A.3.5 Fuel Rods General Standards for 24PT4-DSC

This section provides the temperature criteria used in the 24PT4-DSC thermal evaluation for the safe storage and handling of Westinghouse-CENP, Combustion Engineering 16x16 SFAs in accordance with the requirements of 10CFR 72 to ensure a very low probability of rod failure during long term storage, and to protect against gross failures during short term events. Short term events include transfer operations, off-normal conditions, accident conditions, and other short term operational events.

This section also contains the calculation of the thermal and irradiation growth of the fuel assemblies to demonstrate that adequate space exists within the 24PT4-DSC cavity for the fuel assemblies to grow thermally under all conditions.

In addition, this section provides an evaluation of the fuel rod stresses and critical buckling loads due to accident drop loads.

A.3.5.1 Fuel Rod Temperature Limits for Westinghouse-CENP, Combustion Engineering 16x16 Fuel

A.3.5.1.1 Temperature Limit for Long Term Storage

The maximum fuel cladding temperature limit of 400°C (752°F) is applicable to normal conditions of storage and all short term operations from spent fuel pool to ISFSI pad including vacuum drying and helium backfilling of the 24PT4-DSC per Interim Staff Guidance (ISG) No. 11, Revision 2 [A3.14]. In addition, ISG-11 does not permit thermal cycling of the fuel cladding with temperature differences greater than 65°C (117°F) during DSC drying, backfilling and transfer operations.

A.3.5.1.2 Temperature Limit for Short Term Events

The maximum fuel cladding temperature limit of 570°C (1058°F) is applicable to accidents or off-normal thermal transients [A3.14].

A.3.5.2 Fuel Assembly Thermal and Irradiation Growth

The thermal and irradiation growth of the fuel assemblies were calculated to ensure there is adequate space for the fuel assemblies to grow within the 24PT4-DSC cavity. The reference temperature for material properties is assumed to be 70°F.

The thermal growth is calculated based on the fuel assembly parameters given in Table A.3.5-1. The 24PT4-DSC minimum cavity length is also given in Table A.3.5-1. Thermal expansion coefficients for the materials considered are given in Chapter 4.

Based on the results shown in Chapter A.4, the vacuum drying case produces the highest fuel cladding temperatures coupled with relatively low 24PT4-DSC shell temperatures due to the

water-filled cask annulus. Therefore, this case results in the bounding thermal growth for all operating conditions.

There is adequate space within the 24PT4-DSC cavity for thermal and irradiation growth of the fuel assemblies. The minimum calculated gap is given in Table A.3.5-1.

A.3.5.3 Fuel Rod Integrity During Drop Scenario

Fuel assembly properties are provided in Table A.3.5-2; material properties are provided in Table A.3.5-3 and fuel assembly loads are identified in Table A.3.5-4 for the calculation of fuel rod stresses and critical buckling loads due to cask side and end drop incidents.

A.3.5.3.1 Methodology

A.3.5.3.1.1 Drop

The drop analysis methodology is the same as presented in Section 3.5.3.1 for both side and corner drops.

A.3.5.3.2 Results

Using the geometric and material properties in Table A.3.5-2 through Table A.3.5-4 and the methodology in Section 3.5.3.1, the analysis of the Westinghouse-CENP, Combustion Engineering 16x16 Zircalloy-4 clad fuel assemblies for 75g side and 25g corner drops and the methodology described above gives the following results:

The side drop allowable g-load is calculated to be 156g which exceeds the postulated 75g side load. For the corner drop, the critical axial buckling load is calculated to be 61.2g which, when combined with the side drop component, results in an interaction ratio of 0.35. This provides a factor of safety greater than 2 against fuel rod failure in a corner drop.

A.3.5.4 Fuel Unloading

For unloading operations, the 24PT4-DSC will be filled with spent fuel pool water through the siphon port. During this filling operation, the 24PT4-DSC vent port is maintained open with effluents routed to the plant's off-gas monitoring system. The NUHOMS[®] operating procedures recommend that the 24PT4-DSC cavity atmosphere be sampled before introducing any reflood water into the 24PT4-DSC cavity.

When the pool water is added to a 24PT4-DSC cavity containing hot fuel and basket components, some of the water will flash to steam causing internal cavity pressure to rise. This steam pressure is released through the vent port. The procedures also specify that the flow rate and temperatures of the reflood water be controlled to ensure that the internal pressure in the 24PT4-DSC cavity is maintained at less than or equal to 20 psig. The reflood for the 24PT4-DSC is considered as a Service Level D event. The 24PT4-DSC is also evaluated for a Service Level D pressure of 100 psig. Therefore, there is sufficient margin in the 24PT4-DSC internal pressure during the reflooding event to assure that the 24PT4-DSC will not be over pressurized.

The maximum fuel cladding temperature during reflooding will be significantly less than the vacuum drying condition due to the presence of water/steam in the 24PT4-DSC cavity. Therefore, no cladding damage is expected due to the reflood event. This is also substantiated by the operating experience gained with the loading and unloading of transportation packages like the IF-300 [A3.12] which show that fuel cladding integrity is maintained during these operations and fuel handling and retrieval are not impacted.

Table A.3.5-1
Summary of Fuel Assembly Thermal and Irradiation Growth Calculations

	CE 16x16
Fuel Rod Material ⁽²⁾	Zircalloy-4
Minimum Cavity Length (in)	181.67
Fuel Assembly Temperature (°F)	740
Minimum Calculated Gap (in)	3.43

Notes:

- (2) Thermal growth of fuel assembly conservatively assumes Type 316 stainless properties, not Zircalloy-4.

**Table A.3.5-2
Fuel Assembly Properties⁽¹⁾**

Parameter	CE 16x16
Clad Outside Diameter	0.382 inches
Fuel Rod Thickness	0.025 inches
Active Fuel Rod Length	150.0 inches
Pellet Diameter	0.3255 inches ⁽²⁾
Fuel Rod Pitch	0.506 inches
Average Span Length Between Grid Straps (L)	17.04 inches
Weight of Rod/Unit Length	0.039 lb/inches
Fuel Rod Length	161.9 inches

(1) Nominal values

(2) Bounds pellets with a nominal OD of 0.325".

Table A.3.5-3
Material Properties for Zircalloy Cladding [A3.13]

Temperature (°F)	Modulus of Elasticity (x10⁶ psi)	Yield Stress (x10⁶ psi)	Ultimate Strength (x10⁶ psi)
750	10.4	80,500	99,000

**Table A.3.5-4
Fuel Assembly Loads**

Fuel Assembly	Impact Load (g)	
	Side	Corner
CE 16x16	75	25 ⁽¹⁾

- (1) The postulated 25g corner drop angle is 30°. The axial component is 12.5g and side loading component is 22g.

A.3.6 Supplemental Data

This section presents the structural analyses of the 24PT4-DSC. There is no change to the structural analysis of the AHSM presented in Section 3.6.2.

A.3.6.1 24PT4-DSC Structural Analysis

The 24PT4-DSC shell assembly, shown in Figure A.3.1-1 and Figure A.3.1-2, is described in detail in Section A.3.1.1.1.

The nominal plate thickness for the cylindrical shell is 0.625 inches. The stress analyses conservatively assume a minimum plate thickness of 0.53 inches.

The basket assembly components include the spacer discs, the guidesleeve and neutron absorber plate assemblies, and the support rod assemblies.

Section A.3.6.1.1 presents the structural analyses of the 24PT4-DSC shell assembly and Section A.3.6.1.2 presents the structural analyses of the 24PT4-DSC basket assembly.

A.3.6.1.1 24PT4-DSC Shell Assembly Structural Analysis

The 24PT4-DSC shell assembly is analyzed for the normal, off-normal and postulated accident load conditions specified in Section A.3.1.2.1, utilizing finite element models and/or hand calculations and closed-form classical engineering solutions. The finite element models are developed using the ANSYS [A3.9] computer program.

A.3.6.1.1.1 Applicable Loads and Load Combinations

The 24PT4-DSC loads and load combinations are discussed in Section A.3.1.2.1.3. The 24PT4-DSC load combinations are detailed in Table A.3.6-1.

A.3.6.1.1.2 ANSYS Models for Stress Analysis of the 24PT4-DSC

The 24PT4-DSC shell assembly is analyzed using three finite element models:

- Axisymmetric model of the 24PT4-DSC shell assembly
- Three-dimensional top-end model with top shield plug assembly, outer top cover plate, and part of the 24PT4-DSC shell.
- Three-dimensional bottom-end model with bottom shield plug assembly, outer bottom cover plate, grapple assembly components, and part of the 24PT4-DSC shell.

The axisymmetric model is shown in Figure A.3.6-1. The axisymmetric model is a complete model of the 24PT4-DSC shell assembly which includes both top and bottom shield plug assemblies, cover plates, and the 24PT4-DSC shell. The model is used to analyze axisymmetric loads. The model consists of ANSYS PLANE 42 elements. The adjacent surfaces of the top

cover plate, bottom cover plate, and lead shielding are modeled by ANSYS CONTACT 49 elements. This model is used for analysis of vertical dead weight load, top/bottom end drop loads, and internal/external pressure loads.

The 3D top and bottom end models are shown in Figure A.3.6-2. The three-dimensional top and bottom end models are 180° (half-symmetric) representations, and are used to analyze non-axisymmetric loads. These models consist of eight node 3D solid elements (ANSYS SOLID 45). Each node has three translational degrees of freedom. The adjacent plate surfaces of the top and bottom and components are modeled using nonlinear contact elements (ANSYS CONTACT 49). The contact elements allow the transfer of compressive loads only, allowing interacting surfaces to slide freely with respect to one another. These models are used for the analysis of thermal load, side drop load, and grapple pull/push loads.

A.3.6.1.1.3 24PT4-DSC Dead Load Analysis

Dead load analyses of the 24PT4-DSC are performed for both vertical and horizontal orientations of the 24PT4-DSC. In the vertical orientation, the 24PT4-DSC shell supports its own weight and the weight of the top end components. The weight of the fuel is uniformly distributed over the area of the inner bottom cover plate. When in the horizontal position, the 24PT4-DSC is either in the TC or in the AHSM. In the horizontal orientation, the 24PT4-DSC shell assembly end components and the internal basket assembly bear against the 24PT4-DSC shell. The 24PT4-DSC shell assembly is supported by two 3" wide rails located at $\pm 18.5^\circ$ (in the TC) and $\pm 35^\circ$ (in the AHSM) from the bottom centerline of the 24PT4-DSC, see Figure A.3.6-3.

Dead load stresses are obtained from static analyses performed using the ANSYS finite element models described in Section A.3.6.1.1.2. The axisymmetric model is used to perform analysis for vertical dead weight load and the 3D models are used to perform analysis for horizontal dead weight.

In addition, when the 24PT4-DSC is in the horizontal position, the fuel-loaded spacer discs of the basket assembly bear on the inner surface of the 24PT4-DSC shell. Shell stresses in the region of the spacer discs, resulting from the spacer disc loads, are evaluated using an ANSYS finite element model that includes the spacer disc and a portion of the shell and interfacing TC. This model is described in Section A.3.6.1.2.3.

The 24PT4-DSC shell assembly components are evaluated for primary membrane stress, membrane plus bending stress, and for primary plus secondary stress intensities. Enveloping 24PT4-DSC maximum stress intensities for the dead load condition are summarized in Table A.3.6-2.

A.3.6.1.1.4 24PT4-DSC Pressure Analysis

The 24PT4-DSC shell assembly is analyzed for the normal, off-normal and accident condition pressures listed in Table A.3.1-4.

In addition to internal pressure loads, the 24PT4-DSC is also evaluated for internal and external hydrostatic pressures which may occur during fuel loading operations. Operations which may subject the 24PT4-DSC shell to “external” pressure include the vacuum drying load cases.

Stability of the 24PT4-DSC shell under combined axial load and external pressure is evaluated using the following interaction equation, where the allowables are developed using NB-3133.

$$\frac{\text{applied axial stress}}{\text{allowable axial stress}} + \frac{\text{applied external pressure}}{\text{allowable external pressure}} \leq 1.0$$

Enveloping 24PT4-DSC maximum stress intensities for the normal and off-normal pressure load conditions are summarized in Table A.3.6-2. Maximum stress intensities for the accident pressure of 100 psig are reported in Table A.3.6-3.

A.3.6.1.1.5 24PT4-DSC Thermal Stress Analysis

Chapter A.4 presents the results of the thermal analyses of the 24PT4-DSC for the same ambient temperature conditions, summarized in Table 3.1-8, as the 24PT1-DSC.

The Chapter A.4 temperature distributions are imposed onto the ANSYS models described in Section A.3.6.1.1.2 to evaluate thermal stresses.

The Chapter A.4 results show that similar to the 24PT1-DSC, the thermal gradients in the shell are primarily along the axial and tangential directions of the 24PT4-DSC. No significant thermal gradients exist through the wall of the 24PT4-DSC. Stresses resulting from thermal gradients are classified as secondary stresses and are evaluated for Service Level A and B conditions. Maximum shell stress intensities resulting from the thermal stress analyses are summarized in Table A.3.6-2.

The evaluation for potential interferences due to differential thermal expansion between the 24PT4-DSC shell assembly and the basket assembly components is presented in Section A.3.4.4.2.

A.3.6.1.1.6 24PT4-DSC Operational and Transfer Handling Load Analysis

Stress analyses are performed for two categories of transfer and handling loads: (1) inertial loads associated with moving the 24PT4-DSC (on-site transfer handling loads) and (2) loads associated with loading the 24PT4-DSC into, and unloading the 24PT4-DSC from, the AHSM.

A.3.6.1.1.6.1 24PT4-DSC Onsite Transfer Handling Loads

Transfer handling loads are inertial loads on the loaded 24PT4-DSC resulting from on-site handling and transfer between the fuel handling/loading area and the ISFSI. The inertial conditions during transfer discussed in Section 3.1.2.1.3.4 for the 24PT1-DSC also apply to the 24PT4-DSC. The fuel and guidesleeve assemblies are assumed to bear against the inner bottom (or top) plates during axial handling loads.

The controlling stresses from these analyses are tabulated in Table A.3.6-2.

A.3.6.1.1.6.2 24PT4-DSC Loading/Unloading into AHSM

To load the 24PT4-DSC into the AHSM, the 24PT4-DSC is pushed out of the TC using a hydraulic ram. The applied force from the hydraulic ram, specified in Section 3.1.2.1.3.4, is applied to the center of the 24PT4-DSC outer bottom cover plate. The ANSYS finite element model shown in Figure A.3.6-2 is used to calculate the stresses in the 24PT4-DSC shell assembly.

To unload the AHSM, the 24PT4-DSC is pulled using grapples that fit into the grapple ring. For analysis of grapple pull loading, the 180° ANSYS finite element model of the bottom half 24PT4-DSC assembly is used. The load is applied to the grapple ring plate nodes corresponding to the contact area between the ram grapple arms and the grapple ring plate. The stresses in the 24PT4-DSC outer bottom cover plate and grapple ring resulting from the 24PT4-DSC retrieval load are evaluated.

The controlling stress intensities from these analyses are tabulated in Table A.3.6-2.

A.3.6.1.1.7 Cask Drop

Drop loads are applied as static loads corresponding to the postulated drop accelerations. Drops are postulated for the 24PT4-DSC when positioned inside the TC. A 75g side drop and a 25g corner drop (at 30° from horizontal) are postulated for the 24PT4-DSC. The load path for the postulated side drop is identical to that described in Section A.3.6.1.1.3 for dead weight in a horizontal position.

The controlling stress intensities for the 75g side drop are tabulated in Table A.3.6-3. The 25g corner drop is considered to be bounded by the 75g horizontal drop and the 60g 10CFR 50 and 10CFR 71 end drop.

A.3.6.1.1.8 Seismic Analysis

Seismic analysis of the 24PT4-DSC shell assembly is performed using a procedure similar to that used for on-site transfer loads. Controlling stress intensities are tabulated in Table A.3.6-3.

A.3.6.1.1.9 Summary Discussion of the 24PT4-DSC Stress Analyses Results

The calculated stresses for each load case are combined in accordance with the load combinations presented in Table A.3.6-1. The maximum calculated 24PT4-DSC shell assembly stress intensities for normal, off-normal, and accident load combinations are shown in Table A.3.6-4 through Table A.3.6-6.

A.3.6.1.2 24PT4-DSC Basket Assembly Structural Analysis

A.3.6.1.2.1 Loads and Load Combinations for the Basket Assembly

The detailed load combinations for the 24PT4-DSC are presented in Table A.3.6-1.

A.3.6.1.2.2 Stress Analysis of the Guidesleeve Assemblies

The guidesleeve assemblies consist of guidesleeve tubes, oversleeves, and shim plates, all fabricated from SA-240, Type 304 stainless steel. In addition, neutron absorber plates are sandwiched between the guidesleeves and oversleeves. Depending on its location in the basket, each guidesleeve assembly contains either two or four neutron absorber plates such that there are two absorber plates between any adjacent SFAs. The neutron absorber plates are not welded or bolted to the stainless steel guidesleeve, but are held in place by the oversleeves and shim plates. The oversleeves and shim plates are welded to the guidesleeves.

The structural component of the guidesleeve assembly is the guidesleeve tube. The neutron absorber plates provide criticality control and no credit is taken for the structural capacity of the neutron absorber plates.

Stress analyses of the guidesleeve assemblies are performed using a combination of closed-form calculations and finite element analyses using an ANSYS model of the guidesleeve. Elastic analyses are used for normal conditions, and elastic-plastic analyses are used for the postulated side drop accident load case.

An enveloping temperature of 700°F is used as the basis for the material properties of the guidesleeve assemblies for all load cases, except: (1) vacuum drying, and (2) AHSM storage with blocked vents, for which an enveloping temperature of 800°F is used (per Table A.4.4-2).

Loads applicable to the guidesleeve analyses include loads due to deadweight, onsite handling, 75g side drop and 25g corner drop accidents, and the inertial loads due to a postulated seismic event. As described in Section A.3.4.4.2, fabrication clearances are provided to allow unrestrained expansion of the guidesleeves in the axial and radial directions. Thus, there are no significant stresses resulting from thermal loads.

Also, the guidesleeve assemblies are not affected by pressure loads or loads associated with loading and unloading the AHSM since they are not attached to the DSC shell or the shield plugs.

Lateral loads on the guidesleeve assemblies are evaluated using an ANSYS [A3.9] model of the guidesleeve. Loads considered include horizontal dead weight, on-site handling, seismic, and the 75g side drop accident, as defined in Section A.3.1.2.1.3. In the ANSYS analyses, the load from the fuel is applied as a uniform pressure on the guidesleeve panels, without taking credit for the structural capacity of the fuel assemblies.

As described in Section A.3.1.2.1.2, for axial loading, stability criteria (discussed in Section 3.1.2.1) are applied to the 24PT4-DSC guidesleeves, in addition to the stress criteria of Table 3.1-4.

Table A.3.6-8 shows a summary of the maximum stresses in the guidesleeves for the load cases analyzed. The stresses in the oversleeve and the shim plates are small compared to the stresses in the guidesleeve tubes; therefore, only the stresses for the guidesleeves are summarized. The results show that the guidesleeve assembly stresses meet the stress criteria from Subsection NG.

A.3.6.1.2.3 Stress Analysis of the Spacer Discs

The stress analysis of the spacer discs is performed using 3-D finite element models developed using the ANSYS program [A3.9]. Results from three basic model types are used in the stress qualification of the 24PT4-DSC spacer discs: (1) a half-symmetry (180°) model and a full symmetry (360°) model used for analyzing in-plane loads, (2) a quarter-symmetry (90°) model for analyzing out-of-plane loads, and, (3) a half-symmetry (180°) model for analyzing thermal loads.

Typical in-plane models are shown in Figure A.3.6-4 and Figure A.3.6-5. The in-plane models are used for the horizontal dead weight and horizontal side drop analyses. Included in the model are the spacer disc, 24PT4-DSC shell, TC rails, and inner liner of the TC. The interfaces between these components are modeled using contact elements, with the inner liner of the TC being the outer boundary for the system. The spacer disc, shell, and cask rails are modeled using 3D solid elements (Solid45). The half symmetry (180°) model is used for analyzing symmetric loads, such as horizontal dead weight and the 0° side drop case. The full symmetry (360°) model is used for the 18.5° and 45° side drop cases. The fuel and guidesleeve loads are applied to the spacer disc ligaments as pressure loads.

The out-of-plane model is a 90° (quarter-symmetry) model developed using ANSYS Shell43 elements. A typical model is shown in Figure A.3.6-6. The out-of-plane model is used for the vertical dead weight and end drop analyses. The fuel does not load the spacer discs out of plane; therefore, no fuel loads are applied to the spacer disc. Analyses were performed modeling the connection between the spacer disc and the support rod as both pinned and fixed to determine bounding spacer disc stresses.

The 24PT4-DSC spacer discs are evaluated using the criteria from Subsection NG. The normal and off-normal conditions include vertical and horizontal dead weight, transfer handling, and thermal loads during transfer and storage. Accident loads include the 75g accelerations due to the accidental horizontal drop of the cask and seismic loads due to the design basis earthquake. The spacer discs are not affected by pressure loads.

Thermal stresses are analyzed using a 180° half-symmetry model. The thermal model includes the spacer disc only. The thermal stress analyses are conservatively based on temperature distributions that bound those from the Chapter A.4 thermal analyses. The stress analysis includes the thermal gradients in the plane of the spacer disc, with no gradient through the thickness of the discs.

With the exception of thermal loads, all loads on the spacer discs (e.g., inertial loads, fuel loads) are evaluated and combined within the ANSYS analyses. As required for normal and off-normal conditions, thermal and “non-thermal” loads are combined as follows.

1. For out-of-plane loads, evaluated with the Shell43 models described above, stress intensities at the mid-thickness of the element are classified as general membrane stress, P_m . Stress intensities at the element surfaces (top and bottom) are classified as primary membrane plus bending, $P_m + P_b$. These values are used directly in the compliance evaluations of primary stress.

2. For in-plane loads, evaluated with the Solid45 models described above, stresses are linearized (using ANSYS) across the ligaments at the edges of the fuel cutouts and at critical locations between the fuel cutouts and the outside edge of the spacer disc. The results are classified as P_m and $P_m + P_b$ and are used in the Code compliance evaluations of primary stress.
3. Results from the thermal stress analyses are also linearized across the ligaments at the edges of the fuel cutouts and at critical locations between the fuel cutouts and the outside edge of the spacer disc. The results are classified as secondary membrane and secondary membrane plus bending stress intensities. These stress intensities are classified as secondary (Q).
4. To determine the primary plus secondary stress, the maximum non-thermal membrane plus bending stress intensities ($P_m + P_b$) are combined absolutely with the maximum thermal stress intensities. Since the primary stress intensities ($P_m + P_b$) for the normal loads combinations are typically small, the maximum primary stresses are typically combined with the maximum secondary stresses even though the maximums may occur at different locations in the spacer disc.

The horizontal and vertical deadweight stress intensities are based on the 24PT1-DSC spacer disc analyses. This is acceptable because these are linear-elastic analyses and the differences in elastic modulus between the 24PT1-DSC and the 24PT4-DSC spacer disc material is negligibly small (i.e., 1.0% or less). Stress intensities for the transfer handling cases are computed by scaling stress intensities from the deadweight analyses. The stress checks for handling loads are used to envelop the horizontal deadweight stresses.

For the vacuum drying, horizontal deadweight (combined with thermal), and handling (combined with thermal) analyses, the primary plus secondary stress intensity exceeds $3S_m$ in localized section(s) of the spacer disc. For these locations, qualification is demonstrated using the simplified elastic-plastic analysis methodology of NG-3228.3. NG-3228.3 allows the $3S_m$ limit on primary plus secondary stress to be exceeded provided limits on thermal membrane stress and alternating stresses are satisfied. Additional justification for the acceptability of these stresses is obtained by reviewing a breakdown of the stress. Stresses from thermal gradients across the spacer disc are the most significant part of the primary plus secondary stress in the spacer discs (compare $(P_m + P_b)$ to $(P_m + P_b + Q)$ in Table A.3.6-7). During the transfer and AHSM storage operations, the maximum difference in primary plus secondary stress intensity, for any location on the disc, is about 10.0 ksi from the extreme cold case (-40°F) to the extreme hot case (117°F). Thus the most significant part of the combined $(P_m + P_b + Q)$ stress is a 'one time' initial heatup, followed by cool down over the life of the 24PT4-DSC. The alternating portion of the stress is small, much less than $2S_y$ or $3S_m$, and stresses will "shake down" to elastic action. Thus the secondary stresses in the spacer discs are acceptable.

For the accident side drop analyses, elastic-plastic stress analyses are performed using the in-plane model with a plastic modulus equal to 5% of the elastic modulus. These analyses are based on a spacer disc tributary weight of 2431.5 lbs. Three drop orientations are considered: 0°, 18.5° (directly on the cask rail), and 45°. Results for the drop analyses (enveloping 60g end drop and 75g side drop) are summarized in Table A.3.6-7.

The stress intensities due to seismic loading are enveloped by the 75g side drops and enveloping 60g end drops.

In addition to the stress analyses, an analysis is performed to demonstrate the stability of the spacer discs under in-plane loading. This analysis uses the full-symmetry (360°) in-plane ANSYS model with the spacer disc modeled using SHELL 43 elements to account for both in-plane and out-of plane response of the spacer disc. With the spacer disc loaded by the 75g side drop loads and the thermal loads producing the highest compressive stresses (-40°F in the TC) an eigen value buckling analysis is performed to determine the margin to buckling. The margin (factor of safety) against elastic instability is calculated as 1.70, which meets the stability criteria specified in Section 3.1.2.1.2.

As shown in Table A.3.6-7, the spacer disc stresses are acceptable for all normal, off-normal and postulated accident conditions.

A.3.6.1.2.4 Stress Analysis of the Support Rod/Spacer Sleeve Assemblies

The 24PT4-DSC support rod assemblies, including the support rods, spacer sleeves and support rod to spacer sleeve mechanical connections, are analyzed using the criteria of Subsection NF and Appendix F for linear component supports. The criteria of NF-3322.1(e)(1) and F-1334.5 for combined axial compression and bending are applied to the spacer sleeves. The (tension only) rods are evaluated using the criteria of NF-3322.1(a) and F-1334.1.

The support rod assemblies are designed to meet the allowables for all applicable load combinations for preloads varying from 0 to 65 kips. Support rod temperatures are less than 600°F for all conditions except the (accident) blocked vent storage transient which is limited to 650°F (see Chapter A.4).

For the support rod assembly, the load combinations listed in Table A.3.1-3 are simplified by the following:

- (a) the support rod assemblies are unaffected by pressure loads,
- (b) the support rods are unaffected by loading/unloading the 24PT4-DSC, and
- (c) thermal expansion of the support rod assemblies is not constrained by the 24PT4-DSC cavity.

Accident conditions that affect the support rods are the postulated 75g horizontal drop and 25g corner drop, and the postulated seismic events. The basket assembly components have also been evaluated for the effects of the 10CFR 71 60g end drops. The 25g corner drop is considered to be bounded by the 75g horizontal and the 60g 10CFR 71 end drops. As noted in Section 11, the 60g end drop is not a credible event for on-site (i.e., 10CFR 72) operation of the Advanced NUHOMS[®] System.

The spacer sleeves are loaded in compression by the support rod preload and in compression and bending by the spacer discs.

The analyses of the spacer sleeves are performed using a combination of closed-form calculations and ANSYS [A3.9] finite element analyses.

For loads along the axis of the 24PT4-DSC (e.g., vertical deadweight), the load distributions in the support rod assemblies are evaluated using a simple ANSYS beam model. The model includes the support rods and spacer sleeves with the moment and axial force from each spacer disc applied to the assembly. The stress checks for the spacer sleeves are performed using the interaction equations of NF-3322.1(e)(1).

Table A.3.6-9 summarizes the results for the critical load combinations.

The threaded spacer sleeve mechanical connections are designed to maintain the geometry of the support rod assemblies. A mechanical pin at the bottom spacer sleeve may be used to prevent the bottom spacer sleeve from loosening. To prevent the top spacer sleeve from rotating, a double nut design is used. The outer nut at the top end of the support rod assembly is installed as a "Jam" nut.

As shown in Table A.3.6-9, the support rod assembly stresses meet ASME Code allowables.

A.3.6.1.2.5 Stress Analysis of the Failed Fuel Cans

Failed fuel cans are used to provide confinement for "damaged" fuel assemblies. Since the wall thickness of the Failed Fuel Cans is the same as the thickness of the guidesleeve tubes, the failed fuel can stresses are the same as the guidesleeve stresses. Thus, no specific analysis is presented for the Failed Fuel Cans.

A.3.6.1.3 Fatigue Evaluation

No change.

A.3.6.2 Structural Analysis of the AHSM

The structural evaluations of the AHSM are based on a canister weight of 85,000 lbs. This weight bounds the 24PT4-DSC. Thus, the structural evaluations for the AHSM presented in Section 3.6.2 are applicable to the 24PT4-DSC.

**Table A.3.6-1
24PT4-DSC On-Site Load Combinations**

	Horizontal DW		Vertical DW		Internal Pressure ⁽⁸⁾	External Pressure	Thermal Condition	Lifting Loads	Other Loads	Service Level
	DSC	Fuel	DSC	Fuel						
NON-OPERATIONAL LOAD CASES										
NO-1 Fabrication Leak Testing	—	—	—	—	—	14.7 psi	70°F	—	310 kip axial	Test
NO-2 Fabrication Leak Testing	—	—	—	—	24 psi	—	70°F	—	310 kip axial	Test
NO-3 DSC Uprighting	X	—	—	—	—	—	70°F	X	—	A
NO-4 DSC Vertical Lift	—	—	X	—	—	—	70°F	X	—	A
FUEL LOADING LOAD CASES										
FL-1 DSC/Cask Filling	—	—	Cask	—	—	Hydrostatic	120°F Cask	—	—	A
FL-2 DSC/Cask Filling	—	—	Cask	—	Hydrostatic	Hydrostatic	120°F Cask	—	—	A
FL-3 DSC/Cask Transfer	—	—	Cask	—	Hydrostatic	Hydrostatic	120°F Cask	—	—	A
FL-4 Fuel Loading	—	—	Cask	X	Hydrostatic	Hydrostatic	120°F Cask	—	—	A
FL-5 Transfer to Decon	—	—	Cask	X	Hydrostatic	Hydrostatic	120°F Cask	—	—	A
FL-6 Inner Cover Plate Welding	—	—	Cask	X	Hydrostatic	Hydrostatic	120°F Cask	—	—	A
FL-7 Fuel Deck Seismic Loading	—	—	Cask	X	Hydrostatic	Hydrostatic	120°F Cask	—	Note 9	C
DRAINING & DRYING LOAD CASES										
DD-1 DSC Blowdown	—	—	Cask	X	Hydrostatic+20 psi	Hydrostatic	120°F Cask	—	—	B
DD-2 Vacuum Drying	—	—	Cask	X	0 psia	Hydrostatic+14.7 psia	120°F Cask	—	—	B
DD-3 Helium Backfill	—	—	Cask	X	12 psig	Hydrostatic	120°F Cask	—	—	B
DD-4 Final Helium Backfill	—	—	Cask	X	3.0 psig	Hydrostatic	120°F Cask	—	—	B
DD-5 Outer Cover Plate Welding	—	—	Cask	X	3.0 psig	Hydrostatic	120°F Cask	—	—	B
TRANSFER TRAILER LOADING										
TL-1 Vertical Transfer to Trailer			Cask	X	≤ 20.0 psig	—	0°F Cask	—	—	A
TL-2 Vertical Transfer to Trailer			Cask	X	≤ 20.0 psig	—	120°F Cask	—	—	A
TL-3 Laydown	Cask	X			≤ 20.0 psig	—	0°F Cask	—	—	A
TL-4 Laydown	Cask	X			≤ 20.0 psig	—	120°F Cask	—	—	A

	Horizontal DW		Vertical DW		Internal Pressure ⁽⁹⁾	External Pressure	Thermal Condition	Handling Loads	Other Loads	Service Level
	DSC	Fuel	DSC	Fuel						
TRANSFER TO / FROM ISFSI										
TR-1 Axial Load – Cold	Cask	X	—	—	≤ 20.0 psig	—	0°F Cask	1g Axial	—	A
TR-2 Transverse Load – Cold	Cask	X	—	—	≤ 20.0 psig	—	0°F Cask	1g Transverse	—	A
TR-3 Vertical Load – Cold	Cask	X	—	—	≤ 20.0 psig	—	0°F Cask	1g Vertical	—	A
TR-4 Oblique Load – Cold	Cask	X	—	—	≤ 20.0 psig	—	0°F Cask	½ g Axial+½ g Trans+½ g Vert	—	A
TR-5 Axial Load – Hot	Cask	X	—	—	≤ 20.0 psig	—	104°F Cask	1g Axial	—	A
TR-6 Transverse Load – Hot	Cask	X	—	—	≤ 20.0 psig	—	104°F Cask	1g Transverse	—	A
TR-7 Vertical Load – Hot	Cask	X	—	—	≤ 20.0 psig	—	104°F Cask	1g Vertical	—	A
TR-8 Oblique Load – Hot	Cask	X	—	—	≤ 20.0 psig	—	104°F Cask	½ g Axial+½ g Trans+½ g Vert	—	A
TR-12 Top End Drop	This drop is not credible for the horizontal NUHOMS® system.									
TR-9 Bottom End Drop	This drop is not credible for the horizontal NUHOMS® system.									
TR-10 Side Drop	Note 1	—	—	—	≤ 20.0 psig	—	104°F Cask ⁽²⁾		75G drop ⁽¹⁾	D
TR-11 Corner Drop	Note 1	—	—	—	≤ 20.0 psig	—	104°F Cask ⁽²⁾		25g Drop ⁽¹⁾⁽⁵⁾	D

See the following page for Notes.

**Table A.3.6-1
24PT4-DSC On-Site Load Combinations
(Concluded)**

	Horizontal DW		Vertical DW		Internal Pressure ⁽⁸⁾	External Pressure	Thermal Condition	Handling Loads	Other Loads	Service Level
	DSC	Fuel	DSC	Fuel						
AHSM LOADING										
LD-1 Normal Loading – Cold	Cask	X	—	—	≤ 20.0 psig	—	0°F Cask	+60 kip ⁽¹⁰⁾	—	A
LD-2 Normal Loading – Hot	Cask	X	—	—	≤ 20.0 psig	—	104°F Cask	+60 kip ⁽¹⁰⁾	—	A
LD-3 Off-Normal Loading – Cold	Cask	X	—	—	≤ 20.0 psig	—	0°F Cask	+80 kip ⁽¹⁰⁾	10% Failed Fuel	B
LD-4 Off-Normal Loading – Hot	Cask	X	—	—	≤ 20.0 psig	—	117°F Cask	+80 kip ⁽¹⁰⁾	10% Failed Fuel	B
AHSM STORAGE										
HSM-1 Normal Storage – Cold	HSM	X	—	—	≤ 20.0 psig	—	0°F HSM	—	—	A
HSM-2 Normal Storage – Hot	HSM	X	—	—	≤ 20.0 psig	—	104°F HSM	—	—	A
HSM-3 Off-Normal Storage – Cold	HSM	X	—	—	≤ 20.0 psig	—	-40°F HSM	—	10% Failed Fuel	B
HSM-4 Off-Normal Storage – Hot	HSM	X	—	—	≤ 20.0 psig	—	117°F HSM	—	10% Failed Fuel	B
HSM-5 Off-Normal Storage/Outer-Cold	HSM	X	—	—	≤ 20.0 psig	—	-40°F HSM	—	10% Failed Fuel	B
HSM-6 Off-Normal Storage/Outer-Ho	HSM	X	—	—	≤ 20.0 psig	—	117°F HSM	—	10% Failed Fuel	B
HSM-7 .38g EQ – Cold	HSM	X	—	—	≤ 20.0 psig	—	-40°F HSM	—	.38g EQ+10% FF	Note 11
HSM-8 .38g EQ – Hot	HSM	X	—	—	≤ 20.0 psig	—	117°F HSM	—	.38g EQ+10% FF	Note 11
HSM-9 EQ – Cold	HSM	X	—	—	≤ 20.0 psig	—	-40°F HSM	—	EQ = 10% FF	D
HSM-10 EQ – Hot	HSM	X	—	—	≤ 20.0 psig	—	117°F HSM	—	EQ = 10% FF	D
HSM-11 Blocked Vent Storage	HSM	X	—	—	≤ 100.0 psig	—	117°F HSM/BV ⁽⁴⁾	—	100% Failed Fuel	D
HSM-12 Flood Load (50' H ₂ O) – Cold	HSM	X	—	—	0 psig	22.0 psig ⁽⁹⁾	0°F HSM	—	Flood ⁽³⁾	C
HSM-13 Flood Load (50' H ₂ O) – Hot	HSM	X	—	—	0 psig	22.0 psig ⁽⁹⁾	117°F HSM	—	Flood ⁽³⁾	C

	Horizontal DW		Vertical DW		Internal Pressure ⁽⁸⁾	External Pressure	Thermal Condition	Handling Loads	Other Loads	Service Level
	DSC	Fuel	DSC	Fuel						
AHSM UNLOADING										
UL-1 Normal Unloading – Cold	HSM	X	—	—	≤ 20.0 psig	—	0°F HSM	-60 kip	—	A
UL-2 Normal Unloading – Hot	HSM	X	—	—	≤ 20.0 psig	—	104°F HSM	-60 kip	—	A
UL-3 Off-Normal Unloading – Cold	HSM	X	—	—	≤ 20.0 psig	—	0°F HSM	-60 kip	—	B
UL-4 Off-Normal Unloading – Hot	HSM	X	—	—	≤ 20.0 psig	—	117°F HSM	-60 kip	—	B
UL-5 Accident Unloading – FF/Hot	HSM	X	—	—	≤ 20.0 psig	—	104°F HSM	-80 kip	10% Failed Fuel	C

	Horizontal DW		Vertical DW		Internal Pressure	External Pressure	Thermal Condition	Handling Loads	Other Loads	Service Level
	DSC	Fuel	DSC	Fuel						
DSC UNLOADING / REFLOOD										
RF-1 DSC Reflood	—	—	Cask	X	100.0 ⁽¹²⁾ psig (max)	Hydrostatic	120°F Cask	—	—	D

Notes:

- Drop accelerations include gravity effects. Therefore, it is not necessary to add an additional 1.0g (gravity) load.
- For Level D events, only the maximum temperature case is considered. (Thermal stresses are not limited for Level D events and maximum temperatures result in minimum allowables).
- Flood load is an external pressure equivalent to 50 ft. of water.
- BV = AHSM vents are blocked.
- Corner drop is at 30 degrees from horizontal.
- Not used.
- Not used.
- Normal pressure is based on 1% of fuel rods ruptured, off-normal pressure 10% of rods ruptured, and accident pressure 100% of rods ruptured (see NUREG-1536).
- Fuel deck seismic loads are assumed enveloped by handling loads.
- AHSM insertion loads and internal pressure loads are in opposition.
- Evaluated for fatigue effects on DSC shell components.
- Evaluation performed for 100 psig. However, reflood rate is controlled such that max pressure does not exceed 20 psig during reflood operations.

**Table A.3.6-2
24PT4-DSC Shell Assembly Normal and Off-Normal Operating
Condition Maximum Stress Intensities**

Component	Stress Type	Stress Intensity (ksi) ⁽¹⁾						
		Dead Weight		Normal Internal Pressure	Off-Normal Internal Pressure	Thermal	Normal Handling	Off-Normal Handling
		Vertical	Horiz.					
Shell	Primary Membrane	0.30	1.04	2.62	2.62	N/A	4.13	5.51
	Membrane + Bending	0.65	1.34	11.59	11.59	N/A	16.77	22.26
	Primary + Secondary	N/A	N/A	N/A	N/A	27.78	N/A	N/A
Outer Top Cover Plate	Primary Membrane	0.08	0.74	0.17	0.17	N/A	0.16	N/A
	Membrane + Bending	0.82	0.90	2.14	2.14	N/A	0.82	N/A
	Primary + Secondary	N/A	N/A	N/A	N/A	19.84	N/A	N/A
Inner Top Cover Plate	Primary Membrane	0.22	0.21	2.04	2.04	N/A	0.22	N/A
	Membrane + Bending	0.45	0.41	4.30	4.30	N/A	0.45	N/A
	Primary + Secondary	N/A	N/A	N/A	N/A	18.66	N/A	N/A
Outer Bottom Cover Plate	Primary Membrane	0.42	0.23	1.93	1.93	N/A	16.82	22.43
	Membrane + Bending	0.46	0.45	2.38	2.38	N/A	23.65	31.54
	Primary + Secondary	N/A	N/A	N/A	N/A	18.12	N/A	N/A
Inner Bottom Cover Plate	Primary Membrane	0.11	0.23	0.34	0.34	N/A	2.72	3.63
	Membrane + Bending	0.21	0.25	5.0	5.0	N/A	9.65	12.89
	Primary + Secondary	N/A	N/A	N/A	N/A	24.73	N/A	N/A
Support Ring	Primary Membrane	0.05	0.15	0.89	0.89	N/A	0.07	N/A
	Membrane + Bending	0.07	0.23	0.95	0.95	N/A	0.10	N/A
	Primary + Secondary	N/A	N/A	N/A	N/A	3.12	N/A	N/A

Note:

1. Values shown are maximum irrespective of location.

**Table A.3.6-3
24PT4-DSC Shell Assembly Accident Condition Maximum Stress Intensities**

Component	Stress Type	Stress Intensity (ksi) ⁽¹⁾			
		Flood	Seismic	75g Side Drop	Accident Pressure
Shell	Primary Membrane	9.49	9.02	38.54	13.37
	Membrane + Bending	19.47	13.93	43.75	57.29
Outer Top Cover Plate	Primary Membrane	4.76	6.35	37.60	0.85
	Membrane + Bending	26.87	9.01	47.91	10.77
Inner Top Cover Plate	Primary Membrane	0.3	2.22	11.45	10.27
	Membrane + Bending	0.67	4.40	17.46	21.53
Outer Bottom Cover Plate	Primary Membrane	12.58	3.68	18.72	9.43
	Membrane + Bending	16.69	5.54	22.12	11.60
Inner Bottom Cover Plate	Primary Membrane	0.16	2.06	21.29	1.69
	Membrane + Bending	1.01	3.87	22.56	25.31
Support Ring	Primary Membrane	0.77	1.34	21.53	4.47
	Membrane + Bending	0.85	2.04	26.96	4.75

Note:

1. Values shown are maximum irrespective of location.

Table A.3.6-4
24PT4-DSC Shell Assembly Results for Normal and Off-Normal Load Combinations

Component	Stress Type	Controlling Load Combination	Stress Intensity (ksi) ⁽¹⁾		Stress Ratio
			Calculated	Allowable	
Shell	Primary Membrane	LD-3/LD-4	6.55	17.00	0.39
	Membrane + Bending	UL-3/UL-4	18.11	25.50	0.71
	Primary + Secondary	LD-3	44.01	51.00	0.86
Outer Top Cover Plate	Primary Membrane	TR-4/TR-8	1.73	17.00	0.10
	Membrane + Bending	TR-8	4.35	25.50	0.17
	Primary + Secondary	TR-8	24.19	51.00	0.47
Inner Top Cover Plate	Primary Membrane	TR-4/TR-8	2.57	17.00	0.15
	Membrane + Bending	TR-4/TR-8	5.35	25.50	0.21
	Primary + Secondary	TR-8	24.01	51.00	0.47
Outer Bottom Cover Plate	Primary Membrane	UL-4	18.12	18.60	0.97
	Membrane + Bending	UL-4	24.15	28.00	0.86
	Primary + Secondary	LD-3	38.02	51.00	0.75
Inner Bottom Cover Plate	Primary Membrane	LD-3/LD-4	3.86	17.00	0.23
	Membrane + Bending	LD-3/LD-4	13.14	25.50	0.52
	Primary + Secondary	LD-4	37.87	51.00	0.74
Support Ring	Primary Membrane	TR-4/TR-8	1.23	16.4	0.07
	Membrane + Bending	TR-4/TR-8	1.46	24.60	0.06
	Primary + Secondary	TR-4	4.58	49.2	0.09

Note:

1. Values shown are maximum irrespective of location.

**Table A.3.6-5
24PT4-DSC Shell Assembly Results for Accident Level C Load Combinations**

Component	Stress Type	Controlling Load Combination	Stress Intensity (ksi) ⁽¹⁾		Stress Ratio
			Calculated	Allowable	
Shell	Primary Membrane	HSM-13	10.53	20.4	0.52
	Membrane + Bending	UL-5	23.60	30.6	0.77
	Primary + Secondary	N/A	N/A	N/A	N/A
Outer Top Cover Plate	Primary Membrane	HSM-13	5.62	20.4	.28
	Membrane + Bending	HSM-13	31.67	32.6	.97
	Primary + Secondary	N/A	N/A	N/A	N/A
Inner Top Cover Plate	Primary Membrane	HSM-13	0.51	20.4	0.03
	Membrane + Bending	HSM-13	1.08	30.6	0.04
	Primary + Secondary	N/A	N/A	N/A	N/A
Outer Bottom Cover Plate	Primary Membrane	UL-5	22.29	22.9	0.97
	Membrane + Bending	UL-5	28.79	34.2	0.84
	Primary + Secondary	N/A	N/A	N/A	N/A
Inner Bottom Cover Plate	Primary Membrane	UL-5	2.74	20.4	0.13
	Membrane + Bending	UL-5	7.06	30.6	0.23
	Primary + Secondary	N/A	N/A	N/A	N/A
Support Ring	Primary Membrane	HSM-13	0.92	19.7	0.05
	Membrane + Bending	HSM-13	1.08	29.5	0.04
	Primary + Secondary	N/A	N/A	N/A	N/A

Note:

1. Values shown are maximum irrespective of location.

**Table A.3.6-6
24PT4-DSC Shell Assembly Results for Accident Level D Load Combinations**

Component	Stress Type	Controlling Load Combination	Stress Intensity (ksi) ⁽¹⁾		Stress Ratio
			Calculated	Allowable	
Shell	Primary Membrane	TR-10	37.83	50.20	0.75
	Membrane + Bending	HSM-11	59.08	61.20	0.97
Outer Top Cover Plate	Primary Membrane	TR-10	37.60	50.20	0.75
	Membrane + Bending	TR-10	47.90	64.60	0.74
Inner Top Cover Plate	Primary Membrane	HSM-11	10.55	40.8	0.26
	Membrane + Bending	TR-9	27.95	64.60	0.43
Outer Bottom Cover Plate	Primary Membrane	TR-9	23.30	50.20	0.46
	Membrane + Bending	TR-9	27.58	64.6	0.43
Inner Bottom Cover Plate	Primary Membrane	TR-10	21.49	50.20	0.43
	Membrane + Bending	TR-12	29.51	64.60	0.46
Support Ring	Primary Membrane	TR-10	21.53	44.50	0.48
	Membrane + Bending	TR-10	26.96	57.20	0.47

Note:

1. Values shown are maximum irrespective of location.

**Table A.3.6-7
Summary of Spacer Disc Maximum Stress Ratios**

Loading	Service Level	Stress Classification	Stress Intensity (ksi)	Allowable Stress ⁽²⁾ (ksi)	Maximum Stress Ratio
Vertical Dead Weight ⁽⁵⁾	A	P_m	0.35	26.7	0.02
	A	P_m+P_b	1.41	40.1	0.04
Vacuum Drying (DD-2) at Perimeter ⁽⁶⁾	B	P_m+P_b+Q	97.0	Note 1	Note 1
Vacuum Drying (DD-2) at Ligament ⁽⁶⁾	B	P_m+P_b+Q	34.0	80.1	0.42
Horizontal Dead Weight & HSM Storage (HSM-1 through HSM-4)	A/B	P_m	Enveloped by Handling		
	A/B	P_m+P_b			
	A/B	P_m+P_b+Q			
Handling (TR-1 through TR-8) ⁽⁷⁾	A	P_m	4.9	26.7	0.18
	A	P_m+P_b	17.4	40.1	0.43
At Perimeter ⁽⁸⁾	A	P_m+P_b+Q	85.6	Note 1	Note 1
	A	P_m+P_b+Q	35.7	80.1	0.45
End Drop ⁽⁴⁾ (TR-9)	D	P_m	20.2 ⁽⁹⁾	56.0	0.36
	D	P_m+P_b	61.6 ⁽⁹⁾	72.0	0.86
0° Side Drop	D	P_m	53.4	56.0	0.95
	D	P_m+P_b	67.4	72.0	0.94
18.5° Side Drop	D	P_m	52.9	56.0	0.94
	D	P_m+P_b	69.4	72.0	0.96
45° Side Drop	D	P_m	46.6	56.0	0.83
	D	P_m+P_b	69.0	72.0	0.96
Seismic (HSM-9 and HSM-10)	D	P_m	Enveloped by Drops ⁽³⁾		
	D	P_m+P_b			

Notes:

1. Qualification is based on the simplified elastic-plastic analysis methodology of NG-3228.3.
2. Stress allowables are based on the spacer disc maximum temperature.
3. The SRSS resultant of 6g's in each orthogonal direction is 10.4g. Therefore, the level D earthquake is bounded by the 75g side drop and enveloping 60g end drop.
4. The 60g end drop is not a credible event for the 10CFR72 license. However, it is included as a bounding result for other load conditions such as the 25g corner drop and the level D seismic load.
5. Stress intensity results for the 24PT1-DSC are used for this load case.
6. Stress intensity results are based on maximum temperatures and temperature gradients that bound the Chapter A.4 temperatures.
7. Stress intensity results for the 24PT1-DSC are used for these load cases. The maximum tributary weight corresponds to a spacer disc in the active fuel region. The 24PT4-DSC spacer disc tributary weight of 2431.5 lbs is bounded by the 24PT1 spacer disc tributary weight of 2467.5 lbs.
8. The thermal stress component stress intensities are based on maximum temperatures and temperature gradients that bound the Chapter A.4 temperatures.
9. Stresses correspond to 75g end drop.

**Table A.3.6-8
Summary of Guidesleeve Assembly Maximum Stress Ratios**

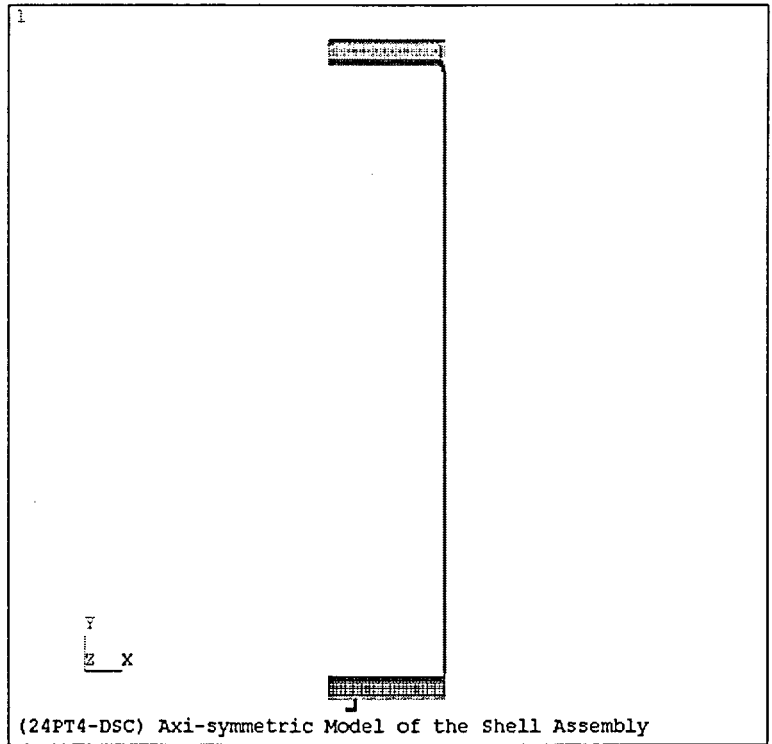
Loading	Service Level	Stress Classification	Stress Intensity (ksi)	Allowable Stress Intensity (ksi)	Maximum Stress Ratio
Vertical Dead Weight	A	f_a	0.11	6.48	0.02
Horizontal Dead Weight	A	P_m	0.09	16.0	.005
	A	P_m+P_b	0.86	24.0	0.04
	A	P_m+P_b+Q	0.86	48.0	0.02
Handling	A	P_m	0.22	16.0	0.01
	A	P_m+P_b	2.16	24.0	0.09
	A	P_m+P_b+Q	2.16	48.0	0.05
	A	f_a	0.28	6.48	0.04
End Drop	D	f_a	6.60	11.0	0.60
Side Drop	D	P_m	8.51	44.5	0.19
	D	P_m+P_b	25.6	57.2	0.45
Seismic	A	P_m	1.04	38.4	0.03
	A	P_m+P_b	10.4	57.6	0.18
	A	f_a	1.32	11.0	0.12

**Table A.3.6-9
Summary of Results for Support Rod Assemblies**

A. Summary of Interaction Ratios in the Spacer Sleeves			
Loading	Service Level	Maximum Interaction⁽²⁾	Allowable
Vertical Dead Weight	A	0.22	1.0
Horizontal Dead Weight	A	0.21	1.0
Handling (Axial)	A	0.24	1.0
Handling (Lateral)	A	0.22	1.0
60g End Drop ⁽⁴⁾	D	0.62	1.0
75g Side Drop	D	0.22	1.0
Seismic	D	Enveloped by Drops	

B. Summary of Support Rod Stresses⁽¹⁾				
Load Combination	Axial Load (Kips)	Axial Stress f_t (ksi)	Allowable Axial Stress F_t (ksi)	Ratio
65K Preload (70°F)	65.0	53.0	54.9 @ 650°F	0.96
65K Preload + 600°F	63.2	51.5	54.9 @ 650°F	0.94
65K Preload + 600°F + 1g	63.0	51.3	54.9 @ 650°F	0.93
65K Preload + 600°F + 60g ⁽⁴⁾	47.5	38.7	92.0 @ 600°F	0.42

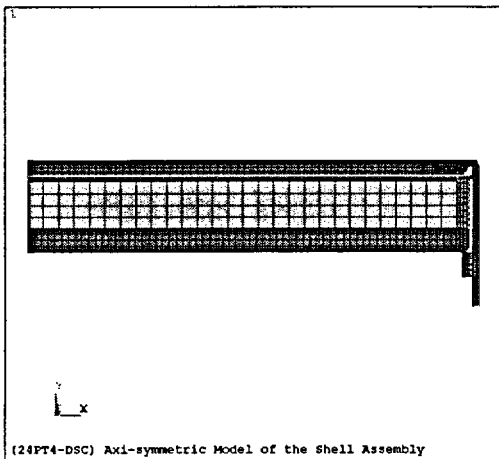
- Notes:**
1. All stresses are calculated using a maximum assembled preload of 65 Kips. Preloads less than 65K are acceptable and will reduce stresses in the support rod assembly. Preload is not required for qualification of the rod assembly.
 2. The reported interaction ratios are the maximum values from Equations 20 through 22 of NF 3322.1(e)(1).
 3. Not used.
 4. End drops are not postulated for on-site operation of the horizontal NUHOMS[®] System. These results are provided to ensure the qualification for postulated 25g 30° corner drop.



ANSYS 5.6.2
 FEB 7 2002
 15:33:23
 PLOT NO. 1
 ELEMENTS
 TYPE NUM

ZV =1
 DIST=109.835
 XF =16.75
 YF =-1.81

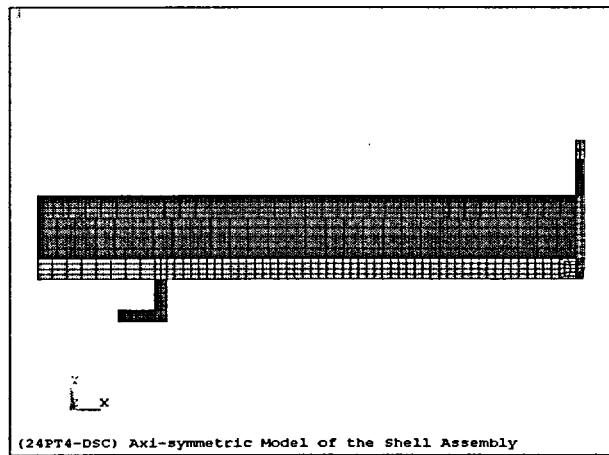
(a) Axi-symmetric Model



ANSYS 5.6.2
 FEB 7 2002
 15:36:49
 PLOT NO. 1
 ELEMENTS
 TYPE NUM

ZV =1
 DIST=18.425
 XF =16.75
 YF =-92.024
 Z-BUFFER

(b) Top End Close-up View

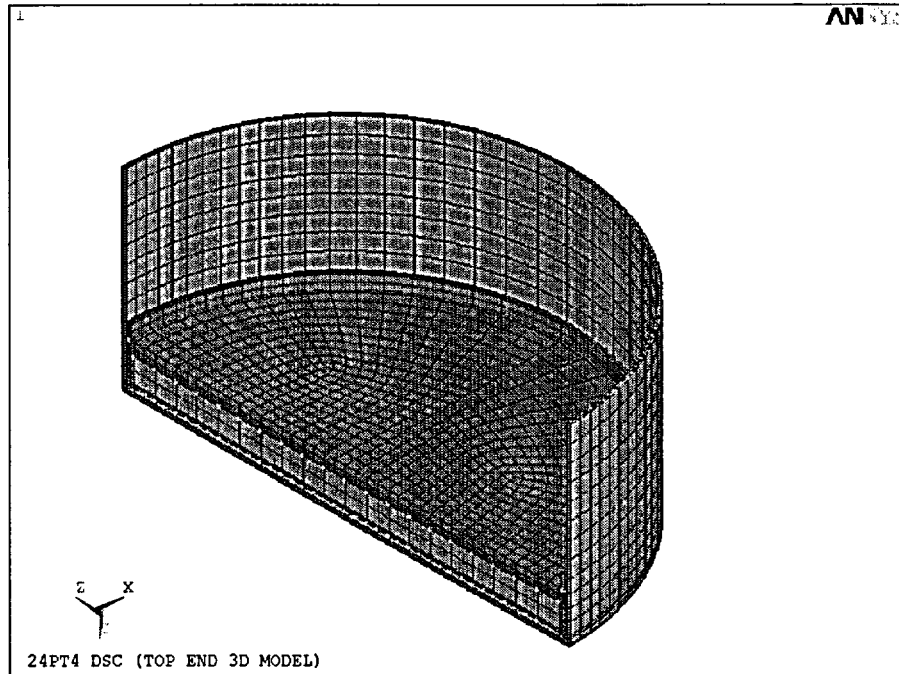


ANSYS 5.6.2
 FEB 7 2002
 15:39:12
 PLOT NO. 1
 ELEMENTS
 TYPE NUM

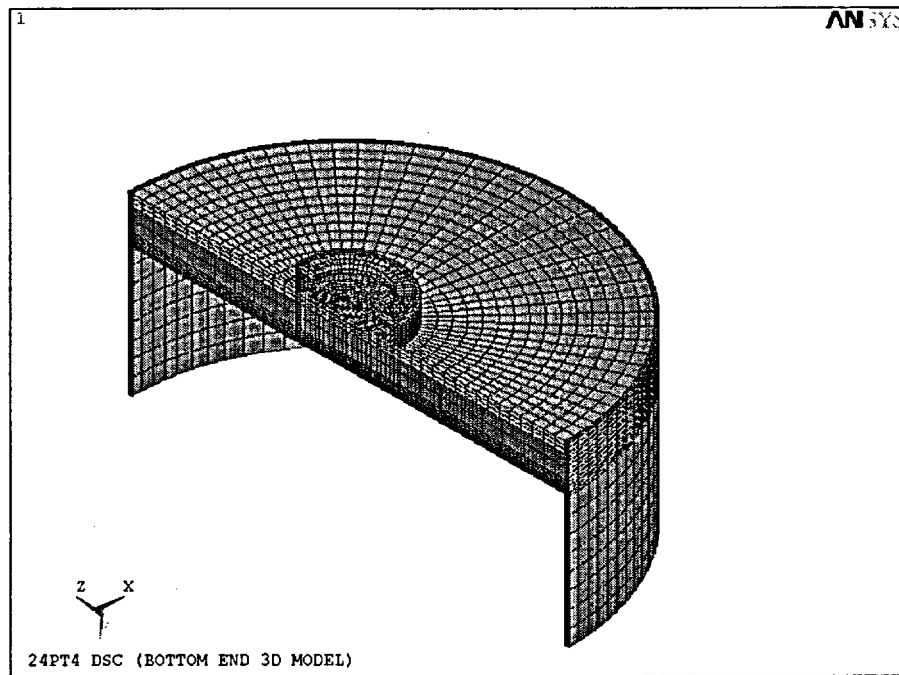
ZV =1
 DIST=18.425
 XF =16.75
 YF =-94.113
 Z-BUFFER

(c) Bottom End Close-up View

Figure A.3.6-1
24PT4-DSC Shell Assembly Axisymmetric Analysis Analytical Model

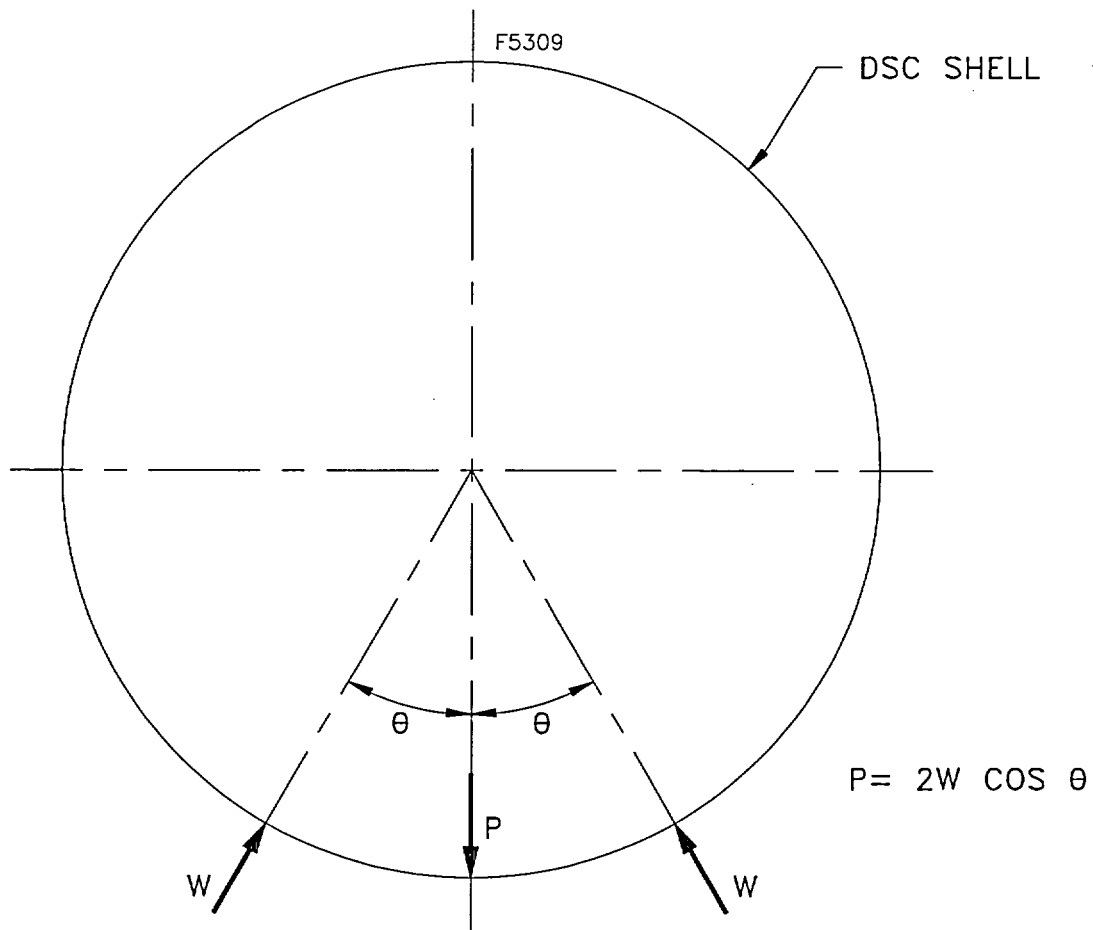


TOP END 3D ANSYS MODEL



BOTTOM END 3D ANSYS MODEL

**Figure A.3.6-2
24PT4-DSC Shell Assembly 3D ANSYS Models**



KEY:
 P= DEAD WEIGHT OF LOADED DSC.
 W= DSC SUPPORT RAIL REACTION.

Figure A.3.6-3
24PT4-DSC Load Support for Shell and Spacer Disc Analyses

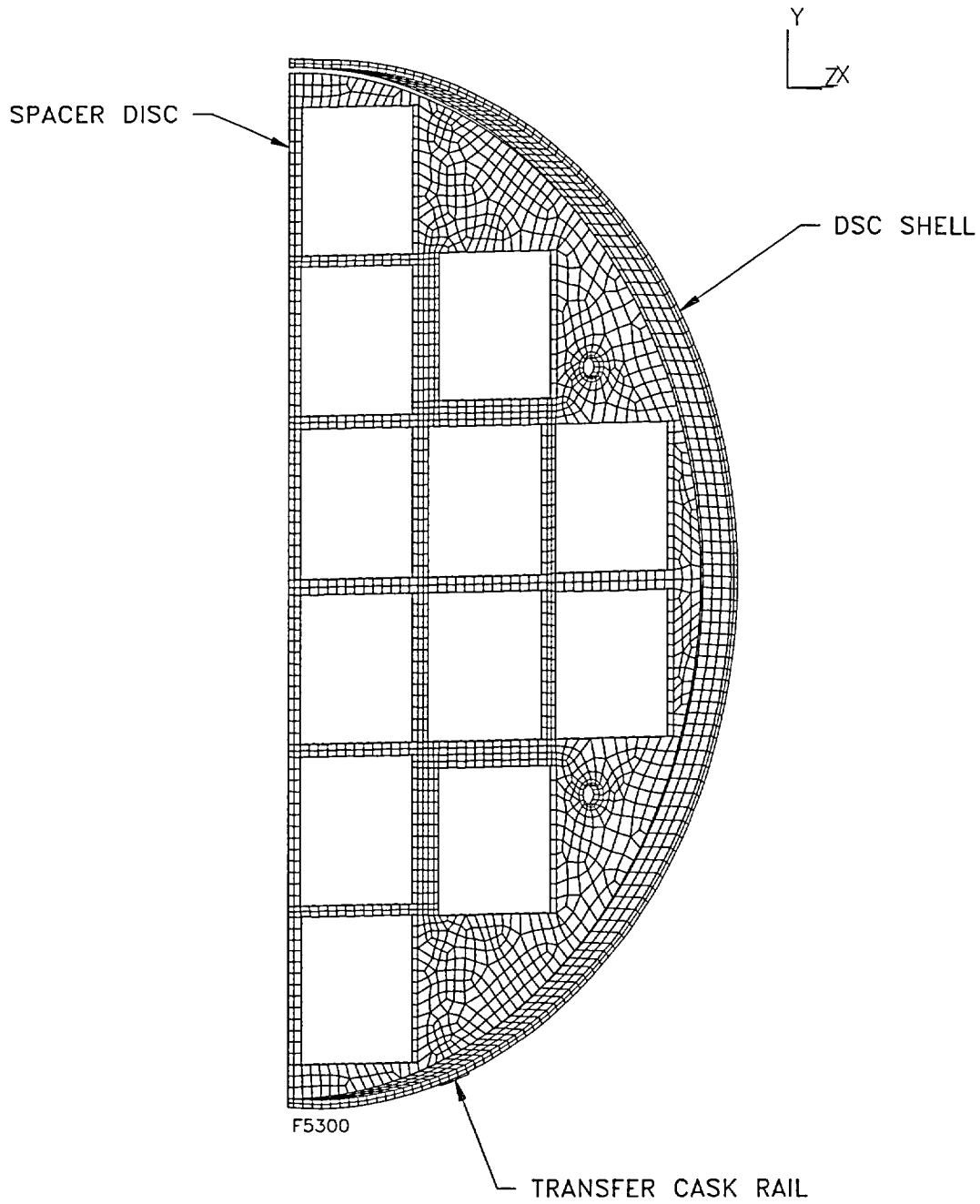


Figure A.3.6-4
Typical 24PT4-DSC Spacer Disc ANSYS Model for In-Plane Loads (Half Symmetry)
(Cask not shown for clarity)

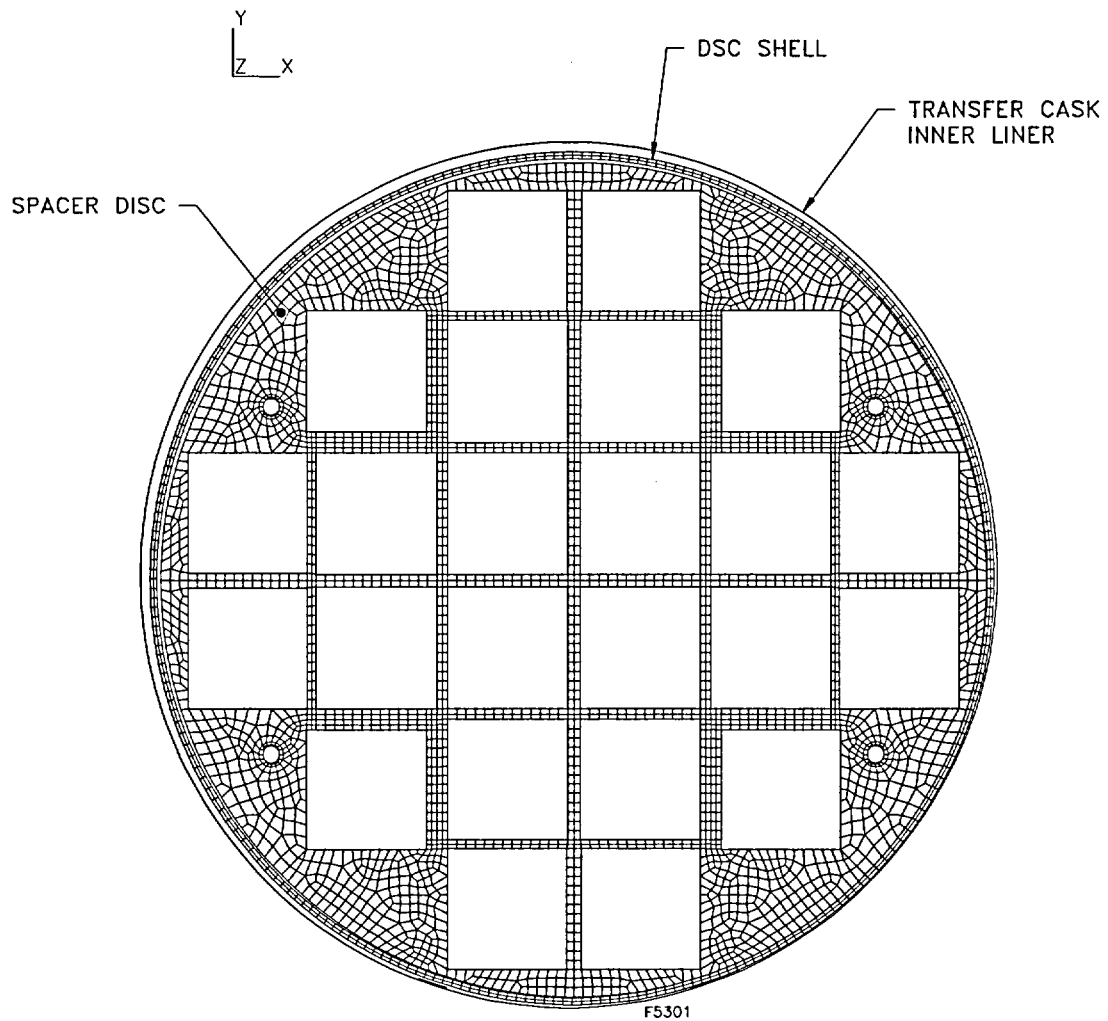


Figure A.3.6-5
Typical 24PT4-DSC Spacer Disc ANSYS Model for In-Plane Loads (Full Symmetry)
(Model shown is for 45° drop orientation)

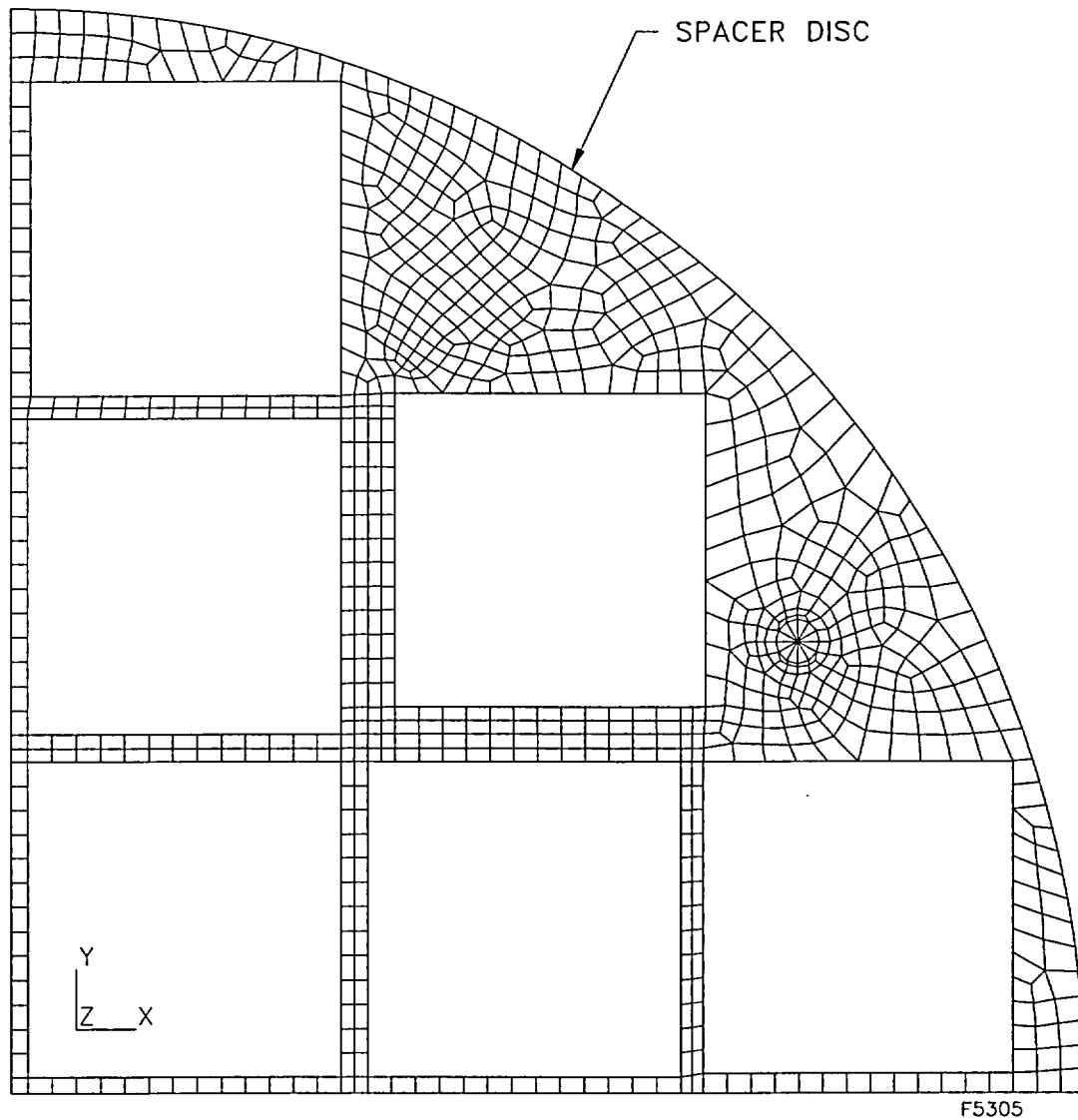


Figure A.3.6-6
Typical 24PT4-DSC Spacer Disc ANSYS Model for Out-of-Plane Loads (Quarter Symmetry)

A.3.7 References

- [A3.1] Nuclear Regulatory Commission, Safety Evaluation Report of Safety Analysis Report for the Standardized NUHOMS® Horizontal Modular Storage System for Irradiated Nuclear Fuel, December 1994, USNRC Docket Number 72-1004.
- [A3.2] American Society of Mechanical Engineers, Boiler & Pressure Vessel Code, Section II, Section III, 1992 Edition with Addenda through 1994 with Code Case N-595-1.
- [A3.3] NRC Spent Fuel Project Office, Interim Staff Guidance, ISG-15, Materials Evaluation.
- [A3.4] American National Standards Institute, ANSI N14.5-1997, Leakage Tests on Packages for Shipment of Radioactive Materials.
- [A3.5] Holman, W.R., Langland, R. T., "Recommendations for Protecting Against Failure by Brittle Fracture in Ferritic Steel Shipping Containers up to Four Inches Thick," NUREG/CR-1815, August 1981.
- [A3.6] Teitz, T. E., "Determination of the Mechanical Properties of a High Purity Lead and a 0.058% Copper-lead Alloy," WADC Technical Report 57-695, ASTIA Document No. 151165, Stanford Research Institute, Menlo Park, CA, April 1958.
- [A3.7] American Society of Mechanical Engineers, *Boiler & Pressure Vessel Code*, Section III, Division 1, Code Case N-499-1, *Use of SA-533 Grade B, Class 1 Plate and SA-508 Class 3 Forgings and their Weldments for Limited Elevated Temperature Service*, Section III, Division 1; Approval Date: December 12, 1994, Reaffirmed October 2, 2000, Expires October 2, 2003.
- [A3.8] Transnuclear, Inc., Final Safety Analysis Report for the Standardized NUHOMS® Horizontal Modular Storage System for Irradiated Nuclear Fuel, Revision 6, October 2001, USNRC Docket Number 72-1004.
- [A3.9] Swanson Analysis Systems Inc., ANSYS Engineering Analysis System User's Manual, Versions 5.3 and 5.6.2, Swanson Analysis Systems, Inc., Pittsburgh, PA.
- [A3.10] Levy, Chin, Simonen, Beyer, Gilbert and Johnson, Recommended Temperature Limits for Dry Storage of Spent Light Water Reactor Zircalloy-Clad Fuel Rods in Inert Gas, May 1987, Pacific Northwest Laboratory, PNL Document PNL-6189.
- [A3.11] Johnson, A. B. and E. R. Gilbert, Technical Basis for Storage of Zircalloy-Clad Spent Fuel in Inert Gas, September 1983, Pacific Northwest Laboratory, PNL Document PNL-4835.
- [A3.12] "Consolidated Safety Analysis Report for IF-300 Shipping Cask", NEDO-10084, Vectra Technologies, Inc., Revision 4, March, 1995.

- [A3.13] UCID – 21246, “Dynamic Impact Effects on Spent Fuel Assemblies,” October 20, 1987.
- [A3.14] Interim Staff Guidance No. 11, Revision 2, “Cladding Considerations for the Transportation and Storage of Spent Fuel”, dated July 30, 2002.

A.4 THERMAL EVALUATION

Sections of this Chapter have been identified as “No change” due to the addition of 24PT4-DSC to the Advanced NUHOMS[®] system. For these sections, the description or analysis presented in the corresponding sections of the FSAR for the Advanced NUHOMS[®] system with 24PT1-DSC is also applicable to the system with 24PT4-DSC.

The 24PT1-DSC results presented in Chapter 4 were developed for a maximum heat load of 14 kW. The 24PT4-DSC is designed for 24 kW and the analyses and results are presented herein.

All AHSM temperature distribution calculations presented in Chapter 4 were generated for 24 kW heat load per DSC, and therefore are not repeated here.

All ambient and accident cases described in Tables 4.1-1 and 4.1-2 are applicable to the 24PT4-DSC when stored within the AHSM and are not repeated here.

This chapter presents the evaluations that demonstrate that the Advanced NUHOMS[®] System with the 24PT4-DSC meets the thermal requirements of 10CFR72 [A4.18]. Thermal analysis methodology for fuel cladding temperature limit criteria is consistent with the guidelines given in ISG-11, Revision 2 [A4.21]. The thermal design and safety evaluation for the AHSM and TC are provided in Chapter 4 of this FSAR. This Chapter builds on those results and provides the thermal evaluation of the 24PT4-DSC. A maximum decay heat load of 24 kW was used for the evaluation of the AHSM (concrete and support steel), the 24PT4-DSC shell assembly, and the basket assembly and fuel cladding.

A.4.1 Discussion

A.4.1.1 Overview and Purpose of Thermal Analysis

The Advanced NUHOMS[®] System is designed to passively reject decay heat under normal and off-normal conditions of storage, and for accident and loading/unloading conditions while maintaining canister temperatures and pressures within specified limits.

To establish the heat removal capability, several thermal design criteria are established for the Advanced NUHOMS[®] System. These are:

- Pressures within the 24PT4-DSC cavity are within design values considered for structural and confinement analyses.
- Maximum and minimum temperatures of the confinement structural components must not adversely affect the confinement function.
- Maximum fuel cladding temperature limit of 400°C (752°F) is applicable to normal conditions of storage, transfer operations from spent fuel pool to ISFSI pad, and all short term operations including vacuum drying and helium backfilling of the 24PT4-DSC per Interim Staff Guidance (ISG) No. 11, Revision 2 [A4.21]. In addition, ISG-11 does not

permit thermal cycling of the fuel cladding with temperature differences greater than 65°C (117°F) during drying and backfilling operations.

- Maximum fuel cladding temperature limit of 570°C (1058°F) is applicable to accidents or off-normal thermal transients [A4.21].
- Thermal stresses for the 24PT4-DSC when appropriately combined with other loads, will be maintained at acceptable levels to ensure the confinement integrity of the Advanced NUHOMS[®] System (see Chapters A3 and A11). Chapter A2 presents the principal design bases for the Advanced NUHOMS[®] System.

Within the canister, the internal basket assembly contains spacer discs, support rods, and guidesleeve assemblies. The guidesleeve assembly consists of a stainless steel guidesleeve and a Boral[®] poison sheet(s) held in place by a thin oversleeve. Heat transfer through the basket structure in the radial direction includes conduction and radiation through the guidesleeve assemblies, spacer disc plates, and the helium cover gas. Heat transfer in the axial direction outside hottest sections between two adjacent spacer discs mid-planes is conservatively neglected in the analysis model.

Three fuel assembly heat load configurations are analyzed to bound those configurations specified in Figures A.2.1-1 through A.2.1-3 and Technical Specifications.

A.4.1.2 Thermal Load Specification/Ambient Temperature

The ambient temperature ranges and the hourly temperature variation for the extreme summer ambient conditions that are considered in the thermal analyses of the 24PT4-DSC are the same as those given in Table 4.1-1 and Table 4.1-2. See Section 4.1.2 for a discussion on the basis for these design temperatures.

The maximum total heat load per DSC is 24 kW (Figures A.2.1-1 and Figure A.2.1-2) or 23.76 kW (Figure A.2.1-3) depending on the specific heat load zoning configurations shown in Chapter A.2. To be conservative, the 24PT4-DSC thermal analysis is based on a maximum heat load of 24 kW from 20 to 24 assemblies. Figure A.4.4-8, Figure A.4.4-9, and Figure A.4.4-10 show the three heat load zoning configurations used in the thermal analysis of the 24PT4-DSC. The maximum heat load per assembly in Configuration #3 of 1.3 kW is higher than the 1.26 kW allowed in Chapter A.2 and 0.8 kW is lower than the 0.9 kW allowed in Chapter A.2. However, use of 1.3 kW and 0.8 kW analyzed here for Configuration #3, results in higher temperatures and differential temperatures, and therefore, is considered as bounding for Configuration #3.

An axial burnup peaking factor for a typical PWR fuel assembly of 1.08 based on Reference [A4.1] is conservatively applied over the entire active fuel length used in the analyses. The parameters of the CE 16x16 fuel assembly type are given in Chapter A.2. A description of the detailed analyses performed for normal conditions is provided in Section A.4.4, off-normal conditions in Section A.4.5, accident conditions in Section A.4.6, and loading/unloading conditions in Section A.4.7. A summary of the results from the analyses performed for normal, off-normal, and accident conditions, as well as maximum and minimum allowable temperatures, is provided in Table A.4.1-1, Table A.4.1-2, and Table A.4.1-3, respectively. The thermal

evaluation concludes that with these heat loads, all design criteria for 24PT4-DSC are satisfied for normal, off-normal, and accident conditions.

The TC was previously licensed for 24 kW [A4.12], which is equal to the maximum heat load of 24 kW for the 24PT4-DSC being licensed in this application. Results are, therefore, not repeated here for the TC.

**Table A.4.1-1
Component Minimum and Maximum Temperatures in the Advanced NUHOMS® System
(Storage or Transfer Mode) for Normal Conditions**

Component		Maximum Storage Mode (°F)	Maximum Transfer Mode (°F)	Minimum ⁽¹⁾ (°F)	Allowable Range (°F) Reference
DSC Shell		399	439	0	0 to 800 [A4.4]
DSC Top Outer Cover Plate		343	464	0	0 to 800 [A4.4]
DSC Top Inner Cover Plate		347	480	0	0 to 800 [A4.4]
DSC Top Plug		346	475	0	0 to 620 [A4.14]
DSC Bottom Plug		412	500	0	0 to 620 [A4.14]
DSC Bottom Inner Cover Plate		418	511	0	0 to 800 [A4.4]
DSC Bottom Outer Cover Plate		402	484	0	0 to 800 [A4.4]
DSC Spacer Disc		650	692	0	0 to 1000 [A4.4]
DSC Guidesleeve or FF Cans		652	694	0	0 to 800 [A4.4]
DSC Oversleeve		652	694	0	0 to 800 [A4.4]
DSC Support Rod/Spacer Sleeve		478	526	0	0 to 650 [A4.4]
DSC Boral® Sheet		652	694	0	0 to 850 [A4.5]
CE 16x16 Zircaloy Cladding	70°F long-term average ambient	638	<695	0	0 to 752 ⁽²⁾ [A4.21]
	104°F short-term maximum ambient	654	695	0	0 to 752 ⁽²⁾ [A4.21]

- (1) For the minimum daily averaged temperature condition of 0°F ambient, the resulting component temperatures will approach 0°F if no credit is taken for the decay heat load.
- (2) These fuel cladding limits apply to the normal conditions of storage and all short term operations, including vacuum drying, helium backfilling and transfer operations from spent fuel pool to ISFSI pad [A4.21].

**Table A.4.1-2
Component Minimum and Maximum Temperatures in the Advanced NUHOMS® System
(Storage or Transfer Mode) for Off-Normal Conditions**

Component	Maximum ⁽²⁾ (°F)	Minimum ⁽¹⁾ (°F)	Allowable Range (°F) Ref
DSC Shell	443	-40	-40 to 800 [A4.4]
DSC Top Outer Cover Plate	468	-40	-40 to 800 [A4.4]
DSC Top Inner Cover Plate	484	-40	-40 to 800 [A4.4]
DSC Top Plug	479	-40	-40 to 620 [A4.14]
DSC Bottom Plug	504	-40	-40 to 620 [A4.14]
DSC Bottom Inner Cover Plate	515	-40	-40 to 800 [A4.4]
DSC Bottom Outer Cover Plate	492	-40	-40 to 800 [A4.4]
DSC Spacer Disc	695	-40	-40 to 1000 [A4.4]
DSC Guidesleeve or FF Can	697	-40	-40 to 800 [A4.4]
DSC Oversleeve	697	-40	-40 to 800 [A4.4]
DSC Support Rod/Spacer Sleeve	529	-40	-40 to 650 [A4.4]
DSC Boral® Sheet	697	-40	-40 to 1000 [A4.5]
CE 16x16 Zircaloy Cladding	698	-40	Storage: 1058 [A4.21] Transfer: 752 [A4.21]

(1) For the minimum daily averaged temperature condition of -40°F ambient, the resulting component temperatures will approach -40°F if no credit is taken for the decay heat load.

(2) Maximum off-normal temperature is during the transfer mode.

**Table A.4.1-3
Component Minimum and Maximum Temperatures in the Advanced NUHOMS[®] System
(Storage and Transfer) for Accident Conditions**

Component	Maximum ⁽²⁾ (°F)	Minimum ⁽¹⁾ (°F)	Allowable Range (°F) Ref
DSC Shell	607	-40	-40 to 800 [A4.4]
DSC Top Outer Cover Plate	470	-40	-40 to 800 [A4.4]
DSC Top Inner Cover Plate	495	-40	-40 to 800 [A4.4]
DSC Top Plug	483	-40	-40 to 620 [A4.14]
DSC Bottom Plug	521	-40	-40 to 620 [A4.14]
DSC Bottom Inner Cover Plate	549	-40	-40 to 800 [A4.4]
DSC Bottom Outer Cover Plate	481	-40	-40 to 800 [A4.4]
DSC Spacer Disc	772	-40	-40 to 1000 [A4.4]
DSC Guidesleeve or FF Can	774	-40	-40 to 800 [A4.4]
DSC Oversleeve	774	-40	-40 to 800 [A4.4]
DSC Boral [®] Sheet	774	-40	-40 to 1000 [A4.5]
DSC Support Rod/Spacer Sleeve	650	-40	-40 to 650 [A4.4]
CE 16x16 Zircaloy Cladding	776	-40	-40 to 1058 [A4.21]

- (1) For the minimum daily averaged temperature condition of -40°F ambient, the resulting component temperatures will approach -40°F if no credit is taken for the decay heat load.
- (2) The maximum accident temperature is during a storage mode blocked vent condition.

A.4.2 Summary of Thermal Properties of Materials

The thermal properties of materials used in the thermal analyses are reported below. The values are listed as given in the corresponding references.

a. Helium

Used for: Blowdown during canister drying operations and for gaps in canister during storage mode. The thermal properties for helium are presented in Section 4.2.a.

b. SA-240, Type 304, ASTM A240, Type 304, 18Cr-8Ni

Used for: Guidesleeves, failed fuel cans and oversleeves. The thermal properties for SA-240, Type 304 stainless steel are presented in Section 4.2.b.

c. SA-240, Type 316, 16Cr-12Ni-2Mo

Used for: 24PT4-DSC shell, outer top cover, outer bottom cover and top shield plug forging. The thermal properties for SA-240, Type 316 stainless steel are presented in Section 4.2.c.

d. SA-533, Gr B, Class 1, Mn-1/2Mo-1/2Ni

Used for: Spacer discs

Temp. °F	Conductivity [A4.4] Btu/hr-ft-°F	Specific Heat, [A4.4] Btu/lbm-°F	Density ⁽¹⁾ [A4.26] lbm/in ³
70	22.3	0.1059	0.284
100	22.6	0.1078	
150	23.1	0.1110	
200	23.4	0.1135	
250	23.7	0.1164	
300	23.8	0.1189	
350	23.8	0.1215	
400	23.8	0.1247	
450	23.7	0.1278	
500	23.5	0.1308	
550	23.2	0.1335	
600	23.0	0.1370	
650	22.7	0.1402	
700	22.3	0.1424	

(1) Density is assumed to be independent of temperature.

e. SA-564, Type 630, 17Cr-4Ni-4Cu

Used for: Support rods, spacer sleeves.

Temp. °F	Conductivity [A4.4] Btu/hr-ft-°F	Specific Heat [A4.4] Btu/lbm-°F	Density ⁽¹⁾ [A4.6] Lbm/in ³
70	9.9	0.107	0.285
100	10.1	0.109	
150	10.4	0.112	
200	10.6	0.114	
300	11.2	0.120	
400	11.7	0.124	
500	12.2	0.130	
600	12.7	0.136	
650	13.0	0.140	

(1) Density is assumed to be independent of temperature.

f. SA-182, Type F316, 16Cr-12Ni-2Mo

Used for: 24PT4 bottom and top shield plug assembly forgings

Temp. °F	Conductivity [A4.4] Btu/hr-ft-°F	Specific Heat, [A4.4] Btu/lbm-°F	Density ⁽¹⁾ [A4.6] lbm/in ³
70	7.7	0.117	0.285
100	7.9	0.118	
150	8.2	0.121	
200	8.4	0.121	
250	8.7	0.124	
300	9.0	0.126	
350	9.2	0.126	
400	9.5	0.128	
450	9.8	0.130	
500	10.0	0.130	
550	10.3	0.132	
600	10.5	0.132	
650	10.7	0.132	
700	11.0	0.134	

(1) Density is assumed to be independent of temperature.

g. ASTM B29 Lead

Used for: Top and Bottom Shield Plugs

Temp °F	Conductivity [A4.14] Btu/hr-ft-°F	Specific Heat ⁽¹⁾ [A4.14] Btu/lbm-°F	Density ⁽¹⁾ [A4.3] lbm/in ³
32	20.1	0.03	0.410
212	19.0		
572	18.0		

(1) Density and specific heat are assumed to be independent of temperature.

h. Boral[®]

Used for: Poison sheets. The thermal properties for Boral[®] are the same as those presented in Section 4.2.e.

i. Water

Used for: Water in 24PT4-DSC cavity during loading operations. The thermal properties for water are the same as those presented in Section 4.2.f.

j. Air

Used for: Cover gas for 24PT4-DSC during vacuum drying (see Section A.4.7.1 for justification). The thermal properties for air are the same as those presented in Section 4.2.g.

k. Concrete/Soil

Used for: AHSM walls and basemat. Soil is under the basemat. The thermal properties are the same as Sections 4.2.h and 4.2.i.

l. Emissivities

Used for: Modeling thermal radiation

Material Emissivities

Material	Nominal ϵ	References
Stainless steel	0.40	[A4.16]
Rolled steel surfaces ⁽¹⁾	0.587	[A4.9]
Carbon steel	0.35	[A4.7]
Electroless nickel coating	0.15	[A4.17]
Boral plate	0.1	[A4.5]
Zircaloy cladding	0.8	[A4.11]

(1) The rolled steel surfaces (DSC shell) will have higher emissivity than the nominal for a smooth steel surface. Reference [A4.10] gives a ϵ of 0.66 for rolled steel, but a value of 0.587 is conservatively used.

m. PWR Fuel with Helium Backfill

The thermal properties for PWR fuel with helium backfill are the same as those presented in Section 4.2.k.

n. PWR Fuel in Vacuum Environment

The thermal properties for PWR fuel with vacuum environment are the same as those presented in Section 4.2.1

A.4.3 Specifications for Components

Allowable temperature ranges for the structural materials used in the design are given in Table A.4.1-1, Table A.4.1-2, and Table A.4.1-3 for normal, off-normal and accident conditions, respectively. Because of the passive design of the Advanced NUHOMS[®] System, there is no need for rupture discs or pressure relief in the safety related components of the 24PT4-DSC.

A.4.4 Thermal Evaluation for Normal Conditions of Storage and Transfer

This section describes the thermal analyses of the 24PT4-DSC for normal conditions of storage and transfer. The analytical models of the 24PT4-DSC within the AHSM and the TC are described and the analysis results are provided in this section. The thermophysical properties of the Advanced NUHOMS[®] System components used in the thermal analysis are listed in Section A.4.2.

A.4.4.1 Overview of Thermal Analysis for Normal Conditions of Storage and Transfer

The thermal analysis of the 24PT4-DSC is carried out for the following cases during normal conditions of storage and transfer.

1. Thermal Analysis of the 24PT4-DSC in the AHSM (See Section 4.4.2),
2. Thermal Analysis of the 24PT4-DSC in the TC (Section A.4.4.3), and
3. Thermal Analysis of the 24PT4-DSC basket (Section A.4.4.4).

A.4.4.2 Thermal Model of the 24PT4-DSC Inside the AHSM

See Section 4.4.2.

A.4.4.3 Thermal Model of 24PT4-DSC in the TC

The thermal analysis of the 24PT4-DSC in the TC is also split into separate models for the 24PT4-DSC and TC. This allows for independent calculation of 24PT4-DSC internal temperatures, using the 24PT4-DSC shell temperatures calculated in the TC model as input.

The purpose of the TC analysis is to determine the 24PT4-DSC shell temperatures to be used as boundary conditions in a subsequent 24PT4-DSC thermal analysis. The thermal analysis of the TC with total heat load of 24 kW is presented in Section 4.4.3. The shell temperatures were provided for 24PT1-DSC for required range of ambient conditions with 24 kW heat load. These shell temperatures are directly applicable for 24PT4-DSC since the shell outside diameter, wall thickness, and materials are the same for both designs. Since the thermal analysis of the TC is based on a homogenized DSC model, a small difference in basket dimensions between 24PT1-DSC and 24PT4-DSC will have a negligible affect on the results.

The maximum temperatures for the top and bottom shield plug assemblies presented in Table A.4.4-1, are computed based on scaling the results for the 24PT1-DSC in the TC. The scaling accounts for changes in the thermal resistances within the top and bottom plug assemblies between the 24PT4-DSC and the 24PT1-DSC and for the change in the surface heat flux due to the different lengths of the two DSC cavities.

A.4.4.3.1 Model Description

The basket component maximum temperatures for the 24PT4-DSC in the TC are computed using a three dimensional ANSYS model of the basket assembly and the 24PT4-DSC shell. For the ANSYS modeling, the 24PT4-DSC shell temperature distribution around the shell is used as boundary conditions for the evaluation of the 24PT4-DSC within the TC (see Section A.4.4.4).

A.4.4.3.2 Description of Cases Evaluated for the 24PT4-DSC inside the TC

The TC thermal analyses are performed for the range of design basis ambient air temperatures defined in Section 4.1 for normal conditions. The TC thermal analysis was not performed for the design life average temperature since this case is needed only for the storage in the AHSM to ensure the integrity of the fuel cladding and is enveloped by the other normal cases.

The thermal stress analysis of the 24PT4-DSC shell assembly is based on the temperature results of 24PT1-DSC shell assembly with 24 kW heat load presented in Section 4.4.3.3. The cases which are used to determine the thermal stresses for normal conditions are listed in Table A.4.4.4.

A.4.4.3.3 TC Thermal Model Results

The calculated temperature for the 24PT4-DSC shell assembly with a 24 kW heat load during transfer operations is presented in Table A.4.4-1. These results are used in the structural analysis described in Chapter A3 and are used as boundary conditions in the 24PT4-DSC basket thermal analysis presented in Section A.4.4.4.

A.4.4.4 24PT4-DSC Basket Thermal Model

A.4.4.4.1 Model Description

For thermal analyses, the internal basket assembly of the 24PT4-DSC is modeled as follows. A three-dimensional slice of the 24PT4-DSC basket assembly and fuel is modeled near the center of the active fuel region. The 3-D slice spans from center to center of two spacer discs to account for the radial effect of conduction through the spacer discs. Heat transfer effects along the axis of the 24PT4-DSC (third dimension) outside hottest section between two adjacent spacer disc mid-planes are conservatively neglected by applying adiabatic boundary conditions to the axial ends of the model. The 24PT4-DSC shell surface is specified as a constant temperature boundary condition equal to that calculated in the AHSM or TC thermal analysis. The fuel regions inside the 24PT4-DSC are modeled as homogenous regions with internal heat sources. The volumetric heat sources are computed using a heat source equal to 1.08 times the decay heat of the assembly to account for the axial peaking factor.

The steady state shell surface temperatures for the 24PT4-DSC resting inside the AHSM are calculated in the AHSM thermal analysis, described in Section 4.4.2. The shell outer surface temperatures for the 24PT4-DSC resting inside the TC are calculated in the TC thermal analysis as described in Section A.4.4.3. The temperatures for the 24PT4-DSC shell presented in Table

A.4.4-1 are used as the constant temperature boundary conditions for the 24PT4-DSC basket model.

The ANSYS computer program [A4.15] is used to perform the thermal analysis of the 24PT4-DSC internal basket assembly and spent fuel assembly regions. Figure A.4.4-1 illustrates the spacer disc layout simulated in the thermal model. The inside dimension of the guidesleeves used in ANSYS model is 8.57" x 8.57", which thermally bounds wider dimension of 8.65" x 8.65" since such a change increases thermal mass of the guidesleeves. The cutout in spacer disc for external guidesleeves assemblies used in ANSYS model is 9.435" instead of 9.45". A sensitivity analysis performed for 9.245" cutout shows that 9.435" value results in conservatively higher 24PT4-DSC components and fuel cladding temperatures. Figure A.4.4-2 illustrates the axial length of the modeled basket slice.

The front and side views of the ANSYS analytical model of the 24PT4-DSC are shown in Figure A.4.4-3. Figure A.4.4-4 illustrates the layout of the finite elements used to model each of the spacer discs. Figure A.4.4-5 presents a perspective view of the finite element modeling of the 24PT4-DSC shell and guidesleeve assemblies, while Figure A.4.4-6 presents a view of the finite element modeling of the fuel assemblies.

The analysis of the guidesleeves is also applicable to the failed fuel can since their configuration is identical, except for the addition of top and bottom closures.

The heat generated within the fuel regions is assumed to be transferred to the guidesleeves and through the guidesleeve walls by conduction. The heat is then transferred through the guidesleeve assembly, including the Boral[®] sheets, oversleeves and gaps by conduction. Conservative helium gaps are modeled within the guidesleeve assemblies between the guidesleeves and the poison plate, between the poison plates and the oversleeves, and between the oversleeves or guidesleeves and the spacer discs. Table A.4.4-7 documents the gaps between the basket components assumed within the ANSYS analytical model of the 24PT4-DSC. Radiation heat transfer across the gaps between guidesleeves and poison plates and between poison plates and oversleeves is conservatively ignored.

For the gaps between adjacent guidesleeve assemblies, heat transfer is assumed to occur by conduction and radiation. In the physical system, conduction in the axial direction would provide an additional mechanism for heat removal from the 24PT4-DSC; however, this mode of heat transfer is conservatively neglected for regions outside hottest section between two adjacent spacer disc mid-planes. Conduction is modeled throughout the entire model. Radiation between adjacent guidesleeve assemblies, between the guidesleeve assemblies and the spacer discs, between the guidesleeve assemblies and the 24PT4-DSC shell, and between the spacer discs and the 24PT4-DSC shell is computed within the ANSYS program using the surface effect elements layout illustrated in Figure A.4.4-7.

In order to simplify the problem and reduce memory requirements and computing time, a portion of the thermal radiation was modeled using radiation link elements (link31). Radiation between the spacer discs and the 24PT4-DSC shell and radiation between the guidesleeves and the spacer discs were modeled by this method. For these link elements, the area, view factor, emissivity, and Stefan-Boltzmann constant are defined as real constants. Because of the close proximity of

the components, it is reasonable to assume a view factor of one. For the emissivity, an effective value is defined as follows [A4.8].

$$\epsilon_{eff} = \frac{1}{\frac{1}{0.587} + \frac{1}{0.15} - 1} = 0.135$$

The area is calculated based on the total area for heat transfer divided by the total number of link elements. The thermal properties used in the ANSYS analytical model, including conductivities and emissivities, are presented in Section A.4.2.

Three different heat load configurations, each with a total canister heat load of 24 kW, are evaluated. These heat load configurations are illustrated in Figure A.4.4-8 to Figure A.4.4-10. The design basis fuel decay heat ranges from 0.80 to 1.3 kW per spent fuel assembly, depending on the load configuration being analyzed. For heat load Configuration #3, the heat load per assembly used is shown in Figure A.4.4-10. This analyzed configuration envelopes the configuration specified for the payload in Figure A.2.1-3 where the 1.3 kW/0.8 kW heat load is replaced with a 1.26 kW/0.9 kW heat load. Heat loads used in the thermal analysis envelopes the total DSC decay heat load and the differential temperatures used in structural analysis in Chapter A.3. The decay heat is applied as a volumetric heat generation uniformly distributed over the homogenous fuel regions inside the guidesleeve assemblies. The resulting volumetric heat density, including a peaking factor of 1.08, which was applied over the active fuel length of 149 inches, are computed as follows:

For 0.8 kW heat load.

$$\ddot{q} = \frac{0.8 \text{ kW} \cdot 1.08 \cdot 3414 \frac{\text{Btu/hr}}{\text{kW}} \cdot \frac{1 \text{ hr}}{60 \text{ min}}}{(8.57 \text{ in})^2 \cdot 149 \text{ in}} = 4.492e-3 \frac{\text{Btu}}{\text{min} \cdot \text{in}^3}$$

For 0.9 kW heat load.

$$\ddot{q} = \frac{0.9 \text{ kW} \cdot 1.08 \cdot 3414 \frac{\text{Btu/hr}}{\text{kW}} \cdot \frac{1 \text{ hr}}{60 \text{ min}}}{(8.57 \text{ in})^2 \cdot 149 \text{ in}} = 5.054e-3 \frac{\text{Btu}}{\text{min} \cdot \text{in}^3}$$

For 1.0 kW heat load.

$$\ddot{q} = \frac{1.0 \text{ kW} \cdot 1.08 \cdot 3414 \frac{\text{Btu/hr}}{\text{kW}} \cdot \frac{1 \text{ hr}}{60 \text{ min}}}{(8.57 \text{ in})^2 \cdot 149 \text{ in}} = 5.615e-3 \frac{\text{Btu}}{\text{min} \cdot \text{in}^3}$$

For 1.2 kW heat load.

$$\ddot{q} = \frac{1.2 \text{ kW} \cdot 1.08 \cdot 3414 \frac{\text{Btu/hr}}{\text{kW}} \cdot \frac{1 \text{ hr}}{60 \text{ min}}}{(8.57 \text{ in})^2 \cdot 149 \text{ in}} = 6.738e-3 \frac{\text{Btu}}{\text{min} \cdot \text{in}^3}$$

For 1.3 kW heat load.

$$\ddot{q} = \frac{1.3 \text{ kW} \cdot 1.08 \cdot 3414 \frac{\text{Btu/hr}}{\text{kW}} \cdot \frac{1 \text{ hr}}{60 \text{ min}}}{(8.57 \text{ in})^2 \cdot 149 \text{ in}} = 7.3e-3 \frac{\text{Btu}}{\text{min} \cdot \text{in}^3}$$

The resulting calculated temperature profiles for the 24PT4-DSC show guidesleeve, failed fuel can, poison plate, and oversleeve temperatures, and other 24PT4-DSC internal component temperatures. These component temperature profiles are used for the evaluation of fuel cladding maximum temperatures and helium temperatures (for use in the 24PT4-DSC pressure evaluation). These temperatures are also used to evaluate the thermal stresses in the 24PT4-DSC shell and the spacer discs as described in Chapters A.3 and A.11.

A.4.4.4.2 Mesh Sensitivity

In order to check the sensitivity of the model to the mesh density, number of model elements was increased by 19%. The maximum model components temperature increase for this refined mesh for long-term storage conditions (70°F ambient) is ~0.2°F. Such a negligible effect shows that model is not mesh sensitive.

A.4.4.4.3 Description of Cases Evaluated for the 24PT4-DSC Basket

The 24PT4-DSC basket and fuel assembly heat transfer analyses with the 24PT4-DSC inside the AHSM, or TC, are performed for the normal ambient air temperature cases defined in Table 4.1-1. A total of five normal cases corresponding to the conditions described in Section 4.4.2.3 for the AHSM and Section A.4.4.3.2 for the TC are performed. The 70°F case is not performed for the TC since it is enveloped by the other cases.

Temperature profiles for the spacer disc are used to determine thermal stresses shown in Chapter A.3. The normal cases which are considered are listed in Table A.4.4-4.

A.4.4.4.4 24PT4-DSC Thermal Model Results

The results obtained from the ANSYS analytical model for each of the three heat load configurations are in the form of temperature profiles. From these analytical results, the 24PT4-DSC component temperatures bounding all configurations are extracted and summarized in Table A.4.4-2. The bounding fuel cladding temperature results are summarized in Table A.4.4-3. Generally, the results for heat load Configuration #1 provide the bounding basket component temperatures. The basket components and fuel cladding maximum temperatures are compared against their limits in Table A.4.1-1. The results demonstrate that all the material temperature limits are satisfied and there is a very low probability of cladding failure during storage or transfer.

A.4.4.5 Test Model

The detailed, conservative evaluations described above for the AHSM, TC, and 24PT4-DSC ensure that the Advanced NUHOMS[®] System is capable of dissipating the design basis heat load. The conservative approach precludes the necessity to perform thermal testing.

For the 24PT4-DSC thermal models, each fuel assembly in the basket is homogenized in its guide sleeve region and effective fuel properties are used for the homogenized fuel assembly region to calculate maximum fuel temperature. This maximum fuel temperature correlates to the maximum fuel cladding temperature based on the validation of fuel effective conductivity values used for the NUHOMS[®] system design against the NUHOMS[®]-07P test data obtained from the PNL/EPRI testing [A4.20] as documented in Appendix B.3 of the NUHOMS[®] CoC 1004 FSAR [A4.12].

In the specific case of the NUHOMS[®]-07P test data obtained from the PNL/EPRI testing [A4.20], the peak system temperatures noted under helium backfill conditions were <365°F. These temperature levels are less than the typical peak design temperatures for initial storage conditions of approximately 650°F. Despite this fact, the use of NUHOMS[®]-07P test data is appropriate for validating the thermal model intended for use at the higher temperature level based on the justification provided in section B.3.4 of Appendix B.3 of the NUHOMS[®] CoC 1004 FSAR [A4.12] and the following:

- For a thermal model that captures the basic thermophysical processes (i.e., conduction, convection, and radiation) present, the primary areas of uncertainty will be the modeling of the geometry and the thermal properties used for each component. Once the correct geometry and thermal properties are captured, the effect of higher temperature levels on the fundamental heat transfer processes involved is well understood and documented. Thus, simply changing the temperature level for a simulation will not necessarily increase the uncertainty level for the thermal model.
- Changes to the thermal conductivity of the metallic components with temperature are well understood and documented for temperature levels well in excess of 700°F. As such, the effect is easily captured through the use of temperature dependent properties.

- Radiation heat transfer is a function of view factor, surface area, and emissivity. View factors and surface area do not change with increased temperature level. As such, a thermal model that incorporates radiation exchange and which has been validated at a lower temperature will typically be conservative (i.e., yield higher temperatures) for application at the higher temperature level.

Therefore, a thermal model that has been properly constructed and validated using the lower temperature data from the NUHOMS[®]-07P test can be fully expected to yield accurate results at higher temperature levels similar to the 24PT4-DSC design.

For additional justification, a confirmatory thermal analysis of the 24PT4-DSC was conducted using a totally independent approach and software code. The results of this confirmatory thermal analysis demonstrated that the safety analysis presented herein using the ANSYS analytical model provides accurate peak fuel cladding temperatures and bounding temperature results for the 24PT4-DSC basket components. Section A.4.8 provides a discussion of the confirmatory modeling and a comparison of predicted 24PT4-DSC basket temperatures for one selected storage condition. Section A.4.8 also includes documentation of the benchmarking of the confirmatory analysis model to the NUHOMS[®] test data.

A.4.4.6 Maximum Temperatures

The peak temperatures for the 24PT4-DSC structural components are listed in Table A.4.4-1 and Table A.4.4-2 for the range of operating conditions. The peak fuel cladding temperatures are listed in Table A.4.4-3 for the full range of operating conditions.

A.4.4.7 Minimum Temperatures

For the minimum daily averaged temperature condition of 0°F ambient, the resulting component temperatures will approach 0°F if no credit is taken for the decay heat load. Since the 24PT4-DSC materials, including confinement structures and welds, continue to function at this temperature (structural materials are stainless steel, or carbon steel), the minimum temperature condition has no adverse effect on the performance of the Advanced NUHOMS[®] System during storage. See Technical Specifications for controls applicable to moving a loaded TC/24PT4-DSC as a function of temperature and location.

A.4.4.8 Maximum Internal Pressure

Based on the results of the 24PT4-DSC thermal analysis, the initial pressure of the helium fill gas during loading operations, and the characteristics of the fuel assemblies being stored, a conservative prediction of the maximum gas pressure within the 24PT4-DSC cavity during normal conditions is determined.

The characteristics of the fuel assemblies are given in Table A.4.4-5. The parameters in Table A.4.4-5 are used to determine the amount of fuel rod fill gas and fission gas moles for 24 CE 16x16 Zircaloy clad fuel assemblies.

Based on the basket temperature results in Table A.4.4-2 and the fuel cladding temperature results of Table A.4.4-3, the maximum pressure in the 24PT4-DSC cavity for normal conditions will occur while in the TC at peak summer ambient condition. To calculate the average gas temperature within 24PT4-DSC cavity, a volume weighted average temperature was calculated for the helium using the ANSYS element table function. The equation used to calculate the average gas temperature is:

$$T_{gas\ aver} = \frac{\sum (T_{element} \cdot V_{element})}{\sum V_{element}}$$

The resulting maximum average helium temperature for the normal case is given in Table A.4.4-6.

The helium pressure during the backfill operation is limited to 3 psig (1.5 psig \pm 1.5 psi). For this condition, a uniform helium temperature of 230°F is assumed, which is approximately equal to the maximum temperature of water in the TC/DSC annulus expected during the loading operations. This assumption is conservative for the following reasons; (1) the assumption of a lower temperature will yield the maximum number of moles of helium gas at the time of backfill and, thus, the maximum predicted canister pressure at steady-state conditions, and (2) the canister and fuel assemblies have ample time during decontamination, welding, blowdown, and vacuum drying described in Chapter A.8 to heatup. The quantity of helium fill gas is then calculated using the ideal gas equation.

For normal conditions, 1% failure of the fuel rods is assumed. For the ruptured rods, 100% release of the fuel rod fill gas and 30% release of the fission gas is assumed, based on guidance in Reference [A4.2]. Based on this guidance the maximum normal pressure is calculated using the ideal gas law and is presented in Table A.4.4-6.

A.4.4.9 Maximum Thermal Stresses

The maximum thermal stresses during normal conditions of storage are presented in Chapter A.3 for the 24PT4-DSC basket and shell assemblies. The AHSM thermal stresses are presented in Chapter 3. The cases that were evaluated for the AHSM and 24PT4-DSC are listed in Table A.4.4-4.

A.4.4.10 Evaluation of System Performance for Normal Conditions of Storage and Transfer

The thermal analysis for normal storage and transfer concludes that the 24PT4-DSC design meets all applicable requirements. The maximum temperatures calculated using conservative assumptions are within the criteria set forth. The predicted maximum fuel cladding temperature is well below the allowable fuel temperature limits given in Table A.4.1-1. The comparison of the results with the allowable material temperature ranges is tabulated in Table A.4.1-1.

**Table A.4.4-1
24PT4-DSC Maximum Shell Assembly Temperatures at 24 kW**

Configuration Ref	T _{amb} (°F)	T _{shell} (°F)	T _{toc} (°F)	T _{tip} (°F)	T _{tp} (°F)	T _{bp} (°F)	T _{boc} (°F)	T _{bsp} (°F)
24PT4-DSC in AHSM	104	399	343	347	346	412	402	418
24PT4-DSC in AHSM	-40	271	218	222	220	290	279	297
24PT4-DSC in AHSM	117	408	352	356	355	420	411	426
24PT4-DSC in AHSM Blocked vent accident	117	607	470	495	483	521	481	549
24PT4-DSC horizontal in TC	-40	380	368	393	385	432	412	445
24PT4-DSC horizontal in TC	104	439	464	480	475	500	484	511
24PT4-DSC horizontal in TC, Loss of sunshade and neutron shield	117	<607	<470	<495	<483	<521	<481	<549
24PT4-DSC horizontal in TC, Fire transient	117	527	<470	<495	<483	<521	<481	<549

Nomenclature used in table

- T_{amb} Ambient temperature
- T_{shell} 24PT4-DSC shell temperature
- T_{toc} 24PT4-DSC top outer cover plate temperature
- T_{tip} 24PT4-DSC top inner plate temperature
- T_{tp} 24PT4-DSC top plug temperature
- T_{bp} 24PT4-DSC bottom plug temperature
- T_{boc} 24PT4-DSC bottom outer cover plate temperature
- T_{bsp} 24PT4-DSC bottom shield plug temperature

**Table A.4.4-2
24PT4-DSC Basket Temperature Results⁽²⁾**

Configuration	T _{amb} (°F)	T _{sp} (°F)	T _{sr} (°F)	T _{gs} (°F)	T _{Boral®} (°F)
24PT4-DSC in AHSM	0	592	403	595	595
24PT4-DSC in AHSM	104	650	478	652	652
24PT4-DSC in AHSM	-40	570	373	572	572
24PT4-DSC in AHSM	117	656	488	658	658
24PT4-DSC in AHSM, blocked vent accident	117	772	650	774	774
24PT4-DSC horizontal in TC	0	661	486	662	662
24PT4-DSC horizontal in TC	104	692	526	694	694
24PT4-DSC horizontal in TC	-40	652	475	654	654
24PT4-DSC horizontal in TC with shade	117	695	529	697	697
24PT4-DSC horizontal in TC loss of sunshade and neutron shield ⁽¹⁾ accident	117	<772	<650	<774	<774
24PT4-DSC horizontal in TC, Fire transient	117	<772	<650	<774	<774
Vacuum drying following DSC blowdown with air	120	617	398	632	632
Vacuum drying following DSC blowdown with helium	120	555	349	557	557

- (1) The accident results in the TC are bounded by the result for the blocked vent accident in the AHSM.
- (2) The results are shown for Configuration #1 which produces highest component temperatures except for support rods, which have maximum temperatures for Configuration #3.

Nomenclature used in table

- T_{amb} Ambient temperature
T_{sp} Maximum spacer disc temperature
T_{sr} Maximum support rod temperature
T_{gs} Maximum guidesleeve temperature
T_{Boral®} Maximum poison plate temperature

**Table A.4.4-3
Maximum Fuel Cladding Temperature Results, 24 kW**

Case	Calculated Maximum Cladding Temperature (°F)	Fuel Temperature Limit (°F)
24PT4-DSC in AHSM, 0°F amb	597	752
24PT4-DSC in AHSM, 70°F amb	638	752
24PT4-DSC in AHSM, 104°F amb	654	752
24PT4-DSC in AHSM, -40°F amb	575	1058
24PT4-DSC in AHSM, 117°F amb	660	1058
24PT4-DSC in AHSM, 117°F amb, blocked vent accident	776	1058
24PT4-DSC horizontal in TC, -40°F amb	655	752
24PT4-DSC horizontal in TC, 0°F amb	664	752
24PT4-DSC horizontal in TC, 104°F amb	695	752
24PT4-DSC horizontal in TC, 117°F amb with sunshade	698	752
24PT4-DSC horizontal in TC, 117°F amb loss of sunshade and neutron shield accident	<776 ⁽²⁾	1058
24PT4-DSC horizontal in TC, Fire transient	<776 ⁽²⁾	1058
Vacuum drying following DSC blowdown with air	659	752
Vacuum drying following DSC blowdown with helium	559	752

- (1) All results are shown for Configuration 1, which produces the highest fuel cladding temperatures.
- (2) The accident results in this TC are bounded by the result for the blocked vent accident in the AHSM.

**Table A.4.4-4
Summary of Cases Considered for Thermal Stress Analysis**

Component	Operation	Heat Load (kW)	Ambient Temperature (°F)	Condition
24PT4-DSC Shell Assembly	Transfer	24	-40	Off-Normal
24PT4-DSC Shell Assembly	Transfer	24	100 ⁽¹⁾	Normal
24PT4-DSC Shell Assembly	Storage	24	-40	Off-Normal
24PT4-DSC Shell Assembly	Storage	24	104	Normal
24PT4-DSC Shell Assembly	Storage	24	117	Off-Normal
24PT4-DSC Basket	Storage	24	-40	Off-Normal
24PT4-DSC Basket	Storage	24	117	Off-Normal
24PT4-DSC Basket	Transfer	24	-40	Off-Normal
24PT4-DSC Basket	Transfer	24	104	Normal
24PT4-DSC Basket	Transfer	24	117	Off-Normal
24PT4-DSC Basket	Vacuum Drying	24	120	Normal

(1) These results are taken from the previous analysis to support CofC 1004. This ambient condition is not based on a daily average temperature as was derived in Section A.4.1. Therefore, this temperature still bounds the daily average defined in Section A.4.1 for a maximum of 104°F.

**Table A.4.4-5
Fuel Assembly Characteristics for Pressure Analysis**

Parameter	CE 16x16 Zircaloy Clad
Number of fuel rods	236
Maximum rod fill pressure (psig)	380 ± 15
Maximum rod void volume (in ³)	1.53
Quantity of fission gas per assy (g-moles)	44.15

**Table A.4.4-6
24PT4-DSC Cavity Pressure Analysis Summary**

Condition	$T_{He,ave}$ (°F)	n_{He} (g-mole)	n_{fill} (g-mole)	n_{fiss} (g-mole)	P (psig)	Thermal Criteria (psig) ⁽¹⁾	Pressures Used in Stress Analysis (psig) Table A.3.1-6
Normal	546.7	240.4	1.65	3.56	11.7	20	20
Off-Normal	550.1	240.4	16.5	35.55	16.8	18	20
Accident	667.0	240.4	164.59	355.48	74.7	90	100

(1) These criteria are used for thermal analyses only. The off-normal and accident thermal criteria have additional margin to account for the effect of the fission gases in the 24PT4-DSC cavity on the thermal results.

Nomenclature used in table

$T_{He,ave}$ Average helium temperature
 n_{He} Number of moles of helium backfill
 n_{fill} Number of moles of fuel rod fill gas released to 24PT4-DSC cavity
 n_{fiss} Number of moles of fission gas released to 24PT4-DSC cavity
P 24PT4-DSC cavity pressure

**Table A.4.4-7
Gaps between Components of ANSYS Model at the Spacer Disc Plane**

Component of the model (Along the first column of fuel assemblies from axis Y from the top to the bottom of DSC)	Gap width, in	Total gap for composite guide sleeve regions, in	Note
Shell			See Figure 4.4-11 for details
Gap	0.19		
Spacer disc			
Gap	0.1874		
Guide sleeve			
Exterior Fuel Assembly			
Guide sleeve			
Gap 1			
Poison plate		Gap 1 + Gap 2	
Gap 2		0.0125	
Over-sleeve			
Gap	0.1874		
Spacer disc			
Gap	0.1072		
Over-sleeve			
Gap 3			
Poison plate		Gap 3 + Gap 4	
Gap 4		0.0125	
Guide sleeve			
Interior Fuel Assembly			
Guide sleeve			
Gap 5			
Poison plate		Gap 5 + Gap 6	
Gap 6		0.0125	
Over-sleeve			
Gap	0.1072		
Spacer disc			
Gap	0.1072		
Over-sleeve			
Gap 7			
Poison plate		Gap 7 + Gap 8	
Gap 8		0.0125	
Guide sleeve			
Interior Fuel Assembly			
Guide sleeve			
Gap 9			
Poison plate		Gap 9 + Gap 10	
Gap 10		0.0125	
Over-sleeve			
Gap	0.1072		
Spacer disc			

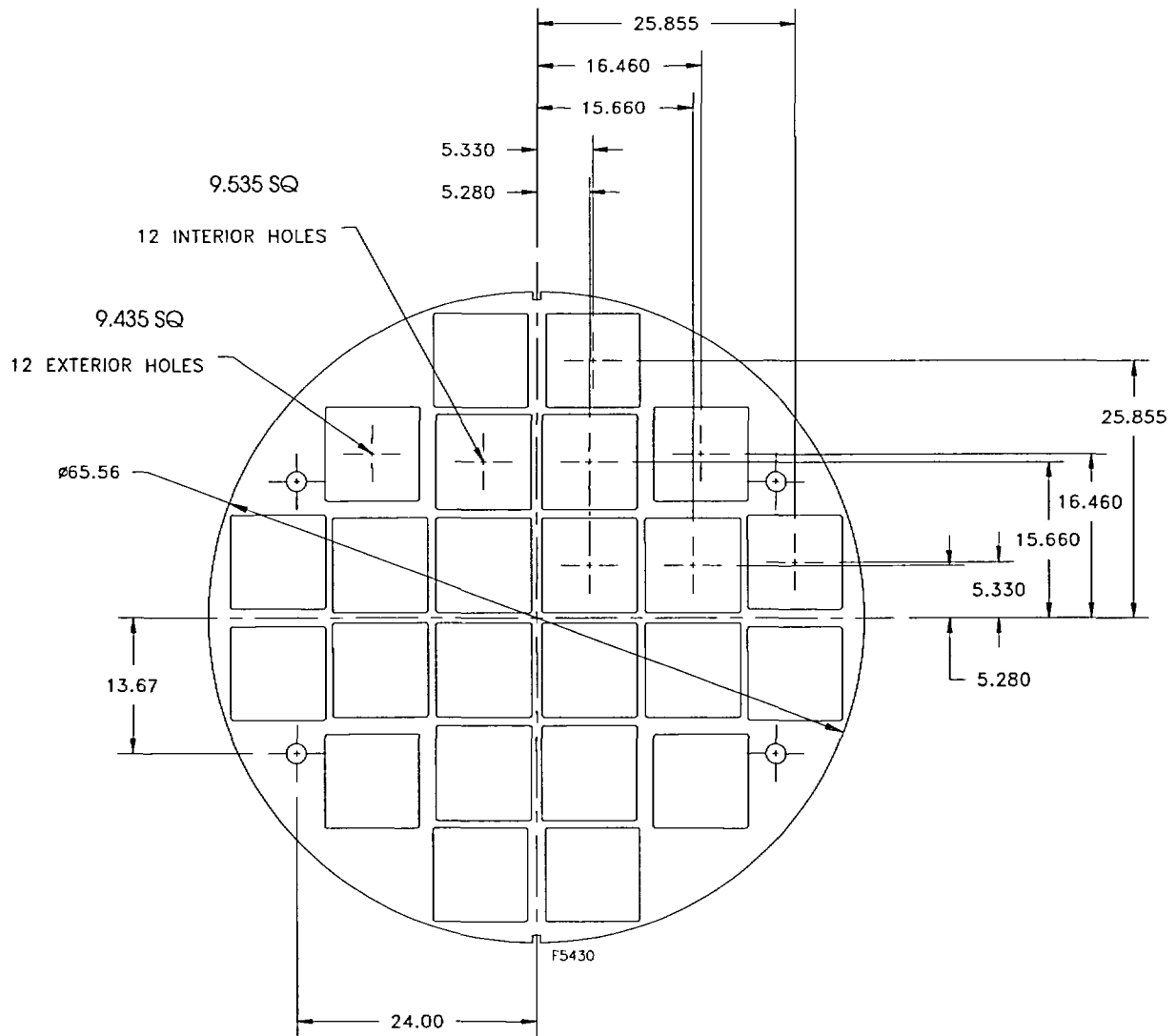


Figure A.4.4-1
24PT4 Spacer Disc Schematic

Note – All dimensions are in inches

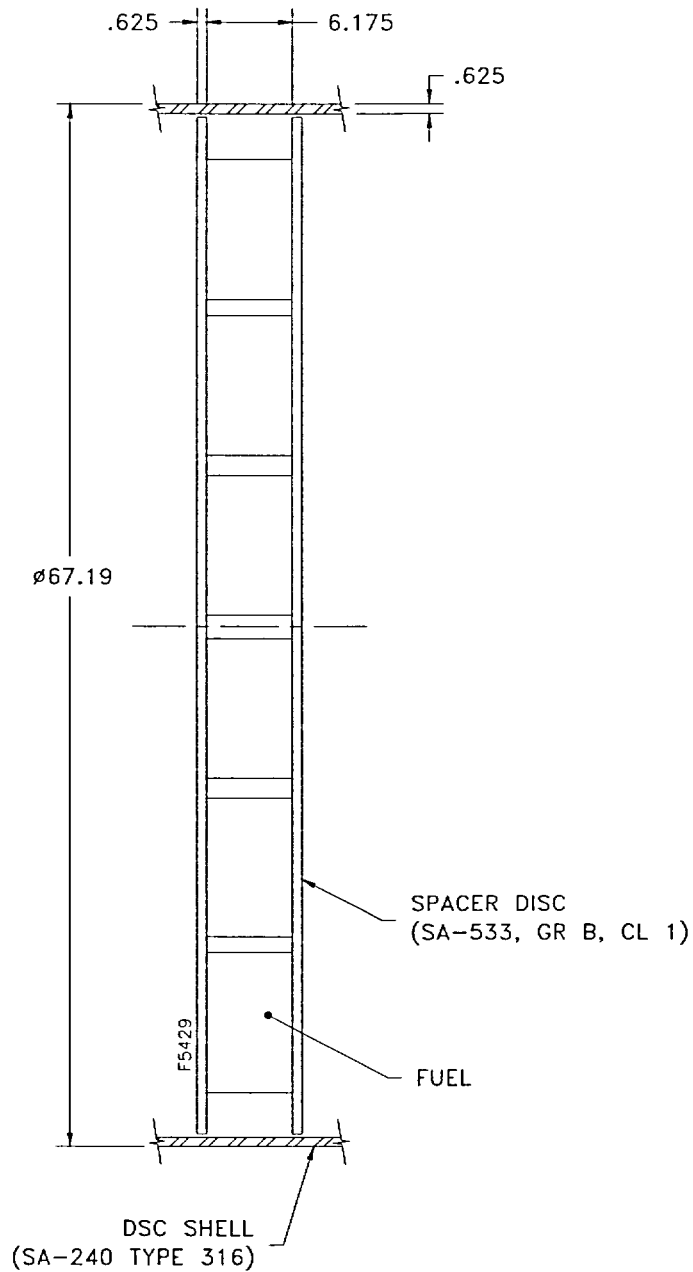


Figure A.4.4-2
Simplified Axial View of the 24PT4-DSC Basket Model

Note – All dimensions are in inches

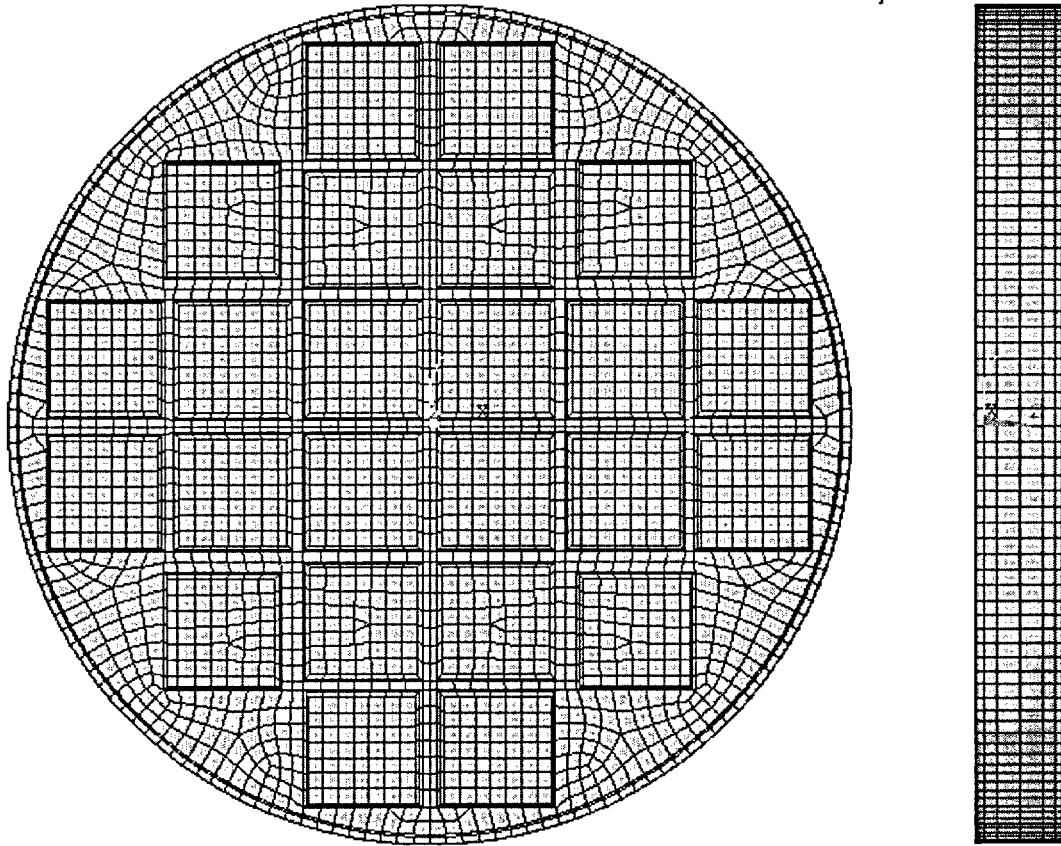


Figure A.4.4-3
24PT4-DSC ANSYS Thermal Model; Front And Side Views

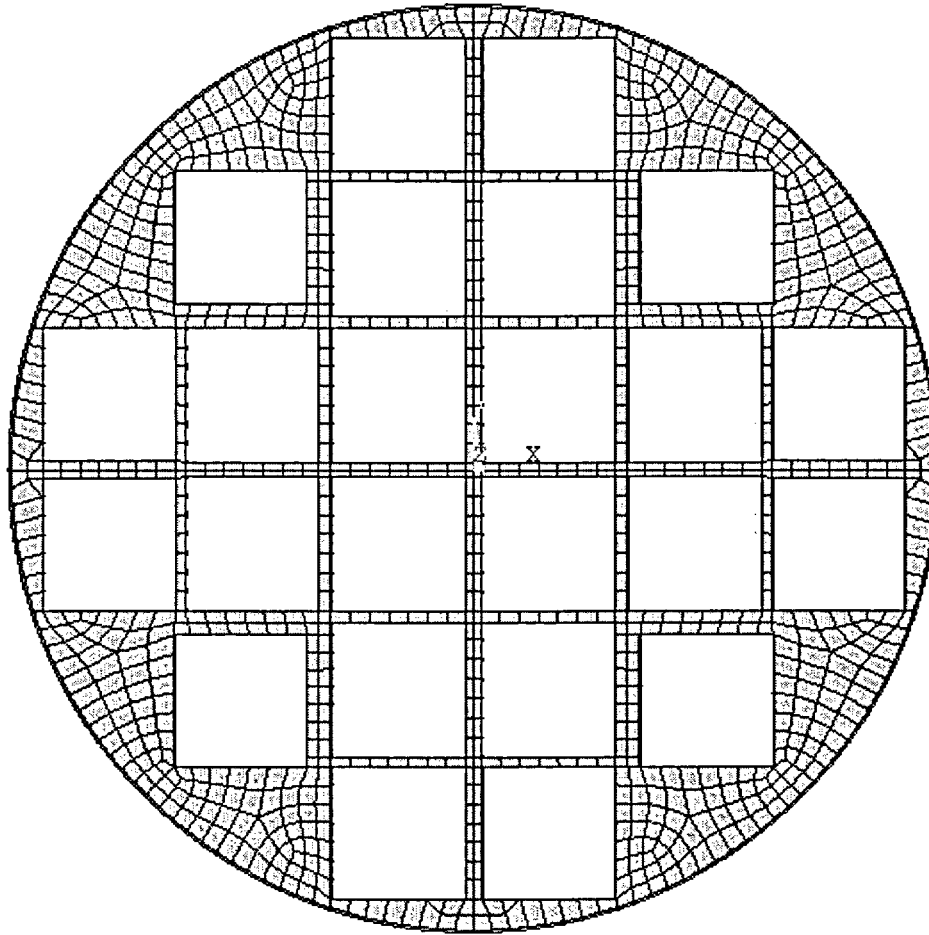


Figure A.4.4-4
24PT4-DSC ANSYS Thermal Model, Spacer Disc

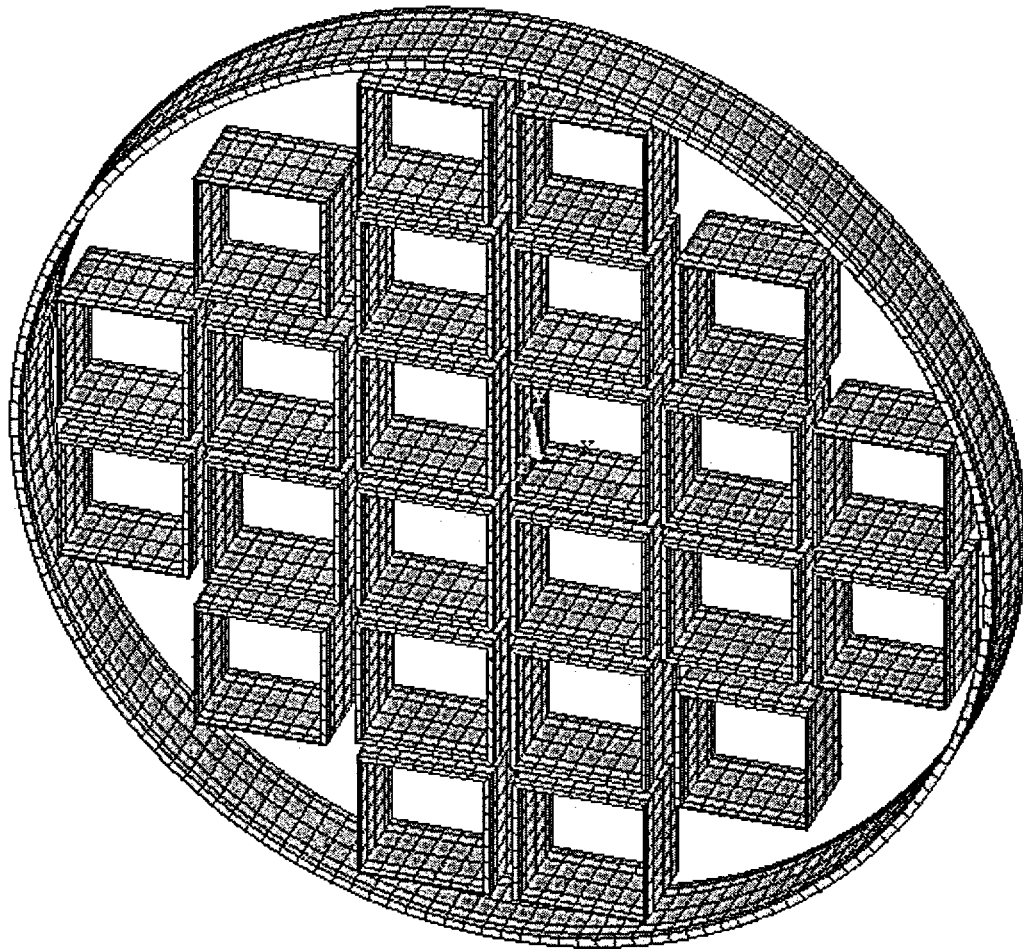


Figure A.4.4-5
24PT4-DSC ANSYS Thermal Model, Shell and Guidesleeve Assembly

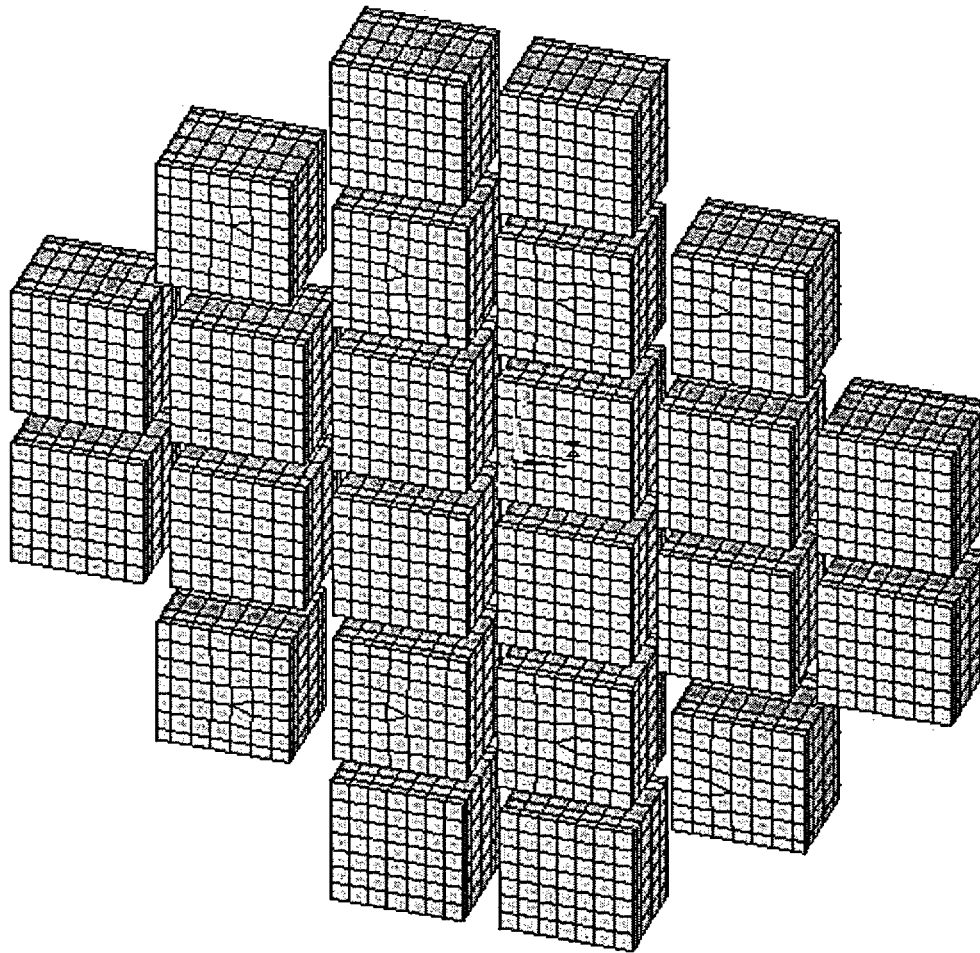


Figure A.4.4-6
24PT4-DSC ANSYS Thermal Model, Fuel Assemblies, Load Configurations #1 and #2

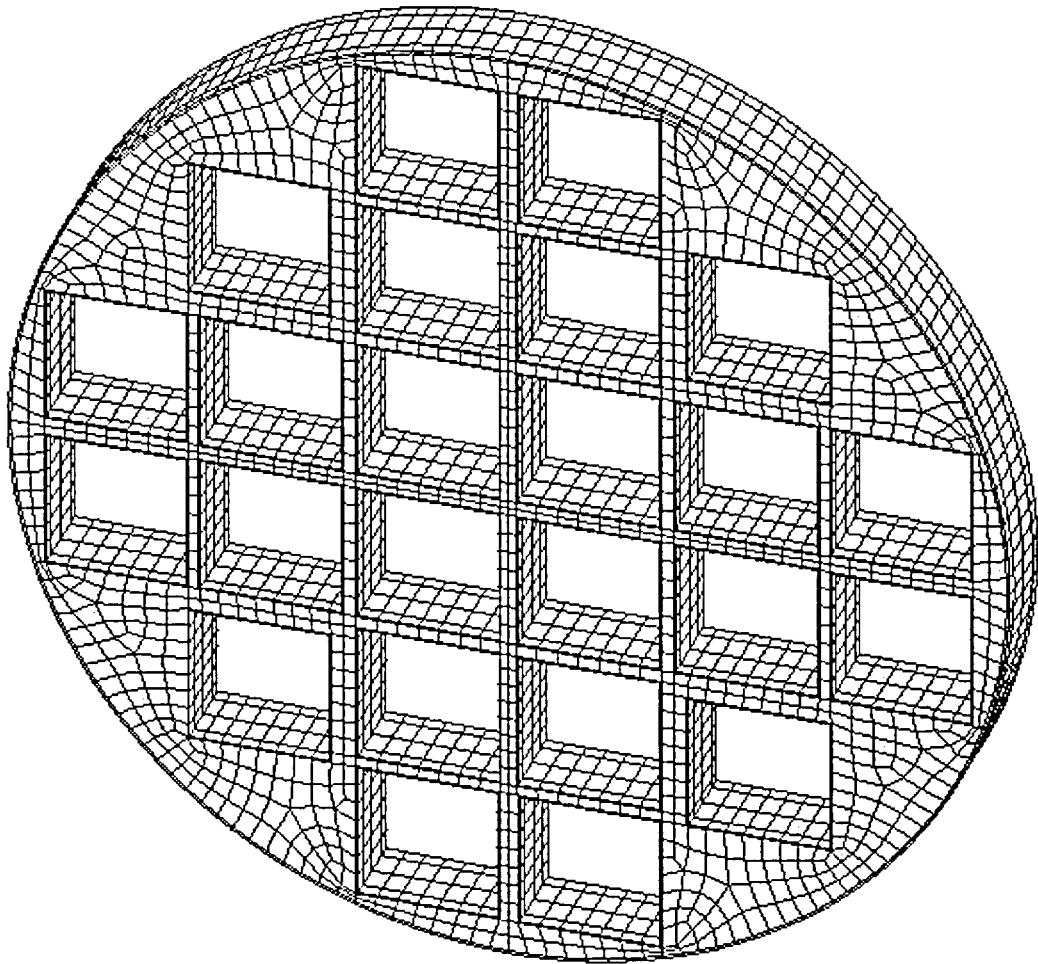


Figure A.4.4-7
Surface Elements for Radiation View Factor Calculation

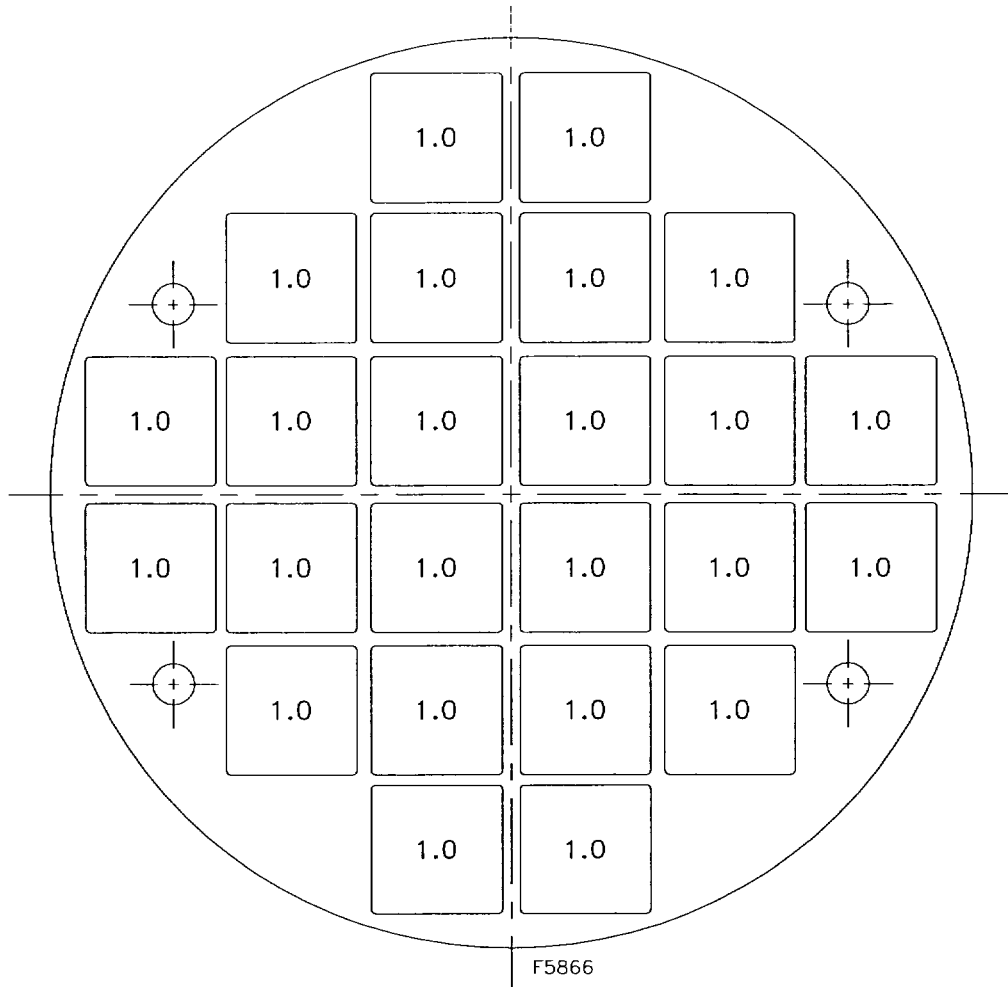


Figure A.4.4-8
24PT4-DSC Heat Load Configurations #1, kW/Assembly

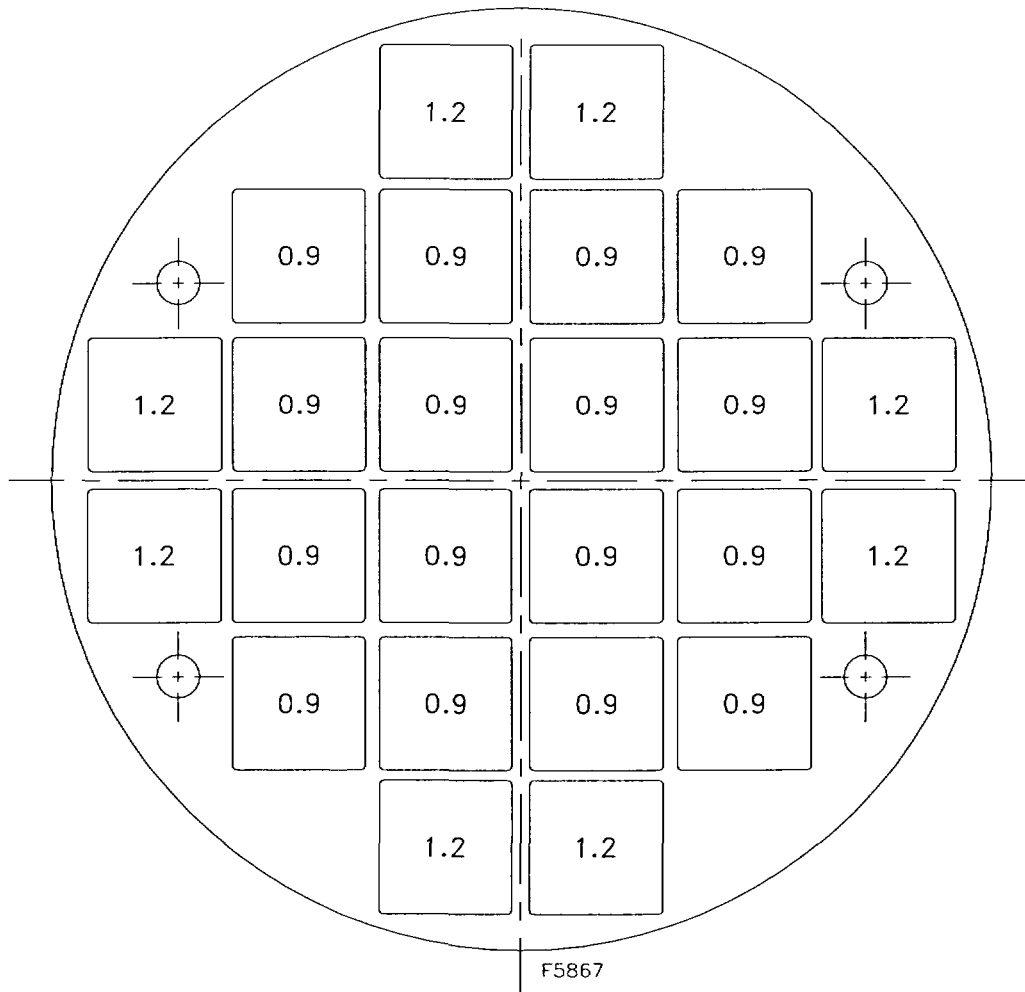
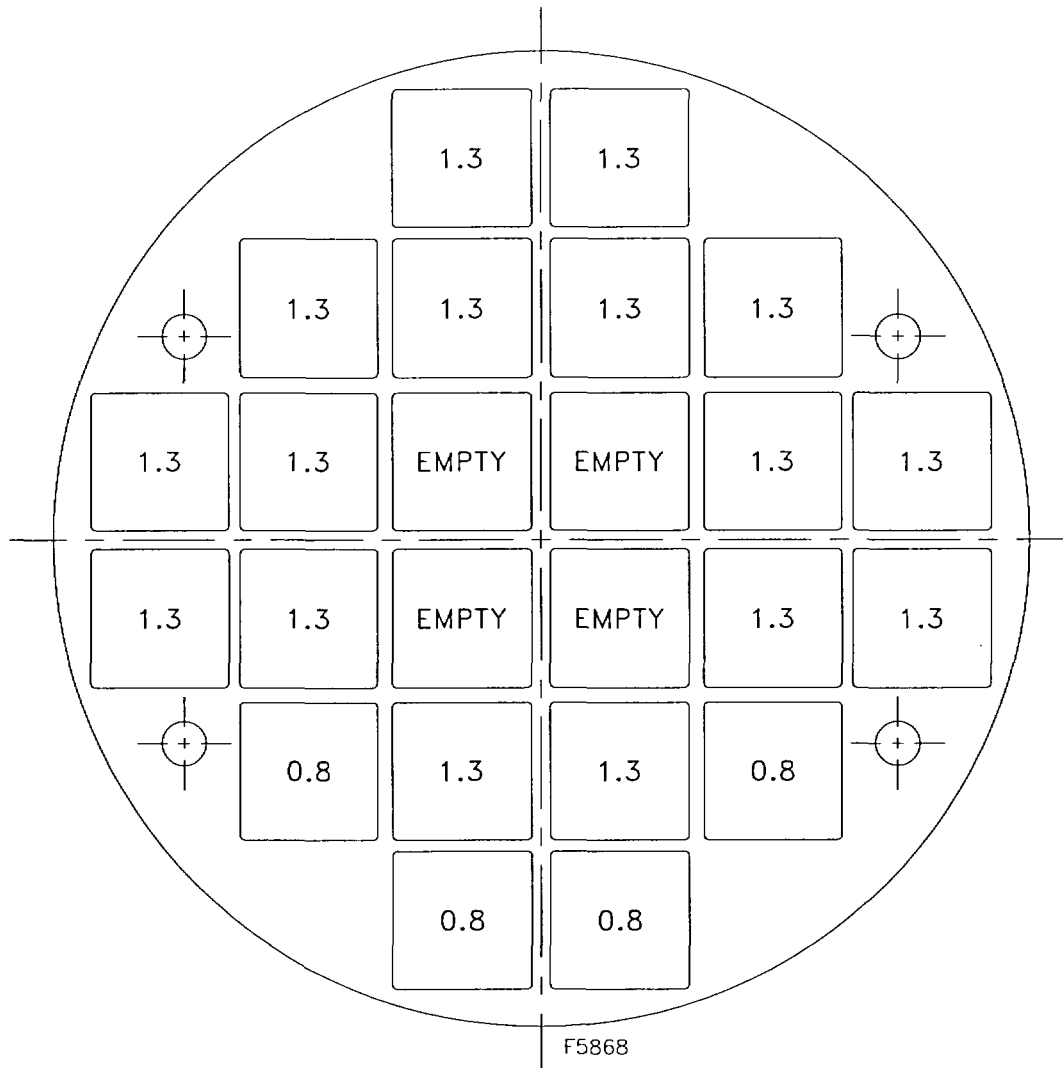


Figure A.4.4-9
24PT4-DSC Heat Load Configurations #2, kW/Assembly



Notes:

1. This analyzed configuration envelopes the configuration specified for the payload in Chapter A.2 where the 1.3 kW / 0.8 kW heat load is replaced with a 1.26 kW / 0.9 kW heat load. Thermal analysis envelopes the total DSC heat load and the differential temperatures used for structural analysis.
2. Fuel Assemblies with a 0.8 kW heat load may be placed anywhere in the 12 locations along the outside periphery of the basket.

Figure A.4.4-10
24PT4-DSC Heat Load Configurations #3, kW/Assembly

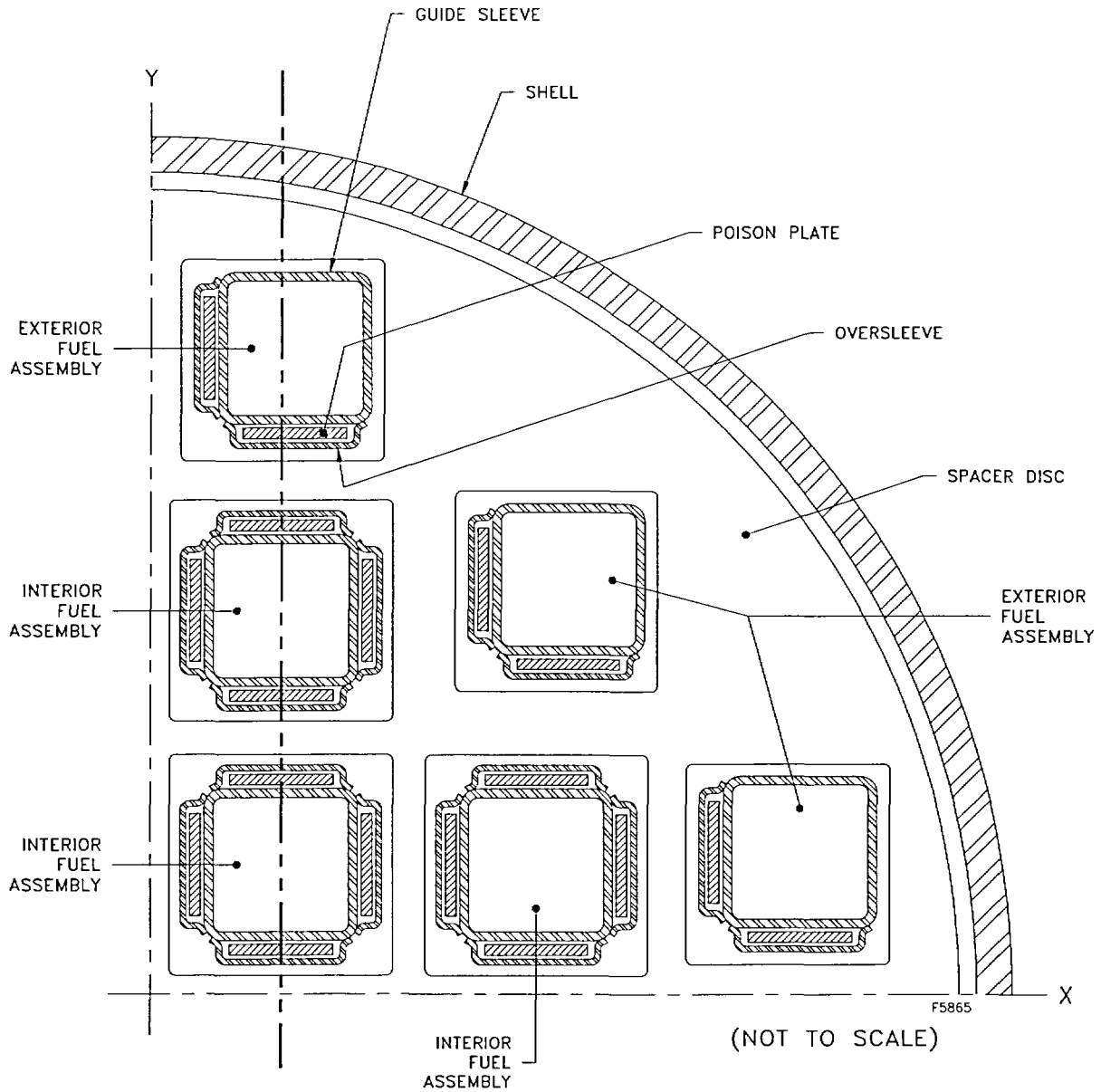


Figure A.4.4-11
Gaps between Components of ANSYS Model Corresponding to Table 4.4-7

A.4.5 Thermal Evaluation for Off-Normal Conditions

A.4.5.1 Overview of Off-Normal Analysis

For off-normal conditions of storage, the 24PT4-DSC components are evaluated for the range of extreme ambient temperatures listed in Table 4.1-1. Should these extreme conditions ever occur, they would be expected to last for a very short time. Nevertheless, these ambient temperatures are conservatively assumed to occur for a sufficient duration to cause a steady-state temperature distribution in the 24PT4-DSC components. For off-normal and accident summer ambient conditions, an insolation of 123 BTU/hr.-ft², is conservatively applied to the AHSM roof surface. The enveloping solar heat flux of 123 Btu/hr-ft² [A4.13] for the extreme off-normal case is based on a flat horizontal surface averaged over a 24 hour day [A4.2]. Solar heat loads are conservatively neglected for the AHSM thermal analysis for off-normal winter ambient conditions.

The off-normal thermal analysis is performed using the same models as those used for the 24PT4-DSC inside the AHSM, the TC, and the 24PT4-DSC basket for normal conditions as described in Sections A.4.4.2, A.4.4.3, and A.4.4.4, respectively. A sunshade is required to be placed over the TC for ambient temperatures above 100°F. This requirement is in Reference [A4.12].

A.4.5.2 Thermal Analysis Results

The maximum 24PT4-DSC shell assembly and basket temperature results for off-normal conditions are given in Table A.4.4-1 and Table A.4.4-2, respectively. The maximum fuel cladding temperature results for off-normal conditions is given in Table A.4.4-3. The 24PT4-DSC and fuel cladding maximum temperatures are compared against their limits in Table A.4.1-2 for off-normal conditions.

The cases providing data for thermal stress analyses are given in Table A.4.4-4.

A.4.5.3 Maximum Pressure

The methodology for calculating the maximum pressure in the 24PT4-DSC cavity during off-normal conditions is the same as that described in Section A.4.4.8 for normal conditions. The criterion for the off-normal pressure is established by accounting for the possible presence of fission gases in the 24PT4-DSC cavity which will reduce the effective cover gas conductivity, and thus increase temperatures and pressures.

As demonstrated in Section A.4.4, the maximum pressure in the 24PT4-DSC cavity will occur while it is in the TC during the peak off-normal summer ambient conditions. The normal operating temperatures presented in Section A.4.4, bound the maximum off-normal ambient temperature case because of the required sunshade over the cask. The resulting maximum average helium temperature for the off-normal case is given in Table A.4.4-6.

For off-normal conditions, 10% failure of the fuel rods is assumed with 100% release of the fuel rod fill gas and 30% release of the fission gas for the ruptured rods assumed, based on guidance

in [A4.2]. The peak off-normal pressure is calculated using the ideal gas law and is presented in Table A.4.4-6.

A.4.5.4 Evaluation of System Performance for Off-Normal Conditions of Storage and Transfer

The thermal analysis for off-normal storage and transfer concludes that the Advanced NUHOMS[®] System design meets all applicable requirements. The maximum temperatures calculated using conservative assumptions are within the criteria set forth. The predicted maximum fuel cladding temperature is well below the allowable fuel temperature limits given in Table A.4.1-2. The comparison of the results with the allowable material temperature ranges is tabulated in Table A.4.1-2.

A.4.6 Thermal Evaluation for Accident Conditions

A.4.6.1 Accident Ambient Conditions

As with the off-normal conditions of storage, the accident conditions for the 24PT4-DSC components are evaluated for the extreme range of design basis ambient temperatures given in Table 4.1-1.

A.4.6.2 Blockage of AHSM Inlet and Outlet Vents

This accident conservatively postulates the complete blockage of the AHSM ventilation air inlet and outlet opening for a maximum of 30 hours concurrent with the extreme hot and cold ambient conditions given in Table A.4.1-1.

A.4.6.2.1 Cause of Accident

Since the NUHOMS[®] AHSMs are located outdoors, there is a remote probability that the ventilation air inlet and outlet openings could become blocked by debris from such unlikely events as floods and tornados. The NUHOMS[®] design features such as the perimeter security fence and the mesh screen covering of the air inlet and outlet openings reduce the probability of occurrence of such an accident. Nevertheless, for this conservative generic analysis, such an accident is postulated to occur and is analyzed.

A.4.6.2.2 Accident Analysis

The thermal effect of this accident results in increased temperatures of the 24PT4-DSC due to the blockage of the AHSM air inlet and outlet openings. The thermal model of the AHSM concrete is identical to the model described in Section 4.4.2.2.

For the postulated blocked vent accident condition, the AHSM ventilation inlet and outlet openings are assumed to be completely blocked for a 40-hour period concurrent with the extreme off-normal ambient condition of 117°F with insolation.

For conservatism, a transient thermal analysis is performed using the 3-D model developed in Section A.4.4.4.1, for heat load zoning configuration 1, 2 and 3. When the inlet and outlet vents are blocked, the air surrounding the DSC in the AHSM cavity is contained (trapped) in the AHSM cavity. The temperature difference between the hot DSC surface and the surrounding cooler heat shield and concrete surfaces in the AHSM cavity will result in closed cavity convection. This closed cavity convection in the AHSM cavity is accounted for by calculating an effective conductivity of air. The AHSM cavity is modeled as a combination of few separate enclosures as described below:

Enclosure 1 – space limited by 24PT4-DSC shell outer circumference and inner surface of heat shields;

Enclosure 2 – space limited by outer surface of heat shields and inner concrete surface opposite the heat shields.

The design of heat shields with an opening at top of enclosures 1 and 2 (otherwise stagnant regions) intensifies the local convection allowing air to flow.

The closed cavity convection everywhere else within AHSM is conservatively neglected.

Heat transfer within AHSM air cavity is modeled by radiation among internal surfaces and free convection with enclosure-wise film coefficient.

For enclosures of closed cavity convection, an increase of thermal conductivity of air from k_{air} , to new value k_{eff} , which accounts for a free convection, an empirical formula [A4.8] for natural convection between two concentric cylinders was applied:

$$\frac{k_{eff}}{k} = 0.386 \cdot \left(\frac{Pr}{0.861 + Pr} \right)^{1/4} \cdot (Ra_c^*)^{1/4},$$

$$Ra_c^* = \frac{\left[\ln \left(\frac{D_o}{D_i} \right) \right]^4}{\delta^3 \cdot \left(D_i^{-3/5} + D_o^{-3/5} \right)^5} \cdot Ra_\delta,$$

$$Ra_\delta = \frac{g \cdot \beta \cdot (T_i - T_o) \cdot \delta^3}{\nu^2} \cdot Pr,$$

where:

Ra_c^*, Ra_δ	–Raleigh numbers,
D_i, D_o	–inner and outer diameters of enclosure,
T_i, T_o	–wall temperature at inner and outer diameters of enclosure,
$\delta = (D_o - D_i)/2$	–thickness of enclosure,
g	–gravitational acceleration,
β	–volumetric coefficient of expansion,
ν	–kinematic viscosity,
$Pr = c_p \cdot \mu / k_{air}$	–Prandtl number,
c_p	–specific heat,
μ	–dynamic viscosity,
k_{air}	–thermal conductivity of air.

Based on Nusselt number :

$$Nu_\delta = k_{eff}/k_{air} = h \cdot \delta / k_{air},$$

a mean film coefficient h for the enclosure was calculated as:

$$h = k_{air} \cdot Nu_\delta / \delta = k_{eff} / \delta .$$

An iterative process was used to determine the mean temperatures for air property calculations. The results are given in table below:

Summary of Closed Cavity Convection Calculation

Enclosure within AHSM	OD	ID	δ	\bar{T}_{hot}	\bar{T}_{cold}	\bar{T}_{mean}	k_{air}	β	ν	Pr	Ra_{δ}	Rac	h
	in	in	in	°F	°F	°F	Btu/min-in.°F	1/°R	ft ² /s	-	-	-	Btu/(in ² -min-°F)
Enclosure 1 – DSC shell-heat shield gap	73	67.19	2.905	587	429	508	3.43e-5	0.00103	4.60e-4	0.679	2.39e+5	4.945e+3	3.12e-5
Enclosure 2 – Heat shield-concrete gap	77	73.21	1.895	429	316	372.5	3.04e-5	0.00120	3.58e-4	0.683	9.17e+4	1.156e+3	2.95e-5

These film coefficients were used in the HEATING 7 AHSM model to determine the transient DSC shell temperatures during blocked vent accident. The calculated DSC shell temperatures described in Chapter 4 were then used as boundary conditions for ANSYS 24PT4-DSC model to calculate the basket and fuel cladding temperatures during blocked vent transient.

The accident duration is assumed for 40 hours, at which time the air inlet and outlet opening obstructions would be cleared by site personnel and natural circulation air flow restored to the AHSM.

The temperature of the spent fuel assemblies and the 24PT4-DSC basket components will rise quickly to the higher temperature increasing heat transfer by radiation, conduction, and convection to the AHSM internal surfaces. In turn, the AHSM surface heatup is limited by the heatup of the entire AHSM. Because the heatup rate of the AHSM is much slower than that of the 24PT4-DSC or the spent fuel, the 24PT4-DSC is assumed to be at steady state at any instant in time and transferring 24 kW of heat to the AHSM. Therefore, the calculated surface temperatures of the 24PT4-DSC shell from the AHSM thermal model are used to determine the maximum 24PT4-DSC basket component and fuel cladding temperatures with a steady state evaluation of the 24PT4-DSC basket.

The initial conditions for the transient analysis correspond to the steady state temperatures calculated at the off-normal analysis extreme ambient temperatures. The maximum concrete temperature during the blocked vent condition was previously calculated and is given in Table 4.4-3.

Figure A.4.6-1, Figure A.4.6-2, and Figure A.4.6-3 present the transient temperature response during the blocked vent accident for the 24PT4-DSC shell, fuel cladding, and support rods for heat load configurations #1, #2, and #3, respectively. The time limit for the heat-up of the 24PT4-DSC basket components is limited by the material temperature limit for the support rods, which reaches the 650°F temperature limit at 31.5, 32.1, and 30.6 hours for load configurations #1, #2, and #3, respectively.

The maximum 24PT4-DSC shell assembly and basket component temperatures for the blocked vent accident are given in Table A.4.4-1 and Table A.4.4-2, respectively. The maximum fuel cladding temperature for blocked vent accident (heat load Configuration #1 at 31.5 hours) is given in Table A.4.4-3.

These temperatures are below the associated safety limits for the AHSM or 24PT4-DSC. The short time exposure of the 24PT4-DSC and the spent fuel assemblies to the elevated

temperatures will not cause any damage. The maximum 24PT4-DSC internal pressure during this event is calculated in Section A.4.6.6.

A.4.6.3 TC Loss of Neutron Shield and Sunshade

The TC and 24PT4-DSC are analyzed for a postulated accident in which the TC loses the annular water neutron shielding and the required sunshade during transfer at the extreme off-normal summer ambient condition. Even though such a scenario would likely result in an immediate corrective action, the duration of the accident is conservatively assumed to result in steady state temperature distributions in the TC and 24PT4-DSC. This analysis was previously performed to support the addition of the TC to the NUHOMS[®] design described in Reference [A4.12]. Therefore, the cask has already been analyzed for such an event.

The maximum shell temperature for this case is 536°F.

Comparison of this shell temperature of 536°F with shell temperature of 602°F for the blocked vent accident for heat load Configuration #3 shows that the TC loss of neutron shield and sunshade accident analysis is bounded by the blocked vent analysis presented in Section A.4.6.2. Hence, end point criteria for the 24PT4-DSC under the blocked vent scenario, such as cavity pressure, fuel cladding integrity, compliance of the 24PT4-DSC structural materials with ASME B&PV Code temperature limit criteria, etc., provide a bounding analysis for the postulated accident in the TC.

A.4.6.4 Fire Accident Evaluation

The fire accident evaluation of the 24PT4-DSC is conducted under the same conditions, and in the same manner, and is described for the Advanced NUHOMS[®] System with 24PT1-DSC in Section 4.6.4. The results for the first 600 minutes are included in Figure A.4.6-4. The maximum calculated DSC shell temperature for the conservative fire condition analyzed is 527°F at 8000 minutes from the beginning of the transient. Comparing this to the results for the 24PT4-DSC in Table A.4.4-1 shows that this extremely conservative fire accident is bounded by the blocked vent accident. Therefore, the end point criteria of the fire for the 24PT4-DSC shell assembly, basket assembly, and fuel cladding are bounded by the blocked vent condition, including accident pressure, fuel cladding and 24PT4-DSC structural component temperatures.

Further, based on the discussion presented in Section 4.6.4, a fire at the inlet of the AHSM with a 24PT4-DSC located within the AHSM is bounded by the analysis provided for a fire accident with the 24PT4-DSC in the TC. Similarly, a fire occurring during transfer operations (i.e., during 24PT4-DSC transfer between the cask and AHSM) will be bounded by the cask/AHSM scenarios discussed above.

Based on the thermal analyses results and the criteria evaluated for the fire accident conditions, the 24PT4-DSC can withstand the hypothetical fire accident event without compromising its confinement integrity and fuel retrievability.

A.4.6.5 Flood Accident

The Advanced NUHOMS[®] System was evaluated for the impact of a worst case flood accident which completely covers the AHSM. The thermal consequences of such an accident are beneficial. The 24PT4-DSC shell temperatures shown in Table A.4.4-1 for the design basis decay heat are higher than the saturation temperature of water. Under these conditions, any water that contacts the 24PT4-DSC surface would eventually boil, providing an extremely effective heat removal mechanism for the 24PT4-DSC. Calculations performed using a boiling correlation show that, given the expected heat flux of the design basis heat load on the 24PT4-DSC surface, the temperature of the canister cannot differ more than 5°F from the water temperature, which is limited by the boiling process. Therefore, the thermal effects of the flood accident are bounded by the other thermal accidents which are considered.

A.4.6.6 Maximum Pressure

The methodology for calculating maximum pressure in the 24PT4-DSC cavity during accident conditions is described in Section A.4.4.8.

Based on evaluation of the basket temperature results in Table A.4.4-2 and the fuel cladding temperature results of Table A.4.4-3, the peak pressure in the 24PT4-DSC cavity for accident conditions will occur during the blocked vent condition. The resulting maximum average helium temperature for the accident case is given in Table A.4.4-6.

For accident conditions, 100% failure of the fuel rods with 100% release of the fill gas from fuel rod and 30% release of the fission gas is assumed, based on guidance in [A4.2]. The maximum accident pressure is calculated by using the ideal gas law and is presented in Table A.4.4-6. The criteria for the accident pressure is established by adding additional margin to the calculated values to account for the presence of fission gases in the 24PT4-DSC cavity which might reduce the effective cover gas conductivity, and thus increase temperatures and pressures.

A.4.6.7 Evaluation of System Performance for Accident Conditions of Storage and Transfer

The thermal analysis for storage and transfer accidents concludes that the 24PT4-DSC design meets all applicable requirements. The maximum temperatures calculated for components necessary to ensure structural integrity, confinement and retrievability of the fuel using conservative assumptions are within the criteria set forth. The predicted maximum fuel cladding temperature is well below the allowable fuel temperature limits given in Table A.4.1-3. The comparison of the results with the allowable material temperature ranges is tabulated in Table A.4.1-3.

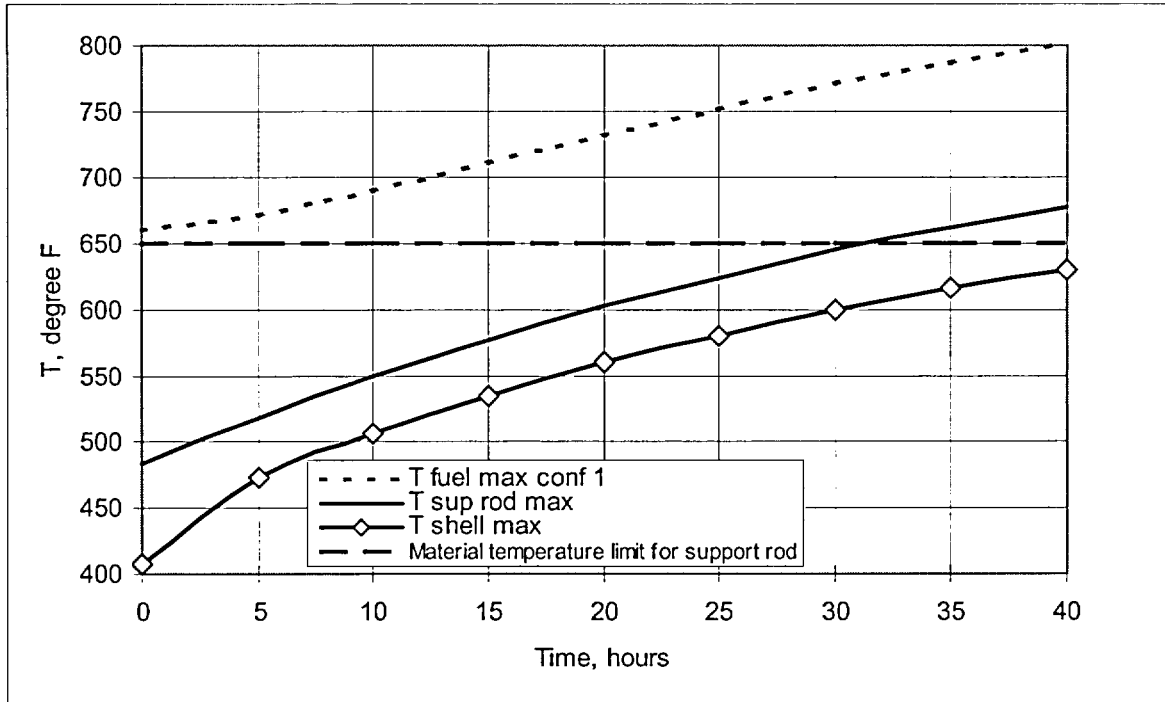


Figure A.4.6-1
Transient Temperatures of 24PT4-DSC Components during Blocked Vent Case – Heat Load Configuration #1

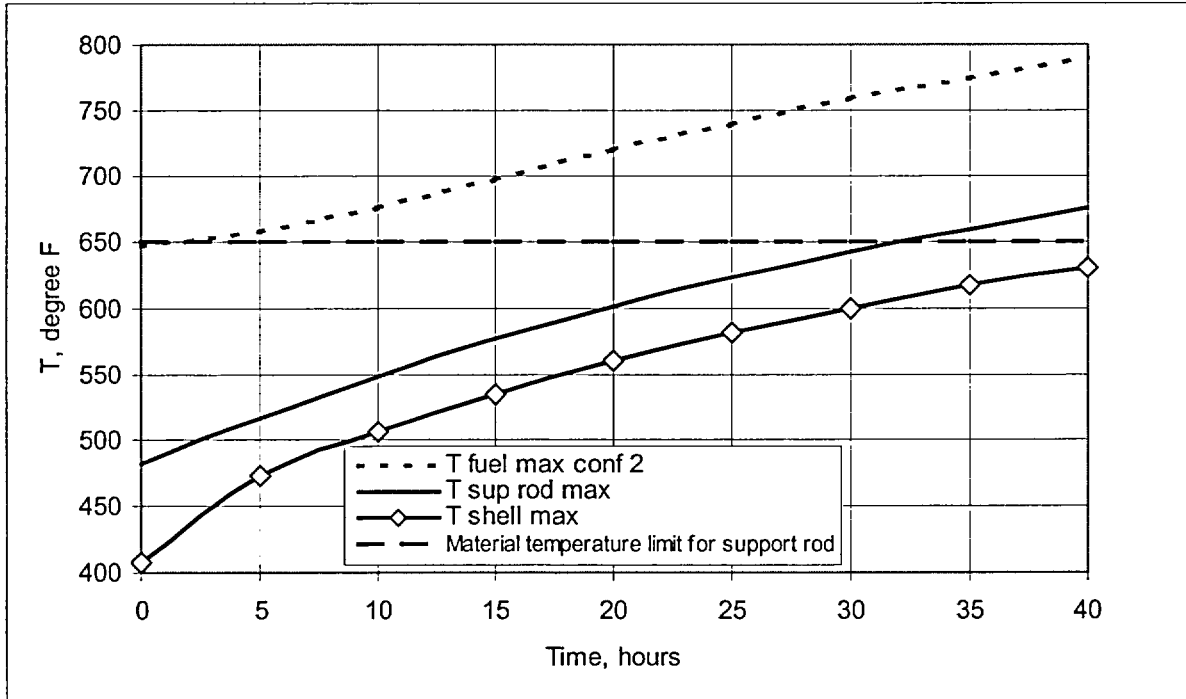


Figure A.4.6-2
Transient Temperatures of 24PT4-DSC Components during Blocked Vent Case – Heat Load Configuration #2

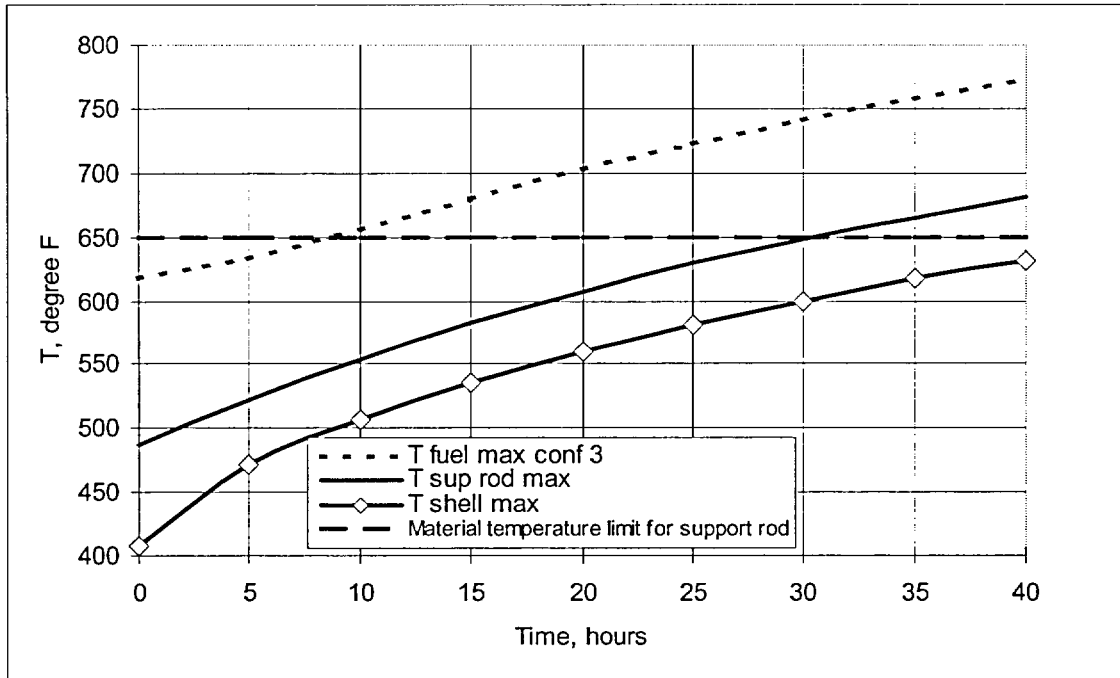


Figure A.4.6-3
Transient Temperatures of 24PT4-DSC Components during Blocked Vent Case – Heat Load Configuration #3

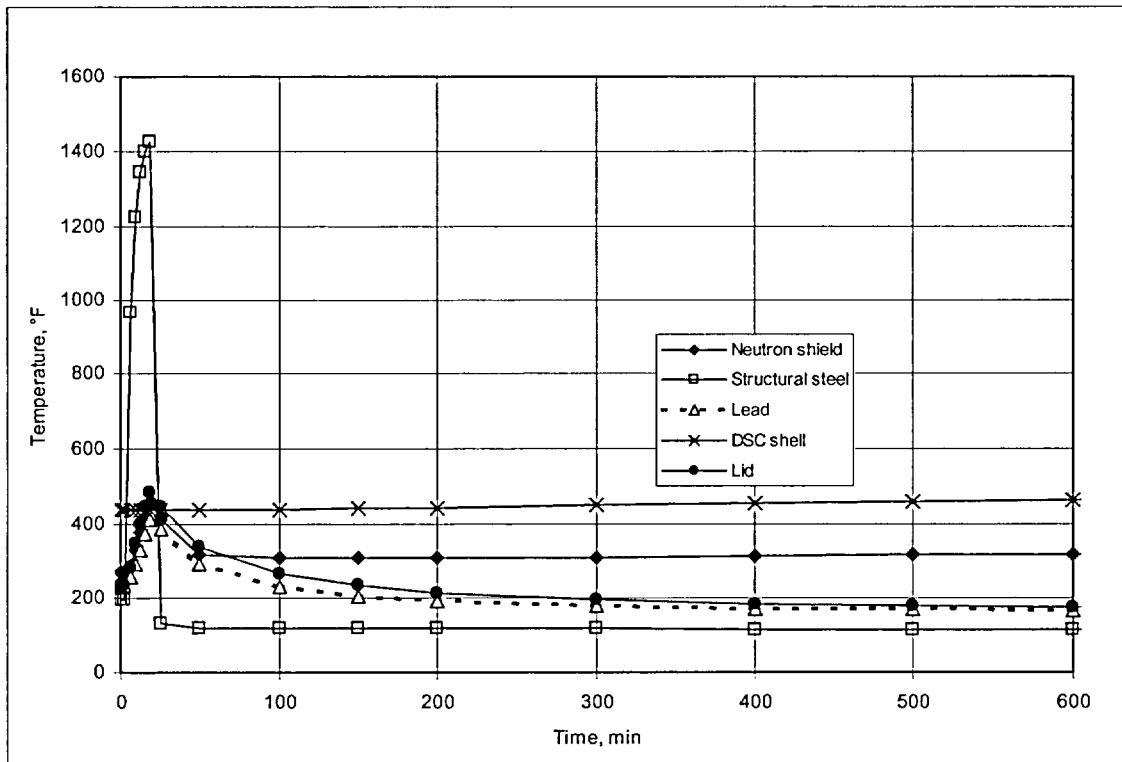


Figure A.4.6-4
OS197H Cask and 24PT4-DSC Response to Fire Accident

A.4.7 Thermal Evaluation for Loading/Unloading Conditions

All fuel transfer operations occur when the 24PT4-DSC is in the spent fuel pool. The fuel is always submerged in free-flowing pool water permitting heat dissipation. After fuel loading is complete, the 24PT4-DSC is removed from the pool, drained, dried, and backfilled with helium.

The three bounding loading conditions evaluated are (1) the heatup of the 24PT4-DSC before the cavity can be backfilled with helium (i.e., prior to blowdown), (2) the vacuum drying transient, and (3) steady state temperatures subsequent to helium backfill. Transient thermal analyses are performed to predict the heatup time history for the 24PT4-DSC components during these events.

The unloading operation considered is the reflood of the 24PT4-DSC with water.

A.4.7.1 Vacuum Drying Thermal Analysis

Analyses were performed for the vacuum drying condition in order to ensure that the steady state fuel cladding and 24PT4-DSC structural component temperatures remain below the maximum allowable material limits shown in Table A.4.7-1. In addition, a transient analysis was performed to ensure the requirements defined by ISG-11 [A4.21] for short-term operations (including vacuum during and helium backfilling operating conditions) are satisfied. According to ISG-11, the maximum fuel cladding temperature cannot exceed $T_{\text{ISG limit}} = 400^{\circ}\text{C}$ (752°F) and the temperature difference during the thermal cycling of the cladding cannot exceed $\Delta T_{\text{ISG limit}} = 65^{\circ}\text{C}$ (117°F).

During vacuum drying operation, water in the DSC cavity is forced out of the cavity (blowdown operation) before the start of vacuum drying. Two alternate options for the gas medium used for the water blowdown operation are evaluated.

In the first option, air is used as the gas medium to remove water and subsequent vacuum drying occurs with air environment in the DSC cavity. In the second option, helium is used as the medium to remove water and subsequent vacuum drying occurs with helium environment in the DSC cavity.

In the thermal analysis for the vacuum drying transient, either air or helium is used as the medium present in the DSC cavity during vacuum drying process. Details of the thermal analysis performed for these two alternate options are described in the following sections.

A.4.7.1.1 Vacuum Drying with Air during Blowdown

For the vacuum drying analysis, the 24PT4-DSC model is similar to that described in Section A.4.4.4. The exception is that the helium regions are replaced with air. Assuming that the cavity is filled with air during the vacuum drying operation provides conservative results since the void volume is typically filled with a mixture of air, water and water vapor, and no credit is taken for evaporation of water, which is a strong cooling mechanism that takes place during this operation. Air thermal conductivity does not change significantly at lower pressures, therefore, the use of a thermal conductivity for a pressure higher than 3 Torr is acceptable. As stated in Chapter A8,

water is required to be in the annulus between the 24PT4-DSC and the TC during the vacuum drying process. Therefore, the 24PT4-DSC shell boundary is set to a temperature of 230°F as a conservative estimate of the shell wall temperature during this operation. A heat load of 24 kW is used in computing the maximum fuel cladding and basket component temperatures.

The maximum steady state fuel cladding temperature during vacuum drying, 740°F, does not exceed the ISG-11 limit of 752°F. However, steady state calculations subsequent to helium backfill show a maximum temperature of 559°F, or a ΔT of $740^\circ\text{F} - 559^\circ\text{F} = 181^\circ\text{F}$ for heat load Configuration #1. As this temperature difference exceeds the ISG-11 ΔT limit of 117°F, a time limit must be placed upon vacuum drying so that this limit is not exceeded. A conservative ΔT of 100°F is assumed, resulting in a maximum allowed cladding temperature of $559^\circ\text{F} + 100^\circ\text{F} = 659^\circ\text{F}$ for the vacuum drying transient for heat load Configuration #1. For heat load Configuration #2 the maximum allowed fuel cladding temperature is 644°F. For heat load Configuration #3 the maximum allowed fuel cladding temperature is 606°F. A transient calculation demonstrates that the maximum fuel temperature reaches values of 659°F, 644°F and 606°F at a time of 32.3 hours, 33.4 hours, and 24.5 hours for heat load Configurations #1, #2 and #3, respectively. The results are summarized in Figure A.4.7-2 and Table A.4.7-1. Therefore, the maximum duration for vacuum drying with air during blowdown is conservatively set at 32 hours, 33 hours and 24 hours for heat load Configurations #1, #2 and #3, respectively. The maximum temperatures for vacuum drying using air for blowdown are presented in Table A.4.4-2 and Table A.4.4-3 for the basket structural components and fuel cladding, respectively.

A.4.7.1.2 Vacuum Drying with Helium during Blowdown

For the vacuum drying analysis, the model is similar to that described in Section A.4.4.4. Similar to air, helium thermal conductivity also remains pressure independent down to 3 Torr, [A4.23], therefore, the helium thermal conductivity at normal pressure is used for this analysis. The boundary conditions applied to the model are the same as those used for vacuum drying after blowdown by air.

The maximum steady state fuel cladding temperature during vacuum drying, 559°F, does not exceed the ISG-11 limit of 752°F.

Since the similar material properties and boundary conditions applied to vacuum drying with helium during blowdown and helium backfilling operations, the maximum fuel cladding temperature of 559°F during helium backfilling remains unchanged after vacuum drying in helium, the ISG-11 thermal cycling temperature limit is satisfied and no time limit for vacuum drying in helium required. The results for Configurations #1, #2, and #3 are presented in Table A.4.7-1. The maximum temperatures for vacuum drying using helium for blowdown are presented in Table 4.4-2 and Table 4.4-3 for the basket components and fuel, respectively.

A.4.7.2 Pressure during Unloading of Cask

To unload the fuel from the 24PT4-DSC, reflooding of the cavity is required. This occurs by reducing the pressure in the 24PT4-DSC to atmospheric conditions followed by introducing water into the cavity through the drain port and venting through the vent port. Since fuel

temperatures are expected to be significantly higher than the saturation temperature of water, flooding of the hot 24PT4-DSC will result in steam generation which, if not vented, will result in a higher cavity pressure.

The flow rate of water into the 24PT4-DSC during reflood is controlled during this operation so that the pressure within the 24PT4-DSC stays below the assumed 20 psig for this condition.

A.4.7.3 Cask Heatup Analysis

Heatup of the water within the 24PT4-DSC cavity prior to blowdown and backfilling with helium occurs as operations are performed to decon the cask and drain and dry the 24PT4-DSC. Prevention of boiling in the Advanced NUHOMS[®] System is not required to ensure public health and safety for the following reasons:

1. The criticality analysis considers a wide range of moderator densities which include that of steam (Chapter A6). Criticality limits were shown to be met at conditions of low moderator density (boiling water).
2. The cavity is always vented during the water heatup transient.
3. Although steam may be produced through boiling of the cavity water, its presence in the weld joint area during the top inner cover plate welding operations will be essentially blocked at the interface between the shield plug and the support ring. What little steam that may be present is displaced by the argon shielding gas used in the GTAW process. This shielding gas is heavier than steam and is delivered at a sufficiently high rate (usually 30 – 50 ft³/hr) to assure that the steam is excluded from the weld joint. Finally, if moisture somehow did enter the weld area, the resulting weld bead porosity would be readily detectable by the visual inspection of each pass performed by the welding operator and the dye penetrant (PT) examination performed on the surface of the root pass.

Therefore, the only potential concern associated with steam generation is shielding. An unexpectedly high loss of water within the 24PT4-DSC cavity during these loading operations could result in increased occupational exposure. The following analysis is presented to identify to the licensees the time for the water in the 24PT4-DSC cavity to boil so that corrective action can be planned and implemented as necessary to address ALARA concerns.

The model conservatively does not credit any heat transfer in the axial direction. Homogenized effective thermal properties of the 24PT4-DSC cavity are calculated based on the weight, volume and material of the components. Radiation heat transfer within the 24PT4-DSC cavity is neglected. All temperatures in the 24PT4-DSC are initially assumed to be at the maximum spent fuel pool temperature. The exterior of the cask is assumed to radiate and convect heat to the prevailing ambient conditions of the fuel building. The analyses are performed for a building temperature of 120°F and a fuel pool temperature of 140°F. The results are tabulated in Table A.4.7-2 and shown in Figure A.4.7-1 for canister decay heat loads ranging from 12 to 24 kW.

A.4.7.4 Pressure During Loading of Cask

The maximum pressure during cask blowdown is 20 psig. This is discussed in Chapter A.3.

**Table A.4.7-1
Vacuum Drying Results following Blowdown with Air or Helium**

Component Heat Load	Max ^m Temperature during Vacuum Drying (Air Blowdown)			Max ^m Temperature during Vacuum Drying (Helium Blowdown)			Limit Ref (°F)
	Conf. #1 (°F)	Conf. #2 (°F)	Conf. #3 (°F)	Conf. #1 (°F)	Conf. #2 (°F)	Conf. #3 (°F)	
Fuel	659	644	606	559	544	506	752 [A4.21]
Support Rod	398	398	388	345	343	349	650 [A4.4]
Guidesleeve	632	615	556	557	542	501	800 [A4.4]
Boral [®]	632	615	556	557	542	501	1000 [A4.4]
Spacer Disc	617	607	527	555	539	496	800 [A4.4]

Table A.4.7-2
Summary of Water Heatup Calculation

Decay Heat, kW	Time, hrs	
	$T_{\text{pool}}=140^{\circ}\text{F}$	$T_{\text{sb}}=120^{\circ}\text{F}$
12	31.4	
14	25.9	
16	22.2	
18	19.5	
20	17.4	
22	15.7	
24	14.3	

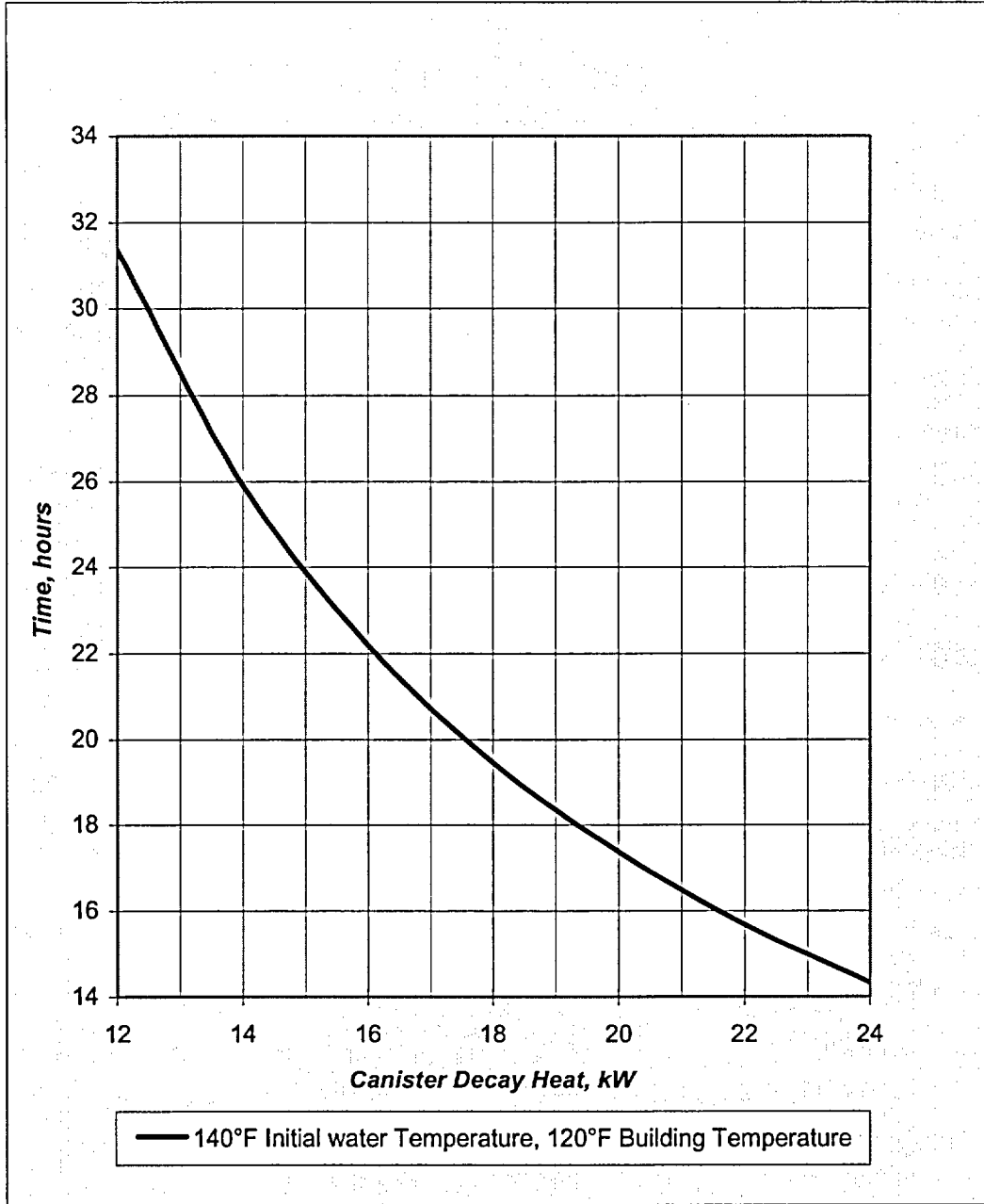


Figure A.4.7-1
Time to Reach Boiling Conditions Inside 24PT4-DSC Cavity

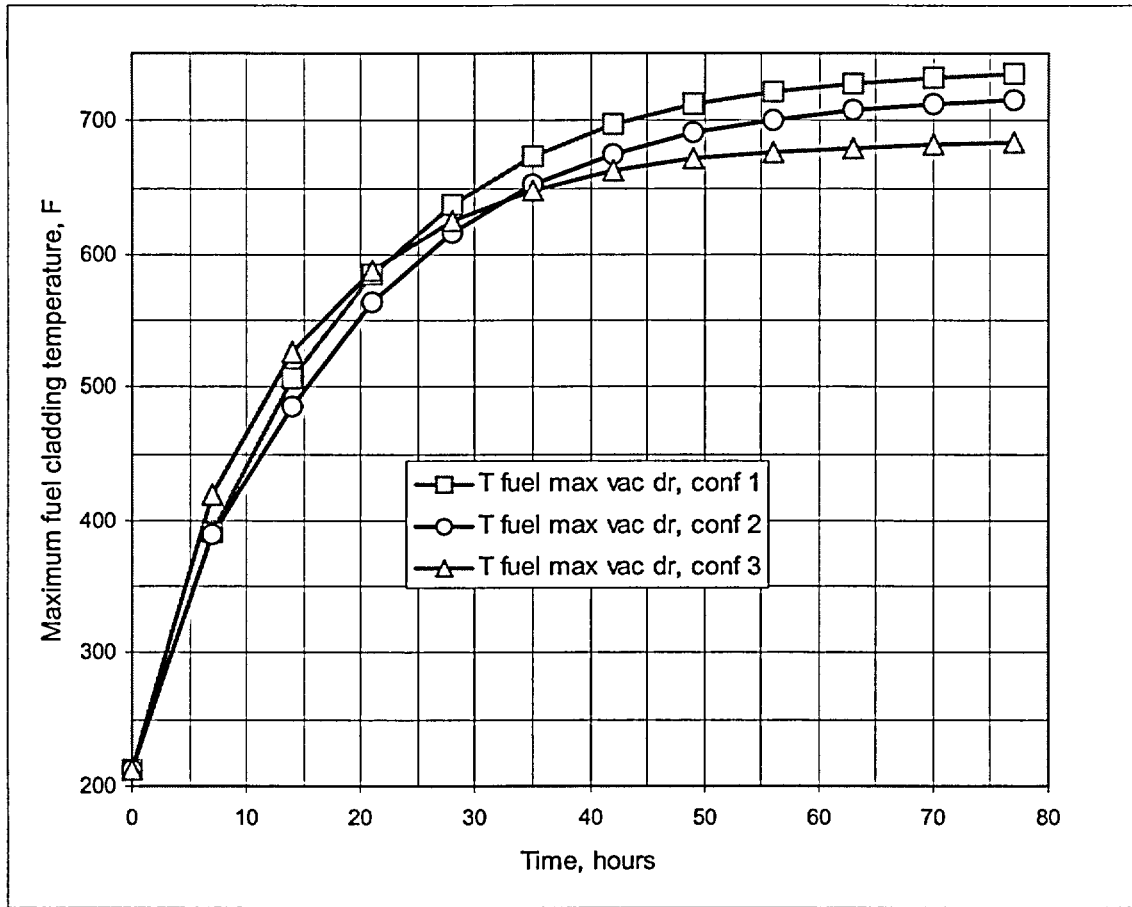


Figure A.4.7-2
Maximum Fuel Cladding Temperature during Vacuum Drying using Air for Blowdown

A.4.8 Confirmatory Thermal Analysis Of The 24PT4-DSC

A confirmatory thermal analysis [A4.22] of the heat transfer within the 24PT4-DSC, including the effects of convection heat transfer, was conducted using the Thermal Desktop™ [A4.25] and SINDA/FLUINT™ software codes [A4.24]. These programs are designed to function together to provide the functions needed to build, exercise, and post-process a thermal model. The Thermal Desktop™ computer program is used to provide graphical input and output display function, as well as computing the radiation exchange conductors for the defined geometry and optical properties. Thermal Desktop™ is designed to run as an AutoCAD™ application. As such, all of the CAD tools available for generating geometry within AutoCAD™ can be used for generating a thermal model. In addition, the use of the AutoCAD™ layers tool presents a convenient means of segregating the thermal model into its various elements.

The SINDA/FLUINT™ computer program is a general purpose code suitable for either finite difference or finite-element models. The code can be used to compute the steady-state and transient behavior of the modeled system. SINDA/FLUINT™ has been validated for simulating the thermal response of spent fuel packages and has been used in the safety analysis of numerous recent license applications to the NRC.

The confirmatory calculation is based on an alternative methodology to that used for the ANSYS analytical model described in Section A.4.4 and is intended to provide a confirmation of the peak fuel cladding and critical basket temperatures determined using the ANSYS analytical model. Comparison of the predicted temperatures obtained using the Thermal Desktop™ and SINDA/FLUINT™ software codes to the test results obtained from a 1/5 scale model of the NUHOMS®-24P design and to a full scale test of the NUHOMS®-7P design provide validation of the calculation methodology employed in the confirmatory analysis.

The thermal model of the 24PT4-DSC developed for use in the confirmatory analysis is based on the same basket geometry (i.e., Figure A.4.4-1 and Figure A.4.4-2), the same gap assumptions (see Table A.4.4-7), and the same material properties (see Section A.4.2) as used for the ANSYS analytical model described in Section A.4.4.

Table A.4.8-1 and Figure A.4.8-1 present a comparison of the component temperatures obtained using the ANSYS analytical model vs. those obtained using the confirmatory analysis methodology. This comparison is for heat load Configuration #1 for the normal storage condition with 70°F ambient temperature. In each case, the shell temperature distribution around the circumference of the 24PT4-DSC was input to the analysis as a boundary condition. As seen from the table, the results from the ANSYS analytical model are 10-16°F higher than predicted by confirmatory analysis for basket components and conservatively bound the confirmatory analysis results.

The peak fuel cladding temperature predicted by confirmatory analysis is within 19°F of peak temperature predicted by ANSYS model.

These results demonstrate the ANSYS analytical model predicts accurate fuel cladding temperatures and conservatively bounding basket component temperature levels for the 24PT4-DSC.

The confirmatory testing methodology has also been validated against NUHOMS[®] system test data [A4.19] and [A4.20]. A comparison of these tests against the SINDA/FLUINT[™] confirmatory analysis model is provided in Table A.4.8-2, Table A.4.8-3, Figure A.4.8-2 and Figure A.4.8-3. These comparisons show a very good agreement between the confirmatory analysis method and the test results.

A comparison of the SINDA/FLUINT[™] analysis as well as the test results to the ANSYS model indicates a more pronounced shift in the maximum temperature toward the top of the DSC. This temperature shift is expected as a result of the convection within the DSC. The convection causes the hot air to shift the peak temperatures toward the top of the horizontally stored DSC.

Figure A.4.8-4 provides a representation of the pictorial convective flow patterns within the DSC.

Table A.4.8-1
Comparison of 24PT4-DSC Component Temperatures, Normal Storage with 70°F Ambient Temperature, Load Configuration #1

EDSC Component	ANSYS Analytical Model	Confirmatory Analysis
Maximum Shell	373°F	373°F
Maximum Guidesleeve	636°F	626°F
Maximum Spacer Disc	634°F	618°F
Maximum Fuel Cladding	638°F	657°F

Table A.4.8-2
Comparison of DSC Component Temperatures for KHI Test, Test Measurements vs. Confirmatory Analysis Methodology

DSC Component	Test Measurement	Confirmatory Analysis Methodology
Maximum Fuel Cladding	N/A	N/A
Maximum Guidesleeve	158°F	156°F
Maximum Spacer Disc	N/A	N/A
Maximum Shell	145°F	145°F

Note:
 Fuel and spacer discs were not simulated in the KHI test configuration.

Table A.4.8-3
Comparison of DSC Component Temperatures for NUHOMS 7P, Test Measurements vs. Confirmatory Analysis Methodology

DSC Component	Test Measurement	Confirmatory Analysis Methodology
Maximum Fuel Cladding	357°F	365°F
Maximum Guidesleeve	341°F	350°F
Maximum Spacer Disc	N/A	330°F
Maximum Shell	240°F	240°F

Note:
 Spacer disc temperature not measured in test. Shell temperature used as boundary temperature the in analysis.

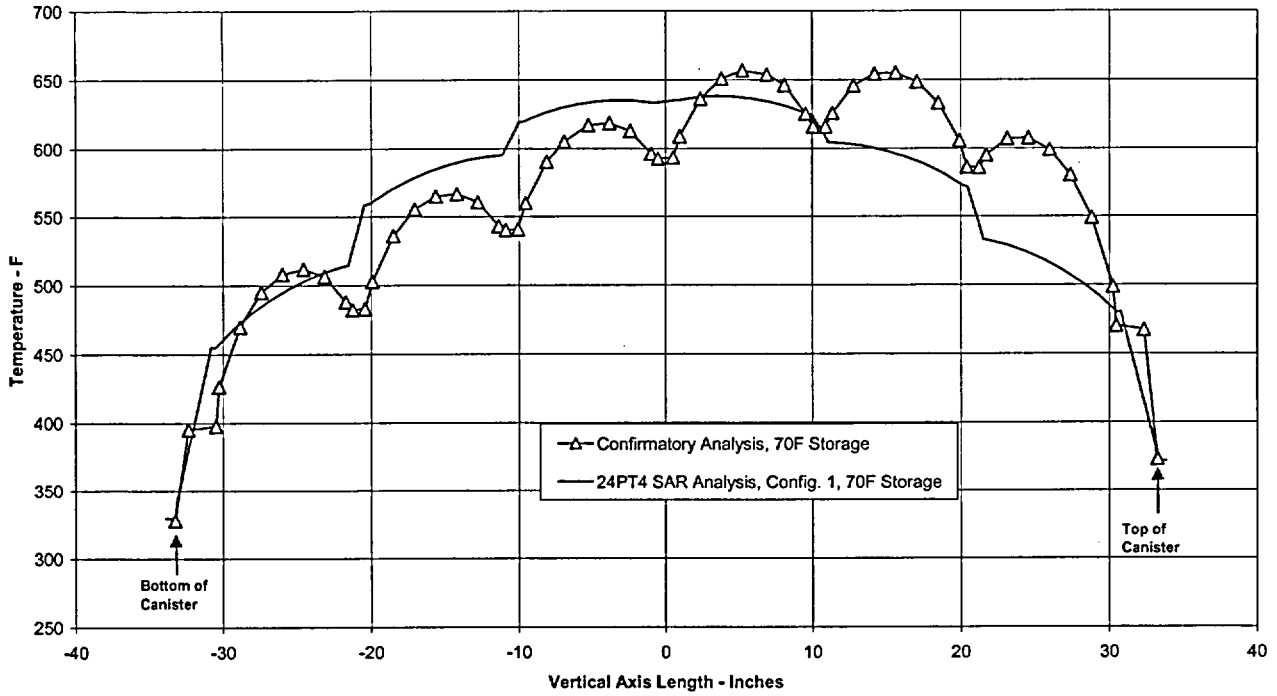


Figure A.4.8-1
Vertical Temperature Profile for 24PT4-DSC, 70°F Normal Storage Condition

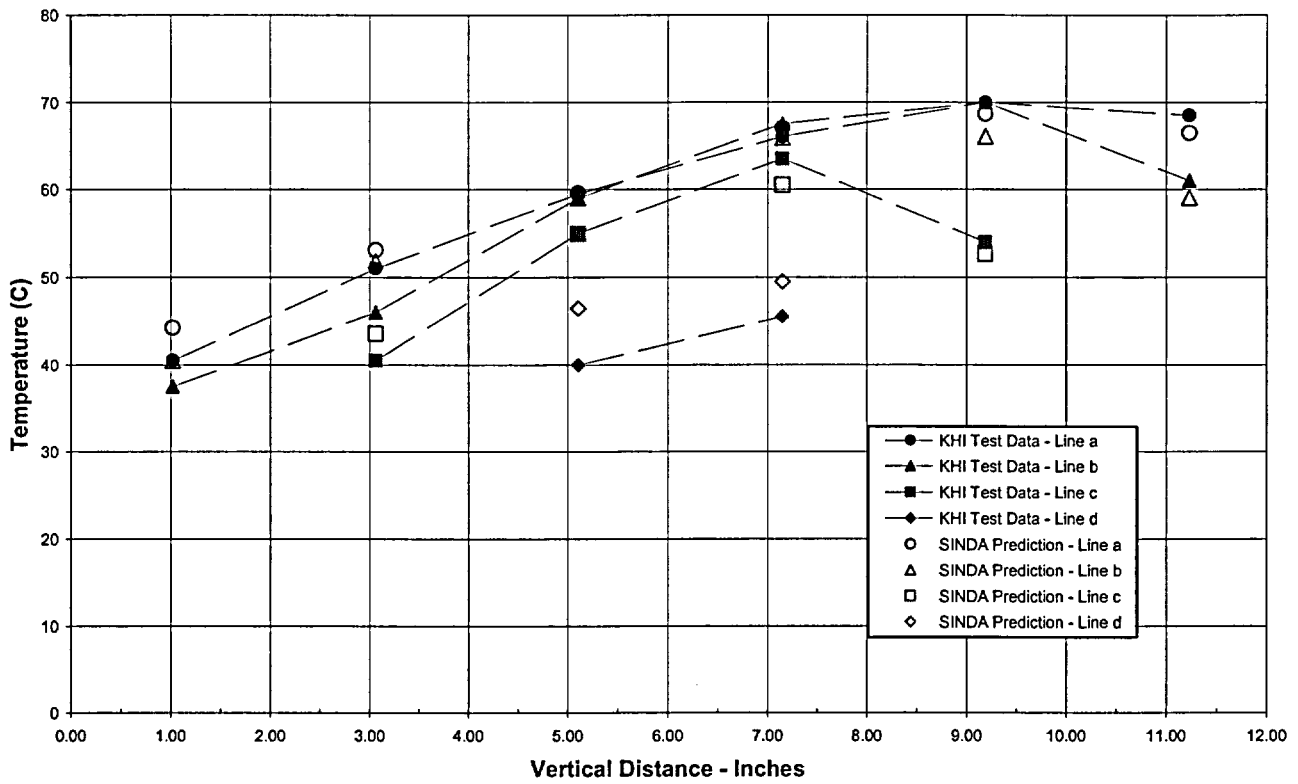


Figure A.4.8-2
Comparison of Predicted SINDA/FLUINT™ Temperatures to KHI Test Results

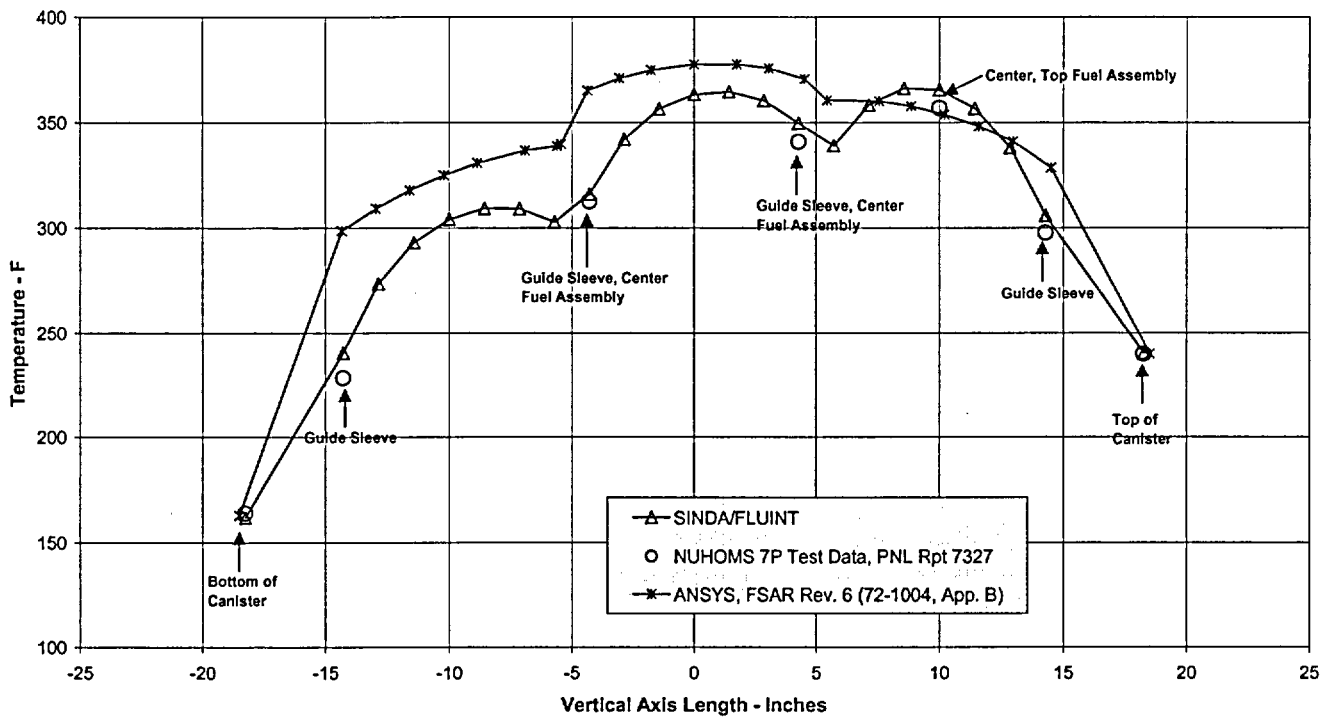


Figure A.4.8-3
Comparison of Predicted vs. Test Results (PNL-7327) for NUHOMS®-7P

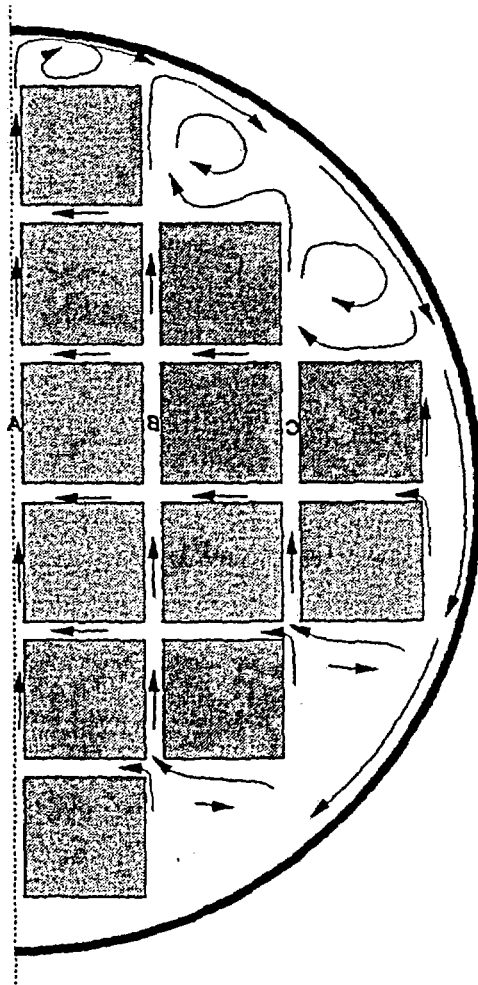


Figure A.4.8-4
General Flow Patterns Expected within Canister

A.4.9 Supplemental Information

A.4.9.1 References

- [A4.1] “Topical Report on Actinide-Only Burnup Credit for PWR Spent Nuclear Fuel Packages,” Office of Civilian Radioactive Waste Management, DOE/RW-0472, Revision 2, September 1998.
- [A4.2] NRC NUREG-1536, Standard Review Plan for Dry Cask Storage Systems, January 1997.
- [A4.3] Bolz, R. E., G. L. Tuve, CRC Handbook of Tables for Applied Engineering Science, 2nd Edition, 1973.
- [A4.4] American Society of Mechanical Engineers, Boiler & Pressure Vessel Code, Section III, 1992 Edition with Addenda through 1994 with Code Cases N-595-1 and N-499-1.
- [A4.5] “Standard Specification for BORAL[®] Composite Sheet,” Specification Number BPS-9000-04, AR Advanced Structures, Livonia, Michigan. PROPRIETARY.
- [A4.6] E. A. Brandes (Editor), Smithells Metals Reference Book, 6th Ed., Butterworths, London, UK, 1983.
- [A4.7] Roshenow, W. M., J. P. Hartnett, and Y. I. Cho, Handbook of Heat Transfer, 3rd Edition, 1998.
- [A4.8] Incropera, F. P., D. P. DeWitt, Fundamentals of Heat and Mass Transfer, 4th Edition, Wiley, 1996.
- [A4.9] Bucholz, J. A., Scoping Design Analysis for Optimized Shipping Casks Containing 1-, 2-, 3-, 5-, 7-, or 10-Year old PWR Spent Fuel, Oak Ridge National Laboratory, January 1983, ORNL/CSD/TM-149.
- [A4.10] Siegel, R. and J. R. Howell, Thermal Radiation Heat Transfer, 2nd Edition, Hemisphere, 1981.
- [A4.11] MATPRO – Version 11: A Handbook of Materials Properties for Use in the Analysis of Light Water Reactor Fuel Rod Behavior, EG&G Idaho, Idaho Falls, February 1979, NUREG-CR/0497.
- [A4.12] TN West, Final Safety Analysis Report for the Standardized NUHOMS[®] Horizontal Modular Storage System for Irradiated Nuclear Fuel, Revision 6, November 2001, NRC Docket No. 72-1004.
- [A4.13] Title 10, Code of Federal Regulations, Part 71 (10CFR71), *Packaging and Transportation of Radioactive Materials*, U.S. Nuclear Regulatory Commission, 1997.

- [A4.14] Frank Kreith, Principles of Heat Transfer, Third Edition, Harper and Row Publishers.
- [A4.15] ANSYS User's Manual for ANSYS Revision 5.6.2.
- [A4.16] Hottel, H. C. and A. F. Sarofim, Radiative Transfer, Chapter 4, p. 164, McGraw-Hill, New York, 1967.
- [A4.17] Fax From DAV-Tech Plating, Emissivity of Electroless Nickel on Carbon Steel, March 30, 2000, Transnuclear Project File SCE-01.0100.
- [A4.18] 10CFR 72, Rules and Regulations, Title 10, Code of Federal Regulations - Energy, U.S. Nuclear Regulatory Commission, Washington, D.C., "Licensing Requirements for the Independent Storage of Spent Nuclear Fuel and High-Level Radioactive Waste."
- [A4.19] Nishimura, M., H. Shibazaki, S. Fujii, and I. Maekawa, *Natural Convection Heat Transfer in the Horizontal Dry Storage System for the LWR Spent Fuel Assemblies*, Journal of Nuclear Science and Technology, Vol. 33, No. 11, pp. 821-828, November 1996.
- [A4.20] "NUHOMS[®] Modular Spent-Fuel Storage System: Performance Testing", Report PNL-7327/UC-812/EPRI NP-6941, Pacific Northwest Laboratory & Carolina Power and Light Company, September 1990.
- [A4.21] Interim Staff Guidance No. 11, ISG-11, Rev. 2, Cladding Considerations for the Transportation and Storage of Spent Fuel, US NRC, July 2002.
- [A4.22] Calculation, "Alternative Thermal Analysis of the 24PT1 and 24PT4 Canister for SCE," Calculation Number SCE-23.0404, Revision 1.
- [A4.23] Lide, David R., CRC Handbook of Chemistry and Physics, 83rd Edition, 2002-2003, CRC Press.
- [A4.24] SINDA/FLUINT[™], Systems Improved Numerical Differencing Analyzer and Fluid Integrator, Version Cullimore and Ring Technologies, Inc., Littleton, CO, 2001.
- [A4.25] Thermal Desktop[™], Version 4.4., Cullimore and Ring Technologies, Inc., Littleton, CO, 2001.
- [A4.26] Manual of Steel Construction, 8th Edition, 1980.

A.5 SHIELDING EVALUATION

Sections of this Chapter have been identified as “No change” due to the addition of 24PT4-DSC to the Advanced NUHOMS[®] system. For these sections, the description or analysis presented in the corresponding sections of the FSAR for the Advanced NUHOMS[®] system with 24PT1-DSC is also applicable to the system with 24PT4-DSC.

The shielding evaluation for the 24PT4-DSC payloads use three dimensional shielding models as opposed to the two dimensional models used for the 24PT1-DSC.

The shielding evaluation presented for the Advanced NUHOMS[®] System demonstrates adequacy of the shielding design for the payload described in Chapter A.2. The geometry of the Advanced NUHOMS[®] System is described in Section A.1.5.2 and 1.5.2 (for the AHSM). The heavy concrete walls and roof of the Advanced Horizontal Storage Module (AHSM) provide the bulk of the shielding for the payload in the storage condition. During fuel loading and transfer operations, the combination of thick steel and lead shield plugs at the ends of the 24PT4-DSC and heavy steel/lead/neutron shield material of the OS197H Transfer Cask (TC) provide shielding for personnel loading and transferring the 24PT4-DSC to the AHSM. Figure A.5.1-1 through Figure A.5.1-4 and Table A.5.1-1 provide the general configuration and (nominal) material thicknesses of the important components of the Advanced NUHOMS[®] System.

The design-basis PWR fuel source terms are derived for the Combustion Engineering 16x16 (CE 16x16) assembly design as described in Section A.5.2.

The 24PT4-DSC is designed to store intact and damaged PWR fuel assemblies with the specifications as described in Tables A.2.1-1 through A.2.1-3. The 24PT4-DSC may store PWR fuel assemblies arranged in any one of the three alternate heat zoning configurations shown in Figures A.2.1-1, A.2.1-2 and A.2.1-3, with a maximum decay heat of 1.26 kW per assembly and a maximum heat load of 24 kW per canister. Evaluation of reconstituted fuel with up to eight (8) stainless steel replacement rods each is discussed in Section A.5.2. The limiting features are burnup, initial enrichment, cooling time, fissile material type, number of fuel rods, number of guide tube/instrument tube holes and initial heavy metal.

The design-basis fuel source terms for this evaluation bound the source term from fuel with the burnup/initial enrichment/cooling time combination given in Tables A.2.1-5 through A.2.1-8 for intact fuel and Tables A.2.1-9 through A.2.1-12 for reconstituted fuel with stainless steel rods, and located in the basket as shown in Figure A.2.1-1, Figure A.2.1-2, or Figure A.2.1-3.

The design basis shielding source terms used in this evaluation are for fuel assemblies with a burnup of 45 GWd/MTU, an initial enrichment of 3.8 wt. % ²³⁵U and five years cooling. These gamma and neutron source terms result in bounding dose rates on the surface of the AHSM and TC. The bounding shielding evaluation presented herein assumes 24 design basis fuel assemblies, which have gamma and neutron source terms in all 24 locations, consistent with a canister total heat load of 30.1 kW, as compared to the 24 kW design basis heat load limit. Therefore, these source terms result in conservative dose rates on and around the AHSM and TC.

The minimum cooling time for the reconstituted fuel assemblies are determined such that the source terms from the reconstituted fuel are bounded by the design basis analyses.

The methodology, assumptions, and criteria used in this evaluation are summarized in the following sections.

A.5.1 Discussion and Results

The dose rates for 24 design basis CE 16x16 PWR fuel assemblies stored in the Advanced NUHOMS[®] System are summarized in Table A.5.1-2 through Table A.5.1-5. These dose rates are calculated using the MCNP three-dimensional Monte Carlo transport code [A5.8]. Table A.5.1-2 provides the dose rates on the surface of the AHSM, while Table A.5.1-3 through Table A.5.1-5 provide the dose rates on and around the TC (sides, top and bottom) during fuel loading and transfer operations.

The source term calculations presented in Section A.5.2, are developed for the design basis fuel with 45 GWd/MTU burnup, a minimum initial enrichment of 3.8 weight % ²³⁵U, and a cooling time of 5 years. Reconstituted assemblies in which damaged fuel rods are replaced with undamaged fuel rods are bounded by this analysis.

A discussion of the method used to determine the design basis fuel source terms is included in Section A.5.2. The model specification and shielding material densities are given in Section A.5.3. Thermal and radiological source terms are calculated with the SAS2H/ORIGEN-S modules of SCALE 4.4 [A5.1]. The method used to determine the dose rates due to 24 design basis fuel assemblies in the Advanced NUHOMS[®] System is provided in Section A.5.4.

Normal and off-normal conditions are modeled with the Advanced NUHOMS[®] System intact, including the filled neutron shield in the TC. The shielding calculations are performed using the MCNP three-dimensional Monte Carlo transport code [A5.8]. Average and peak dose rates on the front, side, top and back of the AHSM and the TC are calculated. Occupational doses during loading, transfer to the ISFSI, and maintenance and surveillance operations are provided in Chapter A.10. Locations where streaming could occur are also discussed in Chapter A.10.

For accident conditions (e.g., cask drop, fire), the TC neutron shield (water) including the steel skin (shown in Figure A.5.1-4) are assumed to be removed. The results of this analysis are addressed in Chapter A.11. Site dose and occupational dose analyses are addressed in Chapter A.10 (including requirements for site specific 72.104 and 72.106 analyses).

**Table A.5.1-1
Advanced NUHOMS® System Shielding Materials**

AHSM

Components	Thickness/Material Modeled
Side Walls	1' concrete
Side Shield Wall	3' concrete
Roof	5' concrete
Rear Wall	Minimum thickness 1' concrete
Rear Shield Wall	3' concrete
Front Door/Front Wall	2' thick concrete

24PT4-DSC

Components	Thickness/Material Modeled
Bottom Shield Plugs/Cover Plates	3.88" Steel 3" Lead
Top Shield Plugs/Cover Plates	3.74" Steel 3.5" Lead
Cylindrical Shell	0.53" Steel
Basket (main components)	28 Steel Spacer Discs, 1.25" thick each, and 24 Steel Guide Tubes with Boral® Sheets

OS197H Transfer Cask

Components	Thickness/Material Modeled
Top Cover Plate	2" NS3 and 3.25" Steel
Bottom Cover Plate	2.25" NS3 and 2.75" Steel
Radial Walls:	
Inner Shell	0.5" Steel
Lead Gamma Shield	3.56" Lead
Structural Shell	1.5" Steel
Neutron Shield	3" Water
Skin	0.19" Steel

**Table A.5.1-2
Summary of AHSM Dose Rates**

Surface	Dose Rate Component	Dose Rate (mrem/hr)	
		Maximum	Average
Rear End of the TSBA ^(b)	Gamma	143.881 ± 15.5% ^(a)	N/A
	Neutron	0.207 ± 4.3%	
	Total	144.088 ± 15.5%	
Back of the Rear Shield Wall ^(b)	Gamma	1.115 ± 4.2%	0.085 ± 3.3%
	Neutron	0.008 ± 1.4%	1.05E-3 ± 1.6%
	Total	1.123 ± 4.1%	0.086 ± 3.3%
Front ^(c)	Gamma	44.318 ± 5.3%	2.154 ± 2.9%
	Neutron	0.838 ± 1.1%	0.138 ± 7.7%
	Total	45.156 ± 5.2%	2.292 ± 2.8%
Roof ^(d)	Gamma	149.298 ± 4.5%	0.011 ± 2.7%
	Neutron	0.279 ± 1.6%	0.001 ± 7.5%
	Total	149.577 ± 4.5%	0.012 ± 2.6%
AHSM Top ^(e)	Gamma	6.657 ± 6.8%	0.474 ± 5.6%
	Neutron	0.016 ± 1.8%	1.56E-3 ± 1.5%
	Total	6.673 ± 6.8%	0.476 ± 5.6%
Side	Gamma	1.790 ± 3.3%	0.309 ± 2.0%
	Neutron	0.074 ± 3.6%	1.06E-3 ± 1.4%
	Total	1.865 ± 3.1%	0.319 ± 1.9%

- (a) Statistical one standard deviation uncertainty in the Monte Carlo calculation.
- (b) The maximum gamma dose rates on the rear concrete surface (of “top” model) but below the roof elevation are less than 0.2 mrem/hr and the maximum gamma dose rates on this surface above the roof level are about 1.12 mrem/hr; i.e., the dose rate above the roof drops off very rapidly with distance in x from the vent (note the dose rate near the edge of the vent is 144.1 mrem/hr).
- (c) These maximum dose rates on the front of the AHSM are based on the results calculated just in front of the entrance of the bottom air inlet.
- (d) The dose rates are calculated on top of the AHSM roof. The maximum dose rates on the roof are based on the dose rates just at the roof vent opening. Knowing dose rates just above the roof vent opening is important, since this area must be accessed to clean the vent screens, if debris accumulates on the screens. For dose rates in front of the Top Shield Block Assembly (TSBA), the “Roof” maximum dose rate is below 1.0 mrem/hr. The average dose rates are calculated over the roof segment in front of the TSBA (before its -x side).
- (e) The dose rates are calculated on the plane enveloping the AHSM from the top. The average dose rate is calculated over the entire plane enveloping the AHSM from the top. This dose rate is used for the site dose rate analysis. The location of the maximum dose rate is near the rear end of the TSBA (its +x side, the side facing rear of the AHSM).

Note: Gamma results include the dose rates from gammas produced from neutrons in the neutron calculation. These partial gamma dose rates and the neutron dose rates have been multiplied by $[1/(1-k)=1/(1-0.45)=1.82]$ to conservatively include neutron multiplication from induced fissions in the source region containing damaged fuel rods.

Note: The averaged dose rates are calculated over the planes enveloping the AHSM geometry, while peak dose rates are for localized areas. The average dose rates are needed for the site dose rate analysis.

**Table A.5.1-3
Transfer Cask (Loading/Unloading/Transfer Operations) Side Dose Rate Summary**

Stage of TC/24PT4-DSC Processing	Dose Rate mrem/hr	On Outside Surface		One Foot from Surface		Three Feet from Surface	
		Gamma	Neutron	Gamma	Neutron	Gamma	Neutron
Wet Welding	Maximum	225.91±0.3%	3.64 ± 3%	143.97±1%	2.37±3%	93.47±1%	1.45±2%
	Minimum	8.41±2%	2.65E-03±24%	8.83±1%	2.16E-02±30%	7.38±3%	6.45E-02±25%
	Average Surface	144.36±0.5%	1.86±1%	97.43±0.4%	1.22±1%	62.95±0.4%	0.78±1%
	At Center Line	206.46±3%	3.09±7%	140.47±2%	2.35±6%	92.51±2%	1.34±5%
Dry Welding	Maximum	1071.69±2%	109.28±1%	758.57±1%	71.25±1%	492.47±3%	43.62±1%
	Minimum	22.82±4%	4.32±9%	18.37±4%	4.02±7%	24.12±3%	3.37±5%
	Average Surface	658.04±0.5%	59.8117±0.5%	459.13±0.5%	38.91±0.4%	301.31±1%	24.78±1%
	At Center Line	1039.90±3%	108.67±3%	752.36±2%	68.58±2%	492.47±3%	43.45±2%
Transfer	Maximum	1072.09±4%	165.11±3%	760.50±2%	107.47±2%	499.16±5%	63.22±2%
	Minimum	15.29±5%	4.45±4%	15.14±3%	4.46±10%	23.69±5%	5.50±8%
	Average Surface	627.99±1%	91.24±1%	445.81±1%	59.22±1%	294.92±1%	37.30±1%
	At Center Line	1072.09±4%	158.62±6%	740.37±3%	94.84±5%	499.16±5%	61.23±5%

**Table A.5.1-4
Transfer Cask (Loading/Unloading/Transfer Operations) Top End Dose Rate
Summary**

Stage of TC/24PT4-DSC Processing	Dose Rate mrem/hr	On Outside Surface		One Foot from Surface		Three Feet from Surface	
		Gamma	Neutron	Gamma	Neutron	Gamma	Neutron
Wet Welding	Maximum	1786.18±6%	0.15±15%	519.48±10%	8.94E-02±18%	257.32±1%	4.67E-02±93%
	Minimum	35.20±1%	2.17E-04±10%	23.30±1%	9.91E-04±7%	15.43±1%	1.48E-03±6%
	Average Surface	119.76±1%	6.16E-02±8%	99.49±1%	3.77E-02±10%	82.59±1%	2.22E-02±16%
	At Center Line	505.76±1%	4.99E-03±10%	431.47±0.4%	3.05E-03±7%	257.32±1%	1.48E-03±6%
Dry Welding	Maximum	5045.57±5%	21.21±20%	1434.42±9%	11.07±1%	568.71±11%	5.35±4%
	Minimum	155.69±1%	6.01±6%	79.92±3%	4.95±8%	40.07±1%	2.99±8%
	Average Surface	265.69±1%	8.98±2%	184.85±2%	6.24±2%	135.93±2%	3.80±3%
	At Center Line	467.209±1%	16.65±1%	391.49±0.4%	11.07±1%	235.07±0.5%	4.91±1%
Transfer-Storage	Maximum	148.73±2%	26.07±3%	76.39±3%	18.76±2%	36.06±1%	9.20±3%
	Minimum	25.69±5%	8.18±6%	18.76±5%	5.94±6%	13.52±4%	4.24±10%
	Average Surface	108.44±1%	14.74±4%	49.78±1%	8.82±4%	19.36±2%	5.05±3%
	At Center Line	71.07±2%	26.07±3%	60.13±1%	18.76±2%	36.06±1%	9.20±3%

**Table A.5.1-5
Transfer Cask (Transfer Operations) Bottom End Dose Rate Summary**

Stage of TC/24PT1-DSC Processing	Dose Rate mrem/hr	On Outside Surface		One Foot from Surface		Three Feet from Surface	
		Gamma	Neutron	Gamma	Neutron	Gamma	Neutron
Transfer	Maximum	1390.13 ± 2%	1006.09 ± 3%	832.61 ± 1%	368.35 ± 3%	278.60 ± 2%	91.35 ± 4%
	Minimum	12.38 ± 7%	20.70 ± 6%	19.52 ± 3%	16.10 ± 9%	20.57 ± 9%	15.31 ± 7%
	Average Surface	124.13 ± 2%	61.05 ± 2%	70.85 ± 1%	44.86 ± 2%	47.10 ± 1%	29.53 ± 2%
	At Center Line	1390.13 ± 2%	1006.09 ± 3%	832.61 ± 1%	368.35 ± 3%	278.60 ± 2%	91.35 ± 4%

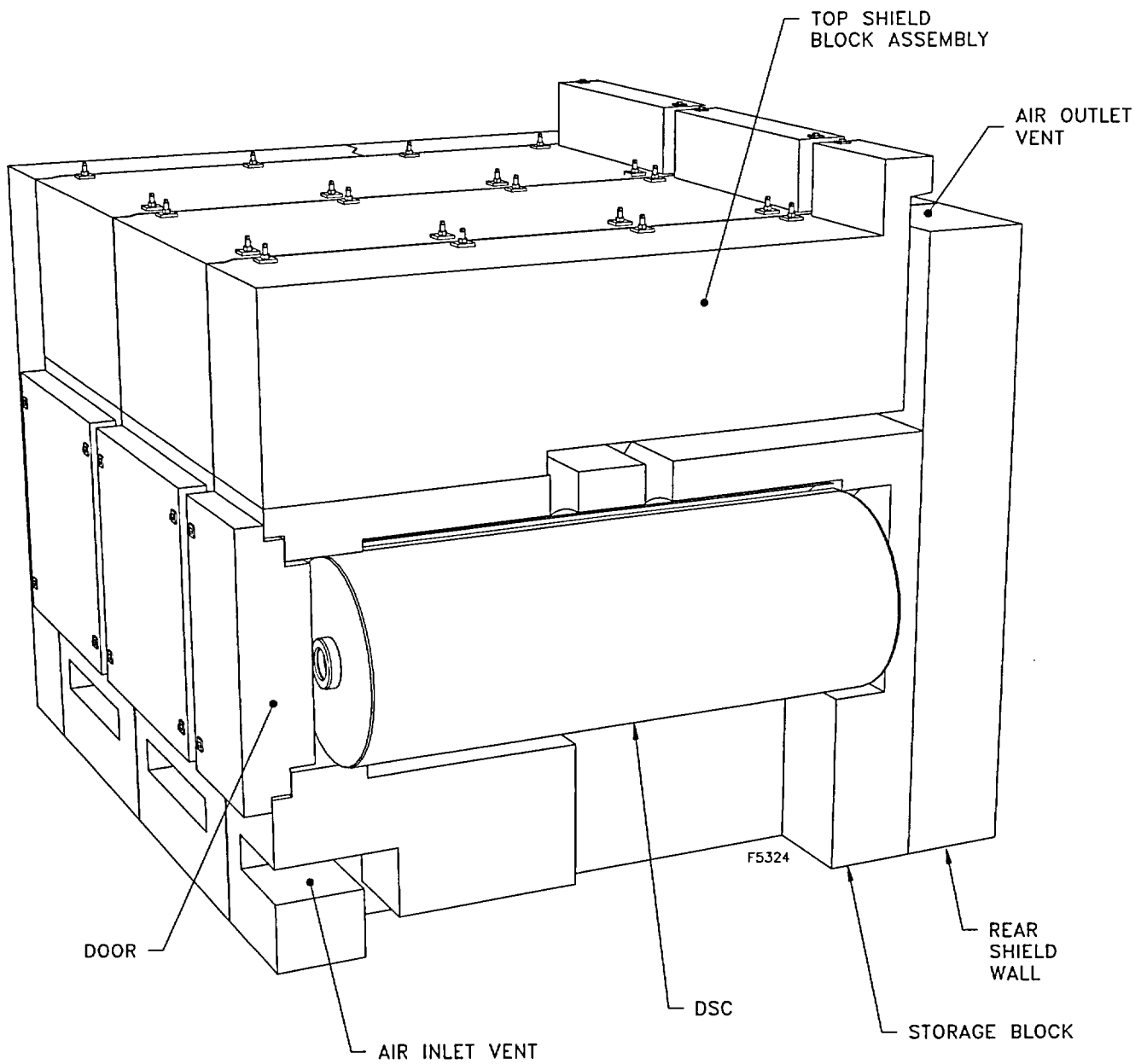


Figure A.5.1-1
Advanced NUHOMS® System (24PT4-DSC in AHSM) Shielding Configuration

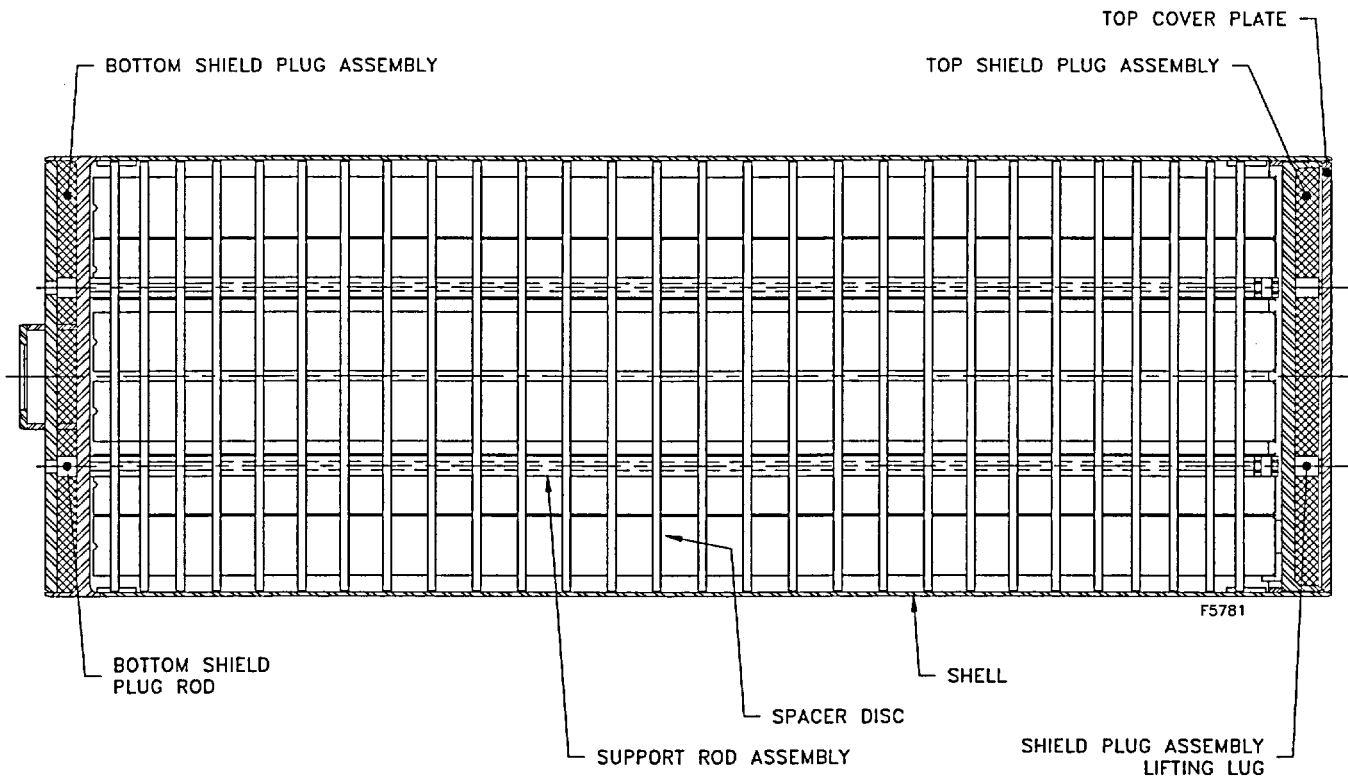


Figure A.5.1-2
24PT4-DSC Shielding Configuration

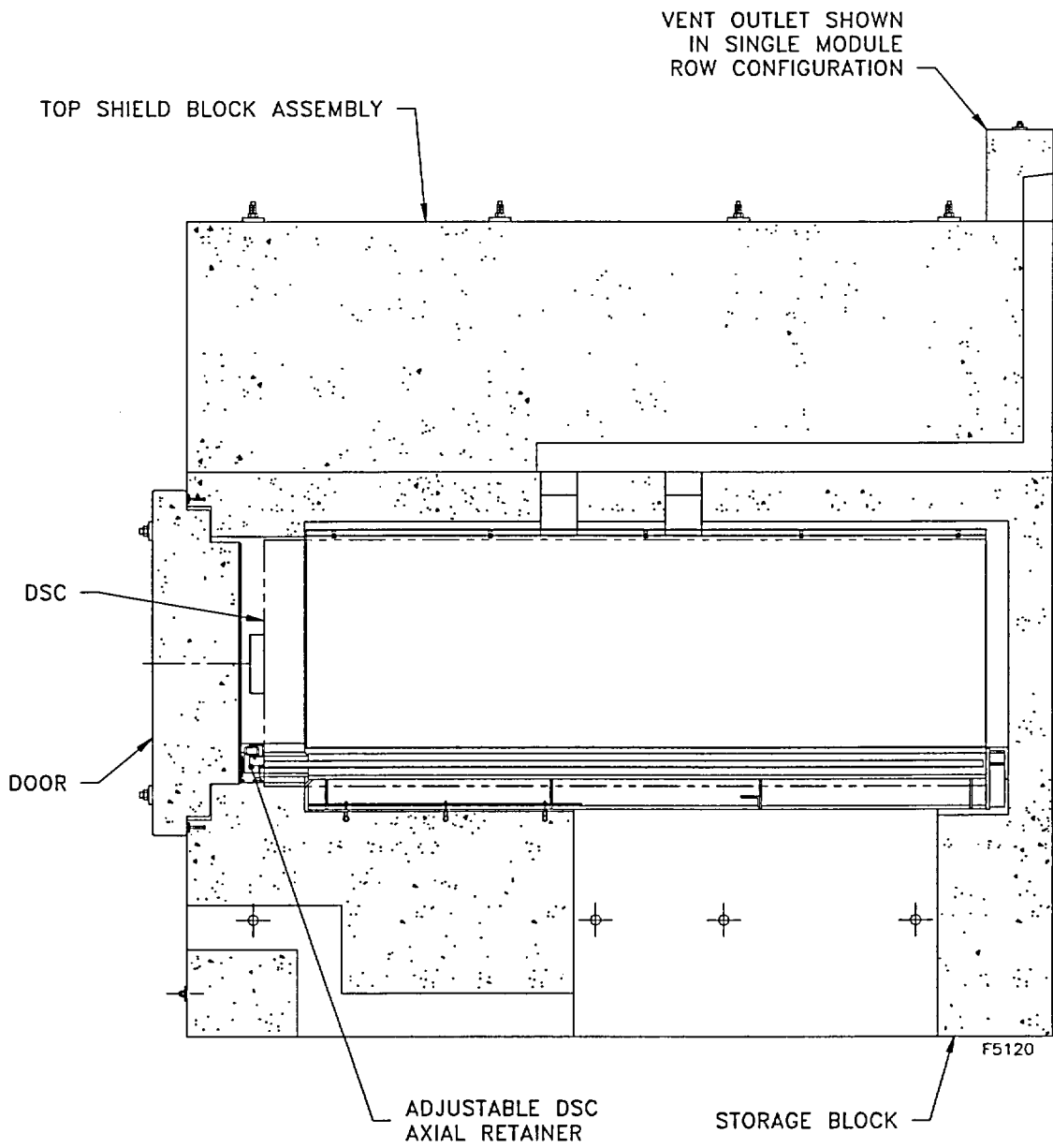


Figure A.5.1-3
Right Elevation Cross Section View of AHSM

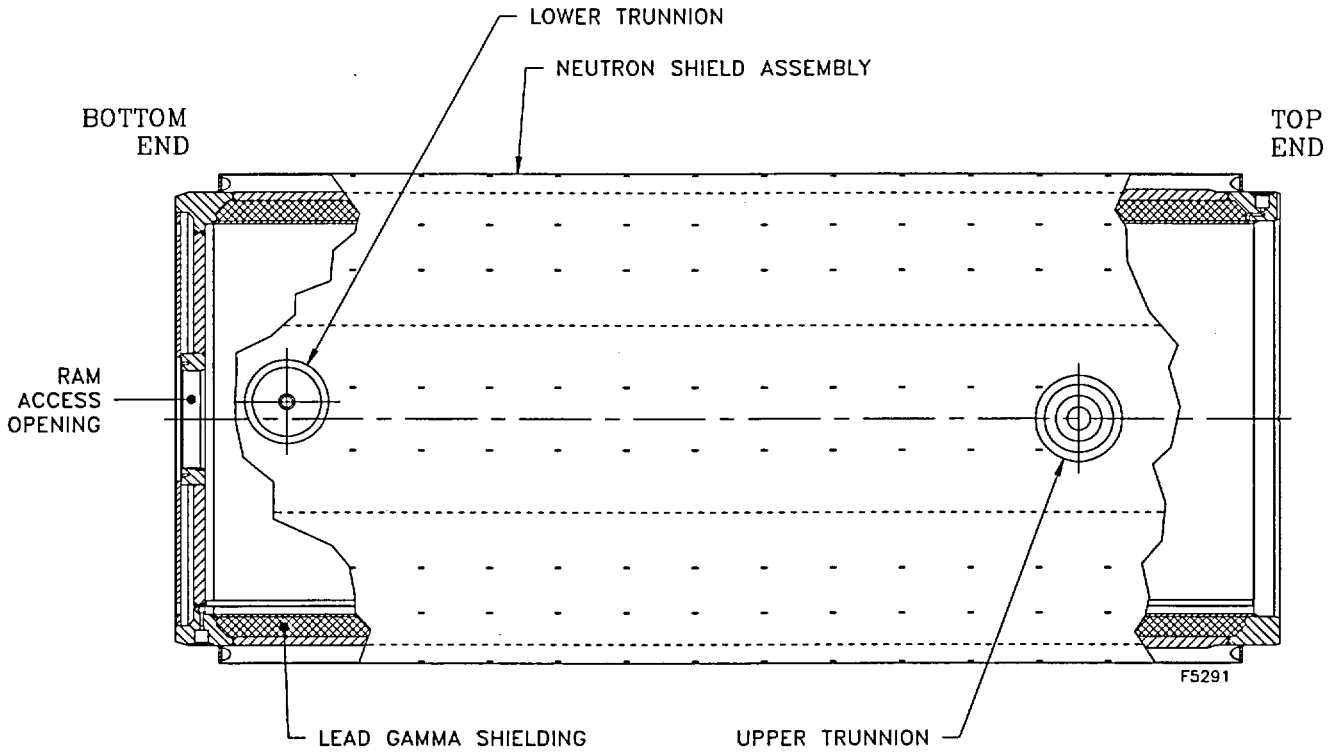


Figure A.5.1-4
Shielding Configuration of the TC

A.5.2 Source Specification

Thermal and radiological source terms are calculated with the SAS2H/ORIGEN-S modules of SCALE 4.4 [A5.1] for the fuel. The SAS2H/ORIGEN-S results are used to develop the fuel qualification tables (Table A.2.1-5 through Table A.2.1-12) and the bounding design basis fuel source terms, which are defined as CE 16x16 fuel with a burnup of 45 GWd/MTU, an initial enrichment of 3.8 wt. % ²³⁵U and a minimum cooling time of 5 years.

A composite CE 16x16 assembly with the maximum initial heavy metal and Co-60 content in each region is chosen as the bounding fuel assembly design for shielding purposes. The neutron flux during reactor operation is peaked in the in-core (active fuel) region of the fuel assembly and drops off rapidly outside the in-core region. Much of the fuel assembly hardware is outside of the in-core region of the fuel assembly. To account for this reduction in neutron flux, the fuel assembly is divided into four exposure "regions." The four axial regions used in the source term calculation are: the bottom (nozzle) region, the in-core (active fuel) region, the (gas) plenum region, and the top (nozzle) region. The CE 16x16 fuel assembly materials and masses for each irradiation region are listed in Table A.5.2-1. The light elements that make up the various materials for the various fuel assembly materials are taken from reference [A5.2] except for the Co-60 content for stainless steel and Inconel, which are conservatively assumed to be higher. The light element compositions are listed in Table A.5.2-2. The design basis source terms are generated using a heavy metal weight of 0.4555 MTU per assembly. These masses are irradiated in the appropriate fuel assembly region in the SAS2H/ORIGEN-S models. To account for the reduction in neutron flux outside the in-core regions, neutron flux (fluence) correction factors are applied to light element composition for each region. The neutron flux correction factors are given in Table A.5.2-3 [A5.3].

The fuel qualification tables are generated based on the decay heat limits for the various heat load zoning configurations shown in Figure A.2.1-1 through Figure A.2.1-3 and to assure that the design basis shielding analysis remains bounding. SAS2H is used to calculate the minimum required cooling time as a function of assembly initial enrichment and burnup for the entries in the various fuel qualification tables. The total decay heat includes the contribution from the fuel as well as the hardware in the entire assembly. Because the decay heat generally increases slightly with decreasing enrichment for a given burnup, it is conservative to assume that the required cooling time for a higher enrichment assembly is the same as that for a lower enrichment assembly with the same burnup.

As discussed above, the shielding analysis, using the MCNP 3-D Monte Carlo transport code models, is based on a source term consisting of the predicted neutron and gamma source terms from an assembly with 45 GWd/MTU burnup, an initial enrichment of 3.8 wt. % U-235 and a cooling time of five years. Evaluations of the existing data with SAS2H and the 44-group ENDF/B-V library used in the analysis are documented in References [A5.12] and [A5.13]. These comparisons all show generally good agreement between the calculations and measurements, and show no trend as a function of burnup in the data that would suggest that the isotopic predictions, and therefore neutron and gamma source terms, would not be in good agreement. A similar conclusion is also reached by the results documented in JAERI report [A5.14]. In fact, for the case with 46,460 MWd/MTU burnup, the isotopic predictions are all

within 2% of those measured. There are ongoing efforts, some of which are documented in Reference [A5.11], to obtain more data for burnups above 45 GWd/MTU. There is no reason to expect that the ongoing evaluations of the higher burnup fuel will result in less favorable comparisons.

As noted in References [A5.15] and [A5.11], there is no public data for the neutron component currently available that bounds a fuel burnup of up to 60 GWd/MTU. However, as documented in Reference [A5.15] and confirmed in the SAS2H analysis, the total neutron source with increasing burnup is more and more dominated by spontaneous fission neutrons. Reviewing the output from the SAS2H runs, the neutron source term is due almost entirely to the spontaneous fission of Cm-244 (~98% of all neutrons both spontaneous fission and (α, n)). After reviewing the measured Cm-244 content compared to the Cm-244 content predicted by SAS2H and the 44-group ENDF/B-V library documented in References [A5.12] and [A5.13] for burnups up to 46,460 MWd/MTU, it is readily apparent that the calculated values are within $\pm 11\%$ of the measured values, with most of the predicted values within $\pm 5\%$ of the measured. Finally, there is no observed trend as a function of burnup in the data that would indicate that the predicted Cm-244 content is significantly different at higher burnups.

As documented in Reference [A5.15] and as observed in preparing the fuel qualification tables, the gamma dose rate increases nearly linearly with burnup relative to the direct gamma component and the neutron dose rate increases with burnup to the fourth power. Therefore, as burnups go beyond 45 GWd/MTU, the contribution from neutron (and associated n, γ) components to the total dose rates measured on the surfaces of the DSC, TC and AHSM increase in relative importance to that of the gamma component. However, this increase in the importance of the neutron source term has a relatively minor effect on the area dose rates on and around the AHSM as these are dominated by the gamma component as shown in Table A.5.1-2 through Table A.5.1-5. The surface dose rates on the AHSM are dominated by the gamma component because the AHSM is constructed of thick reinforced concrete, which is an excellent neutron shield. The ratio of the average neutron to the average gamma dose rate on the surfaces of the AHSM is from 0.061 to 0.003 (See Table A.5.1-2). Therefore, even a postulated substantial increase in the neutron source term would have a relatively minor effect on the site dose rate evaluation presented in Section A.10 of the amendment application.

For the TC, the neutron source term has a relatively minor effect (<15% of total dose rate) on the area dose rates during most of the cask handling operations, since as the DSC cavity and the annulus between the TC and DSC is filled with water and most of the work is done around the top of the cask. The neutron component is of more importance on and around the TC during transfer operations but, in general, only represents approximately 15% the total dose rate on the sides and top of the TC. While the neutron dose rate on the bottom of the TC is just under 45% of the total, relatively little occupational dose is received from this area. The dose rates for the design basis fuel on the surfaces of AHSM and TC are shown in Table A.5.1-2 through Table A.5.1-5. These tables show that gamma dose rates are substantially higher than neutron dose rates. Therefore, the neutron component of the dose is a relatively minor fraction of the total occupational and site boundary dose.

The occupational exposure calculations demonstrate that most of the dose received by workers during cask loading and transfer operations is due to the gammas on and around the cask. The

only surface of the TC that is dominated by neutrons is at the bottom of the cask. Less than 5% of the total occupational exposure is due to the doses around the bottom of the cask because very little work is performed on or around the bottom of the cask with fuel in the TC.

As discussed above, any impact of uncertainties in source terms is expected to be negligible for the Advanced NUHOMS[®] system. Therefore, isotopic depletion calculations with SAS2H for fuel burned above 45 GWd/MTU are appropriate.

The 1-D discrete ordinates code ANISN [A5.4] and the CASK-81 22 neutron, 18 gamma-ray energy group coupled cross section library [A5.7] are used to demonstrate that the design basis source terms used in the evaluation result in dose rates on the surface of the AHSM and TC that are greater than the dose rates due to fuels with burnup, initial enrichment and cooling time combinations given in the fuel qualification tables. The AHSM roof surface and transfer cask radial surface dose rates do not represent regulatory limits, however these surfaces are considered appropriate for comparing neutron and gamma source terms. For a given cask (AHSM or TC), the actual material thicknesses are not important for determining the relative effect of various source terms on total dose rate. What is important are the materials of construction and the general configuration of those materials. The ANISN results due to the 24 design basis assemblies (source terms) on the AHSM roof determines the "target dose rate" for the AHSM for this analysis. Similarly, the ANISN results on the side of the TC using the bounding source term provides the "target dose rate" for this TC. This approach described in detail in Section A.5.2.3 is consistent with the method used to determine the fuel qualification tables for the Standardized NUHOMS[®] 24P and 52B canister [A5.5]. The radiological source terms generated in the SAS2H/ORIGEN-S using 44-group ENDF/B-V library, which includes more accurate evaluation for ¹⁵⁴Eu and ¹⁵⁵Eu, are used in the ANISN evaluations to calculate the surface dose rates.

A sample SAS2H/ORIGEN-S input file for the 45 GWd/MTU, 3.8 wt. % ²³⁵U case is provided in Section A.5.5.2. It is conservatively assumed that a reactor operated at the maximum power from the beginning to the end of each cycle to maximize actinide production rate.

The cobalt concentration used in the various exposure regions and the total for entire fuel assembly are selected to maximize the gamma source terms.

For reconstituted fuel with up to eight (8) stainless steel rods, a series of SAS2H calculations were performed to evaluate the effect of the increased Co-60 content from the stainless steel rods. For a given burnup, initial enrichment and cooling time, the total neutron and decay heat are reduced because of the reduced heavy metal in the assembly. Therefore, the surface neutron dose rates are reduced and the total decay heat is bounded by fuel that has not been reconstituted. The effect on the gamma source term and resulting gamma dose rate is evaluated using the same response function as that used to develop fuel qualification tables A.2.1-5 through A.2.1-8. The fuel qualification tables applicable to fuel with up to eight (8) stainless steel rods are provided in Tables A.2.1-9 through A.2.1-12.

Boron concentration, moderator temperature and density values are selected in the depletion model to over estimate buildup of isotopic activities such as ²⁴⁴Cm resulting in conservative neutron source terms.

A.5.2.1 Gamma Source

Four SAS2H/ORIGEN-S runs are required to determine gamma source terms for the four exposure regions of interest for each fuel assembly; the bottom, in-core, plenum and top regions. The only difference between the runs is in Block #10 "Light Elements" of the SAS2H input and the 82\$\$ card in the ORIGEN-S input. Each run includes the appropriate "Light Elements" for the region being evaluated and the 81\$\$ card is adjusted to have ORIGEN-S output the total gamma source for the in-core region and only the light element source for the plenum, top and bottom nozzle regions.

The SAS2H/ORIGEN-S gamma source is output in the CASK-81 energy group structure shown in Table A.5.2-4 [A5.7]. Gamma source terms for the in-core region include contributions from actinides, fission products, and activation products. The bottom, plenum and top nozzle regions include the contribution from the activation products in the specified region only. The gamma results for the Design Basis fuel for various zones are given in Table A.5.2-5.

Gamma source terms used in the MCNP shielding models are calculated by multiplying the assembly sources by the number of assemblies (24).

A.5.2.2 Neutron Source Term

One SAS2H/ORIGEN-S run is required to determine the total design basis neutron source term for the in-core regions. At discharge, the neutron source is almost equally produced from ^{242}Cm and ^{244}Cm . The other strong contributor is ^{252}Cf , which is approximately 1/10 of the Cm intensity, but its share vanishes after 6 years of cooling time because the half-life of ^{252}Cf is 2.65 years. The half-lives of ^{242}Cm and ^{244}Cm are 163 days and 18 years respectively. Contributions from the next strongest emitters, ^{238}Pu and ^{240}Pu , are lower by a factor of 1000 and 100 relative to ^{244}Cm . Thus, the neutron spectrum for a cooling time of 5 years is totally dominated by ^{244}Cm in both spontaneous fission and (α, n) (~ 2% of total neutron source) components. The results for the design basis fuel are summarized in Table A.5.2-6.

Neutron source terms for use in the MCNP shielding models are calculated by multiplying the assembly sources by the number of assemblies (24).

A.5.2.3 Response Functions for Alternate Nuclear Parameters

To determine if a candidate CE 16x16 fuel assembly with a given burnup, wt. % enrichment and cooling time is bounded by the design basis shielding analysis, the total source term, which includes the contribution from the fuel as well as the hardware in the entire candidate fuel assembly (including end fittings and plenum) is used to calculate its total dose rate and compared to the "target dose" rates on the AHSM roof and TC radial surface using a response function developed using the ANISN code. This response function is only used to determine the relative strength of the various source terms from fuel assemblies to assure that the dose rates calculated on and around the AHSM and TC, with MCNP 3-D models, using the design basis fuel source terms remain bounding. As discussed above, the design basis source terms used in this evaluation are for 24 CE 16x16 fuel assemblies each with a burnup of 45 GWd/MTU, an initial enrichment of 3.8 wt. % ^{235}U and five years cooling loaded in the DSC. Therefore a response

function that is developed assuming a canister loaded with 24 design basis assemblies bounds the four decay heat zones as the response function assumes that all 24 spaces are loaded with same source term which is equivalent to fuel assembly heat load configuration shown in Figure A.2.1-1 and conservative compared to the heat load configurations shown in Figure A.2.1-2 and A.2.1-3.

ANISN [A5.4] determines the fluence of particles throughout one-dimensional geometric systems by solving the Boltzmann transport equation using the method of discrete ordinates. Particles can be generated by either particle interaction with the transport medium or extraneous sources incident upon the system. Anisotropic cross-sections can be expressed in a Legendre expansion of arbitrary order.

The ANISN code implements the discrete ordinates method as its primary mode of operation. Balance equations are solved for the flow of particles moving in a set of discrete directions in each cell of a space mesh and in each group of a multigroup energy structure. Iterations are performed until all implicitness in the coupling of cells, directions, groups, and source regeneration is resolved.

ANISN coupled with the CASK-81 22 neutron, 18 gamma-ray energy group, coupled cross-section library [A5.7] and the ANSI/ANS-6.1.1-1977 [A5.9] flux-to-dose conversion factors is chosen to generate the response functions used to determine the relative strength of the various source terms from fuel assemblies to assure that the dose rates calculated on and around the AHSM and TC, with MCNP, using the design basis fuel source terms remain bounding. ANISN provides an efficient method to calculate the response function.

The response functions are calculated using ANISN models to perform the evaluation for the fuel assembly parameters in the fuel qualification table. The ANISN model used to generate the AHSM Response Function is a 1-D cut through the center of the MCNP AHSM roof model used for the shielding evaluation documented in Section A.5.4. The ANISN model used to generate the TC Response Function is a cut through the center of the MCNP TC side model used for the shielding evaluation documented in Section A.5.4. Figure A.5.2-1 and Figure A.5.2-2 provide sketches for the ANISN models of the AHSM roof and TC centerline respectively.

The material densities used in the ANISN models for the various model regions are identical to those used in the MCNP analysis and are listed in Table A.5.3-1.

To generate the neutron and (n, γ) response functions, ANISN runs for the AHSM roof and TC are run with a starting neutron source of one neutron per second per assembly with a ^{244}Cm spectrum. The resulting calculated total dose rates on the AHSM and TC surfaces are the appropriate neutron and (n, γ) response functions documented in Table A.5.2-7. To generate the response function for each gamma group (CASK-81 group structure), ANISN runs are performed for the AHSM and TC assuming one gamma per second per assembly in that group. The resulting ANISN calculated total dose rates on the AHSM and TC surfaces are the appropriate gamma response functions documented in Table A.5.2-7. An example ANISN input file is included in Section **Error! Reference source not found.** The AHSM and Transfer Cask materials are very similar in all directions; the ANISN models accurately assess the relative

source strengths to assure that all dose rates calculated using MCNP 3-D models, as summarized in Section A.5.4 remain bounded by the design basis source terms.

To determine if the source term from a candidate assembly for a given burnup, wt. % enrichment and cooling time, multiply the total neutron source in n/sec/assembly by the neutron and (n, γ) response functions given in Table A.5.2-7 and the group-wise source in γ /sec/assembly per group times the appropriate gamma group response function given in Table A.5.2-7 and sum the results, thus accounting for the total, i.e. the neutron, (n, γ) and primary gamma contributions from the fuel assembly. If the total dose rate is less than or equal to that determined in the same way for the design basis source term, then the minimum cooling time is adequate for shielding purposes. Note that the decay heat limit must also be verified depending on fuel Zone. If not, the cooling time is increased until the decay heat limit and target dose rate is met for both the AHSM and TC.

The target dose rate calculated with design basis neutron and gamma source terms, using the response function, is 0.079 mrem/hr on the AHSM roof surface and 877.0 mrem/hr on the TC side surface. The corresponding MCNP calculated dose rates are 0.21 mrem/hr on the roof surface and 1231 mrem/hr on the TC cask surface. The ANISN calculated target dose rates are different than those calculated by MCNP at the corresponding location, due to the simplifying assumptions used in the ANISN models for the source and geometry. Calculation of these target dose rates is shown in Table A.5.2-8. Table A.5.2-8 lists the response function for the AHSM and the TC, the total design basis source term for a single assembly and the corresponding target dose rates derived by multiplying the applicable response function by the source term and summing the results.

To evaluate other burnup/initial enrichment/cooling time combinations of candidate fuel assemblies one obtains the total neutron and group-wise gamma source for the applicable burnup/initial enrichment/cooling time combination for a single candidate assembly, which must include the contribution from the fuel as well as the hardware in the entire assembly. An example calculation is presented in Table A.5.2-9 for the 57 GWd/MTU, 3.8 wt. % U-235, 8-year cooled fuel case shown in the fuel qualification table, Table A.2.1-3. The combination of burnup, initial enrichment and cooling time is acceptable for storage in the 1.26 kW/assembly locations identified in Figure A.2.1-3 because the total decay heat is less than 1.26 kW and the total dose rates are less than 0.079 mrem/hr for the AHSM and the 877.0 mrem/hr for the TC.

The response function is used to account for the substantial shift in the gamma spectrum over the range of burnup/initial enrichment/cooling time combinations included in the Fuel Qualification Tables provided in Chapter A.2. The important energy groups contributing to the total dose rate on and around the AHSM and TC are groups 35 to 29 (0.6 – 2.5 Mev) as demonstrated in Table A.5.2-8 and Table A.5.2-9. However depending upon cooling time most notably, the lower energy groups 38 to 40 dominate the total gamma source (gamma/sec) but make no contribution to the dose rate outside the AHSM and TC. The response function is used to remove these low energy gammas from the evaluation. Table A.5.2-10 shows the fraction of the total number of primary gammas and corresponding contribution to the AHSM and TC surface dose rate in groups 35 to 29 and 38 to 40 for the design basis source terms and for 57 GWd/MTU, 3.8 wt. % U-235, 8-year cooled fuel.

**Table A.5.2-1
Fuel Assembly Region Materials, Masses, and Lengths**

Item	Material	Average Weight (lb./assembly)
In-Core Region (149.610 in.)		
Guide Tubes	Zircaloy-4	21
Spacer Grids	Zircaloy-4	23.4
Spacer Grid	Inconel 625	2.6
Cladding	Zircaloy-4	235.2
Fuel Rods	UO ₂	1137 (Total U = 455.5 kg)
Plenum Region (8.638 in.)		
Guide Tubes	Zircaloy-4	1.5
Spacer Grid	Zircaloy-4	1.8
Upper End Cap	Zircaloy-4	1.9
Cladding	Zircaloy-4	15.7
Plenum Springs	Stainless Steel 302	16.5
Spacer Discs	Al ₂ O ₃	1.3
Top Region (11.473 in.)		
Holddown Plate	Stainless Steel 304	24.6
Flow Plate	Stainless Steel 304	
Outer Posts	Stainless Steel 304	
Center Guide Post	Stainless Steel 304	
Guide Tubes	Zircaloy-4	0.3
Holddown springs	Inconel X-750	11.4
Bottom Region (4.703 in.)		
Guide Tubes	Zircaloy-4	0.9
Locking Discs/Sleeve	Stainless Steel 304	0.2
Spacer Grid	Inconel 625	2.6
Spacer Discs	Al ₂ O ₃	1.3
Cladding	Zircaloy-4	0.4
Bottom End Cap	Zircaloy-4	20.6
Lower End Fitting	Stainless Steel 304	13.1

**Table A.5.2-2
Elemental Composition of LWR Fuel-Assembly Structural Materials**

Element	Atomic Number	Material Composition, grams per kg of material			
		Zircaloy-4	Inconel X-750/ Inconel 625	Stainless Steel 302/304	UO ₂ Fuel
H	1	1.30E-02	-	-	-
Li	3	-	-	-	1.00E-03
B	5	3.30E-04	-	-	1.00E-03
C	6	1.20E-01	3.99E-01	8.00E-01	8.94E-02
N	7	8.00E-02	1.30E+00	1.30E+00	2.50E-02
O	8	9.50E-01	-	-	1.34E+02
F	9	-	-	-	1.07E-02
Na	11	-	-	-	1.50E-02
Mg	12	-	-	-	2.00E-03
Al	13	2.40E-02	7.98E+00	-	1.67E-02
Si	14	-	2.99E+00	1.00E+01	1.21E-02
P	15	-	-	4.50E-01	3.50E-02
S	16	3.50E-02	7.00E-02	3.00E-01	-
Cl	17	-	-	-	5.30E-03
Ca	20	-	-	-	2.00E-03
Ti	22	2.00E-02	2.49E+01	-	1.00E-03
V	23	2.00E-02	-	-	3.00E-03
Cr	24	1.25E+00	1.50E+02	1.90E+02	4.00E-03
Mn	25	2.00E-02	6.98E+00	2.00E+01	1.70E-03
Fe	26	2.25E+00	6.78E+01	6.88E+02	1.80E-02
Co	27	2.00E-02	1.00E+01	2.00E+00	1.00E-03
Ni	28	2.00E-02	7.22E+02	8.92E+01	2.40E-02
Cu	29	2.00E-02	4.99E-01	-	1.00E-03
Zn	30	-	-	-	4.03E-02
Zr	40	9.79E+02	-	-	-
Nb	41	-	8.98E+00	-	-
Mo	42	-	-	-	1.00E-02
Ag	47	-	-	-	1.00E-04
Cd	48	2.50E-04	-	-	2.50E-02
In	49	-	-	-	2.00E-03
Sn	50	1.60E+01	-	-	4.00E-03
Gd	64	-	-	-	2.50E-03
Hf	72	7.80E-02	-	-	-
W	74	2.00E-02	-	-	2.00E-03
Pb	82	-	-	-	1.00E-03
U	92	2.00E-04	-	-	8.81E+02

**Table A.5.2-3
Flux Fraction By Assembly Region**

Fuel Assembly Region	Flux Factor
Bottom	0.20
In-Core	1.00
Plenum	0.20
Top	0.10

**Table A.5.2-4
CASK-81 Energy Group Structure**

Neutron Group Number	E _{upper} (MeV)	Gamma Group Number	E _{upper} (MeV)
1	14.9	23	10.0
2	12.2	24	8.0
3	10.0	25	6.5
4	8.18	26	5.0
5	6.36	27	4.0
6	4.96	28	3.0
7	4.06	29	2.5
8	3.01	30	2.0
9	2.46	31	1.66
10	2.35	32	1.33
11	1.83	33	1.0
12	1.11	34	0.8
13	0.550	35	0.6
14	0.111	36	0.4
15	3.35E-03	37	0.3
16	5.83E-04	38	0.2
17	1.01E-04	39	0.1
18	2.90E-05	40 ⁽²⁾	0.05
19	1.07E-05		
20	3.06E-06		
21	1.12E-06		
22 ⁽¹⁾	4.14E-07		

1. Group 22 lower energy boundary is 1.00E-08 MeV
2. Group 40 lower energy boundary is 0.01 MeV

Table A.5.2-5
Design Basis Gamma Sources
 (per assembly)

CASK 81 Energy Group	Top Region γ/s	Plenum Region γ/s	In-Core Region γ/s	Bottom Region γ/s
23	0.000E+00	0.000E+00	2.127E+05	0.000E+00
24	0.000E+00	0.000E+00	1.002E+06	0.000E+00
25	0.000E+00	0.000E+00	5.107E+06	0.000E+00
26	0.000E+00	0.000E+00	1.273E+07	0.000E+00
27	1.550E-10	5.112E-15	1.251E+10	7.091E-11
28	3.880E+05	1.566E+05	1.005E+11	2.513E+05
29	2.502E+08	1.010E+08	3.128E+12	1.621E+08
30	1.984E+03	6.090E+02	1.328E+12	1.213E+03
31	1.054E+13	4.255E+12	5.020E+13	6.829E+12
32	3.733E+13	1.507E+13	1.695E+14	2.418E+13
33	7.516E+10	9.485E+10	3.766E+14	7.814E+10
34	6.458E+08	2.783E+10	2.649E+15	2.941E+10
35	4.817E+08	5.377E+10	8.775E+14	5.645E+10
36	2.026E+09	3.224E+09	7.490E+13	3.833E+09
37	1.536E+09	1.229E+09	1.065E+14	1.633E+09
38	3.092E+10	2.266E+10	3.761E+14	3.069E+10
39	1.279E+11	5.228E+10	4.633E+14	8.352E+10
40	1.006E+12	5.513E+11	2.252E+15	8.020E+11

Table A.5.2-6
Design Basis Neutron Source
(per assembly)

CASK 81 Energy Group	E_{upper} (eV)	Normalized Cm-244 Fission Source	In-Core Region n/s
1	1.49E+07	1.255E-04	4.638E+04
2	1.22E+07	1.067E-03	3.944E+05
3	1.00E+07	2.935E-03	1.085E+06
4	8.18E+06	1.463E-02	5.407E+06
5	6.36E+06	3.705E-02	1.369E+07
6	4.96E+06	4.900E-02	1.811E+07
7	4.06E+06	1.230E-01	4.546E+07
8	3.01E+06	1.007E-01	3.722E+07
9	2.46E+06	2.461E-02	9.096E+06
10	2.35E+06	1.271E-01	4.698E+07
11	1.83E+06	2.265E-01	8.371E+07
12	1.11E+06	2.008E-01	7.422E+07
13	5.50E+05	9.252E-02	3.420E+07
14	1.11E+05	3.986E-06	1.473E+03
15	3.35E+03	0.000E+00	0.000E+00
16	5.83E+02	0.000E+00	0.000E+00
17	1.01E+02	0.000E+00	0.000E+00
18	2.90E+01	0.000E+00	0.000E+00
19	1.01E+01	0.000E+00	0.000E+00
20	3.06E+00	0.000E+00	0.000E+00
21	1.12E+00	0.000E+00	0.000E+00
22	4.14E-01	0.000E+00	0.000E+00
Total		1.000E+00	3.696E+08

Table A.5.2-7
AHSM and TC “Response Function” for Evaluating Fuel with Alternate Parameters

Response Function Parameter	AHSM Response Function in mrem/hr per Particle/Sec per Assembly	TC Response Function in mrem/hr per Particle/Sec per Assembly
Neutron	2.6023E-12	2.9830E-07
(n, γ)	1.1846E-11	7.8700E-08
Group 23 ⁽¹⁾	6.0914E-12	5.1039E-11
Group 24	3.7137E-12	6.6402E-11
Group 25	1.7529E-12	7.3485E-11
Group 26	6.3958E-13	7.1647E-11
Group 27	1.9153E-13	6.0827E-11
Group 28	4.1468E-14	4.2152E-11
Group 29	1.0430E-14	2.4797E-11
Group 30	1.8769E-15	1.0714E-11
Group 31	3.2623E-16	3.4860E-12
Group 32	3.1763E-17	5.5317E-13
Group 33	1.5147E-18	1.5268E-13
Group 34	1.0535E-19	6.6217E-14
Group 35	2.9912E-21	2.5118E-14
Group 36	1.2627E-23	2.4083E-16
Group 37	3.4992E-25	6.8957E-19
Group 38	2.7471E-27	1.6984E-23
Group 39	5.5200E-31	2.6661E-27
Group 40	0.0000E+00	2.8026E-45

(1) Group Structure for CASK-81 Library [A5.7]. (See Table A.5.2-4 for group structure.)

Table A.5.2-8
“Response Function” Evaluation of Design Basis Source Terms

<i>Column A</i>	<i>Column B</i>	<i>Column C</i>	<i>Column D</i>	<i>Column E</i>	<i>Column F</i>
Response Function Parameter	AHSM Response Function in mrem/hr per particle/sec per assembly	TC Response Function in mrem/hr per particle/sec per assembly	Design Basis Source Term particle/sec for single assembly	Column B* Column D AHSM	Column C* Column D TC
Neutron	2.6023E-12	2.9830E-07	3.691E+08	0.0010	110.10
(n,γ)	1.1846E-11	7.8700E-08		0.0044	29.05
Group 23 ⁽¹⁾	6.0914E-12	5.1039E-11	2.124E+05	0.0000	0.00
Group 24	3.7137E-12	6.6402E-11	1.000E+06	0.0000	0.00
Group 25	1.7529E-12	7.3485E-11	5.100E+06	0.0000	0.00
Group 26	6.3958E-13	7.1647E-11	1.271E+07	0.0000	0.00
Group 27	1.9153E-13	6.0827E-11	1.251E+10	0.0024	0.76
Group 28	4.1468E-14	4.2152E-11	1.004E+11	0.0042	4.23
Group 29	1.0430E-14	2.4797E-11	3.127E+12	0.0326	77.55
Group 30	1.8769E-15	1.0714E-11	1.328E+12	0.0025	14.22
Group 31	3.2623E-16	3.4860E-12	7.176E+13	0.0234	250.17
Group 32	3.1763E-17	5.5317E-13	2.459E+14	0.0078	136.01
Group 33	1.5147E-18	1.5268E-13	3.766E+14	0.0006	57.50
Group 34	1.0535E-19	6.6217E-14	2.648E+15	0.0003	175.37
Group 35	2.9912E-21	2.5118E-14	8.771E+14	0.0000	22.03
Group 36	1.2627E-23	2.4083E-16	7.489E+13	0.0000	0.02
Group 37	3.4992E-25	6.8957E-19	1.065E+14	0.0000	0.00
Group 38	2.7471E-27	1.6984E-23	3.761E+14	0.0000	0.00
Group 39	5.5200E-31	2.6661E-27	4.634E+14	0.0000	0.00
Group 40	0.0000E+00	2.8026E-45	2.253E+15	0.0000	0.00

(1) Group Structure for CASK-81 Library [A5.7]
(See Table A.5.2-4 for group structure).

Total mrem/hr (sum of column) **0.079** **877.0**

Maximum decay heat per assembly:
See Figures A.2.1-1 through A.2.1-3

Table A.5.2-9
“Response Function” Evaluation of Candidate Fuel Assembly Source Terms
57 GWd/MTU, 3.8 wt. % U-235, 8-year Cooled Fuel Case

<i>Column A</i>	<i>Column B</i>	<i>Column C</i>	<i>Column D</i>	<i>Column E</i>	<i>Column F</i>
Response Function Parameter	AHSM Response Function in mrem/hr per particle/sec per assembly	TC Response Function in mrem/hr per particle/sec per assembly	57 GWd/MTU, 3.8 wt. % U-235 Enrichment, 8 Year Cooling Time Fuel Source Term particle/sec for single assembly	Column B* Column D AHSM	Column C* Column D TC
Neutron	2.6023E-12	2.9830E-07	8.585E+08	0.0022	256.09
(n,γ)	1.1846E-11	7.8700E-08		0.0102	67.56
Group 23 ⁽¹⁾	6.0914E-12	5.1039E-11	4.944E+05	0.0000	0.00
Group 24	3.7137E-12	6.6402E-11	2.328E+06	0.0000	0.00
Group 25	1.7529E-12	7.3485E-11	1.187E+07	0.0000	0.00
Group 26	6.3958E-13	7.1647E-11	2.957E+07	0.0000	0.00
Group 27	1.9153E-13	6.0827E-11	2.405E+09	0.0005	0.15
Group 28	4.1468E-14	4.2152E-11	1.880E+10	0.0008	0.79
Group 29	1.0430E-14	2.4797E-11	3.484E+11	0.0036	8.64
Group 30	1.8769E-15	1.0714E-11	3.246E+11	0.0006	3.48
Group 31	3.2623E-16	3.4860E-12	5.420E+13	0.0177	188.95
Group 32	3.1763E-17	5.5317E-13	2.129E+14	0.0068	117.78
Group 33	1.5147E-18	1.5268E-13	2.279E+14	0.0003	34.79
Group 34	1.0535E-19	6.6217E-14	2.587E+15	0.0003	171.27
Group 35	2.9912E-21	2.5118E-14	4.688E+14	0.0000	11.78
Group 36	1.2627E-23	2.4083E-16	4.989E+13	0.0000	0.01
Group 37	3.4992E-25	6.8957E-19	7.695E+13	0.0000	0.00
Group 38	2.7471E-27	1.6984E-23	2.667E+14	0.0000	0.00
Group 39	5.5200E-31	2.6661E-27	3.515E+14	0.0000	0.00
Group 40	0.0000E+00	2.8026E-45	1.817E+15	0.0000	0.00

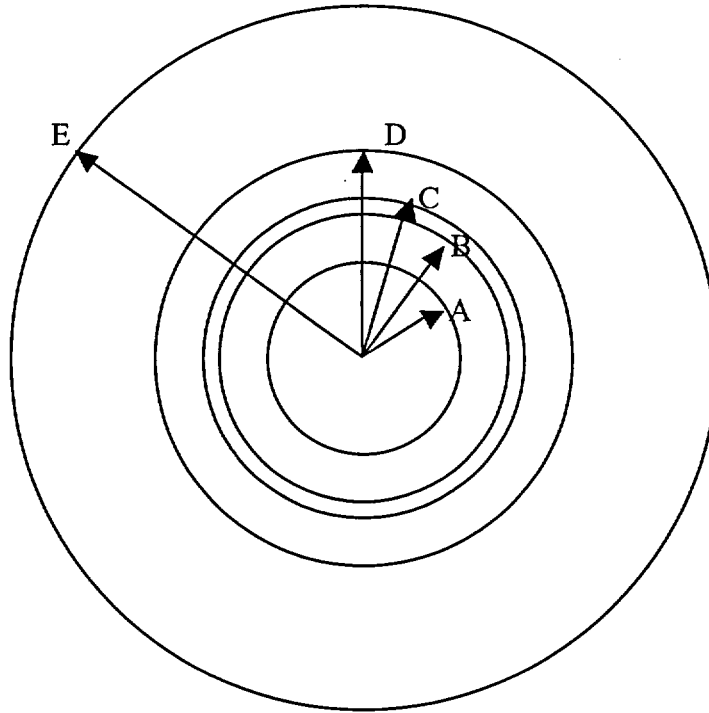
(1) Group Structure for CASK-81 Library [A5.7]
(See Table A.5.2-4 for group structure).

Total mrem/hr	0.0430	861.3
(sum of column)	<0.079	<877.0

Decay heat = 1.24<1.26 kW/FA, therefore only allowed in 1.26 kW/FA locations shown in Figure A.2.1-3.

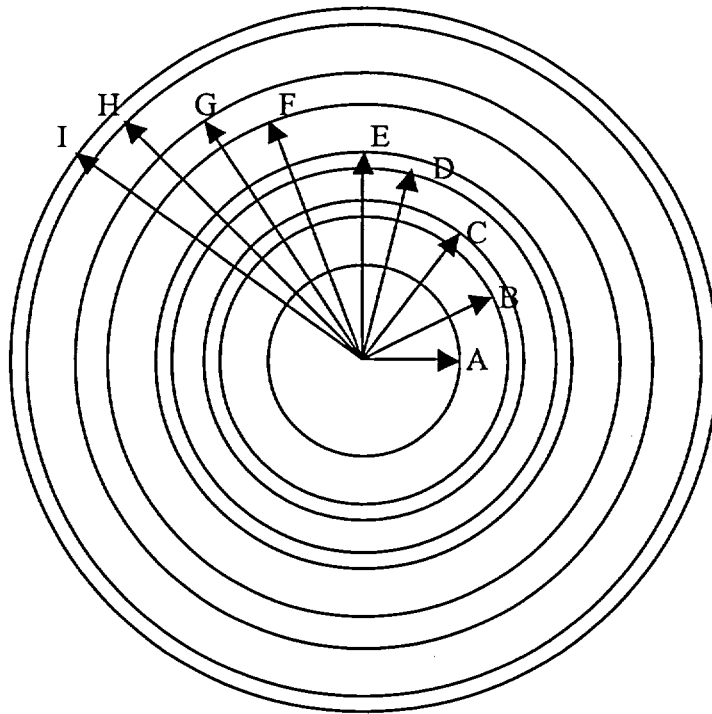
**Table A.5.2-10
Relative Contribution of Source Terms to Dose Rates**

CASK-81 Group	Total γ/s/assembly	Fraction γ/s/assembly	Response Function Dose Rate for AHSM	Fraction of Dose Rate for AHSM	Response Function Dose Rate for TC	Fraction of Dose Rate for TC
Design Basis Source Terms						
35-29	4.224E+15	56%	0.0672	85%	732.8	84%
38-40	3.093E+15	41%	0.0000	0%	0.0	0%
Total	7.498E+15	100%	0.0791	100%	877.0	100%
57 GWd/MTU, 3.8 wt. % U-235, 8-year Cooled Fuel						
35-29	3.551E+15	58%	0.0293	68%	536.7	62%
38-40	2.435E+15	40%	0.0000	0%	0.00	0%
Total	6.113E+15	100%	0.0430	100%	861.3	100%



Region	Material	Outer Radius (cm)	Thickness (cm)	Thickness (in)
A. Source Region	In-Core	71.71	71.71	-
B. Gap between fuel/basket	Air	84.38	12.67	-
C. Canister Wall	Stainless Steel	85.33	0.95	0.37
D. Gap between DSC/AHSM	Air	156.58	71.25	28.05
E. Roof	Concrete	304.80	148.22	58.35

Figure A.5.2-1
ANISN AHSM Model



Region	Material	Outer Radius (cm)	Thickness (cm)	Thickness (in)
A. Source Region	In-Core	71.71	71.71	-
B. Gap between fuel/basket	Air	84.38	12.67	-
C. Canister Wall	Stainless Steel	85.33	0.95	0.37
D. Gap between DSC/Cask	Air	86.36	1.03	0.41
E. Inner Liner of Cask	Stainless Steel	87.63	1.25	0.50
F. Lead Gamma Shield	Lead	96.67	9.04	3.56
G. Cask Body	Stainless Steel	100.48	3.81	1.50
H. Neutron Shield	Water	108.10	7.62	3.00
I. Cask Skin	Stainless Steel	108.59	0.49	0.19

Figure A.5.2-2
ANISN TC Model

A.5.3 Model Specification

The neutron and gamma dose rates on the surface of the AHSM, and on the surface, and at 1 and 3 feet from the surface of the TC are evaluated with the Monte Carlo transport code MCNP-4C2 [A5.8]. In addition, the flux-to-dose conversion factors specified by the ANSI/ANS 6.1.1-1977, Table A.5.3-3, are used [A5.9].

A.5.3.1 Description of the Radial and Axial Shielding Configurations

Figure A.5.1-1 is a sketch of an AHSM with a cut away through the AHSM at its mid-vertical plane. Figure A.5.1-3 is also a cut through the vertical mid-plane of an AHSM with the 24PT4-DSC shown in phantom lines, and the front door at the left hand side. The rear wall of the AHSM has a minimum thickness of 1 foot. A 3-foot shield wall is placed along the rear and sides of the AHSM array, as shown in Figure A.5.1-1.

MCNP computer models are built to evaluate the dose rate along the front wall surface, the rear shield wall surface, the vent openings, the roof surface, and on the side shield walls.

Figure A.5.1-4 shows the shielding configuration of the TC.

A.5.3.1.1 Storage Configuration

The geometry of nearly all components of the AHSM is Cartesian, except for the 24PT4-DSC, which is cylindrical. All relevant features of the AHSM are modeled explicitly in MCNP. In the MCNP coordinate system, the AHSM/DSC length is in the X direction, the width is in the Y direction, and the height is in the Z direction.

Two general classes of models are developed, one for the top of the AHSM and the other for the bottom of the AHSM. The models make use of symmetry by using reflective boundary conditions and modeling only $\frac{1}{4}$ of the DSC in each model. A total of four models are developed: top neutron, bottom neutron, top gamma, and bottom gamma. The geometry is shown in Figure A.5.4-1 through Figure A.5.4-4.

A.5.3.1.2 Loading/Unloading Configurations

The dose rates on the surface, and at 1 and 3 feet from the surface of the 24PT4-DSC/ Transfer Cask are evaluated with MCNP. Three different configurations representing the 3 stages in the loading/unloading of the spent fuel are analyzed. These stages are (1) Cask decontamination, (2) Wet Welding, and (3) Dry Welding.

Definition of Transfer Cask and 24PT4-DSC Loading Stages

Cask decontamination – The 24PT4-DSC and the Transfer Cask are completely filled with water, including the region between 24PT4-DSC and cask, which is referred to as the “Cask/24PT4-DSC annulus.” The 24PT4-DSC outer top cover plate and temporary shielding in

the welding machine is not installed. The geometry for this configuration (top end only) is shown in Figure A.5.4-8.

Wet welding – The water level in the 24PT4-DSC cavity is lowered approximately four inches below the bottom of the shield plug. Temporary shielding consisting of three inches of NS3 and one inch of steel replaces the outer top cover plate, which is not installed. The Cask/24PT4-DSC annulus remains filled with water. The geometry for this configuration (top end only) is shown in Figure A.5.4-9.

Dry welding – The 24PT4-DSC cavity is completely dry, the 24PT4-DSC shield plug and outer top cover plate have been installed, and temporary shielding consisting of three inches of NS3 and one inch of steel covers the outer top cover plate of the 24PT4-DSC. The Cask/24PT4-DSC annulus remains filled with water. The geometry for this configuration (top end only) is shown in Figure A.5.4-10.

Dose analysis results for the above conditions are provided in Table A.5.1-3 through Table A.5.1-5.

A.5.3.1.3 Transfer Configuration

For the transfer configuration the Transfer Cask/24PT4-DSC annulus is completely dry. The 24PT4-DSC shield plug and outer top cover plate are installed. The lid of the Transfer Cask is in place, which consists of a 3" thick carbon steel cover plate, a 2" thick solid neutron shield, and a ¼" thick stainless steel plate cover over the NS-3 shield. The geometry for this configuration is shown in Figure A.5.4-5 through Figure A.5.4-7.

The Z-axis in the MCNP models coincides with the axis of rotation of the Transfer Cask and the 24PT4-DSC. Minor features, such as the 24 Neutron Shield Panel (NSP) support angles, the 4 trunnions, relief valves, clevises, eyebolts, etc., are not modeled. With the exception of the 24 neutron shield support angles and the trunnions, the balance of these items are local features that increase the shielding in a small area without replacing any of the shielding material which is included in the model. The additional shielding material that these features provide is not smeared into the bulk shielding, nor is any credit taken for it for the occupational exposure calculation. The 24 neutron shield support angles provide support for the neutron shield skin, which contains the water for the neutron shield. The steel that forms these angles is not smeared with the water in the neutron shield; rather it is modeled as water. This is conservative for gamma radiation because water is less than one seventh the density of steel. The density of the neutron shield water used in the cask MCNP models is 0.96 g/cm³. The resultant reduction in the hydrogen density as compared to full density water results in the water attenuating the neutron dose rate at about the same rate as that for full density steel. Therefore, replacing the steel with the lower density water results in little to no effect on the neutron dose rate outside the cask.

The trunnions penetrate the neutron shield, which locally changes the shielding configuration of the neutron shield. The trunnions are thick steel structures filled with NS-3 neutron shielding material. These structures protrude well past the neutron shield and are made of materials which provide more gamma shielding and comparable neutron shielding as compared to the 0.96 g/cm³

water that these replace. In addition, with the exception of the neutron shield support angles, none of these features is located near the axial center of the cask where the surface dose rate is the largest due to the axial peaking of the fuel.

A.5.3.2 Shield Regional Densities

The actual fuel layout in the 24PT4-DSC is a cartesian array of fuel assemblies inside guidesleeves surrounded by sheets of poison material. These regions are smeared into a homogenous cylinder of equal volume and material loading. This smeared geometry represents a major part of the shielding (fuel, steel, Boral[®] sheets, etc.) and contains the neutron and gamma source volumetric distribution itself. As for the source, when the source is smeared into a cylinder, the source is moved closer to the surface of the source region. This results in less self-shielding of the source in the model as compared to the actual geometry, which results in an overestimate of the surface dose rates.

For dose rate evaluations made on surfaces that are parallel to the spacer disks (perpendicular to the DSC longitudinal axis), credit is taken for the presence of the carbon steel spacer disks and the fuel spacer grids by smearing them in the fuel material regions. For dose rate evaluations made on surfaces that are perpendicular to the spacer disks (parallel to the DSC longitudinal axis), a considerable fraction of the radiation will travel between the spacer disks, without being attenuated by the spacer disks. Therefore, the spacer disks and fuel spacer grids are not included in the smeared region number densities. For the AHSM evaluation, for conservatism, no credit is taken for the shielding properties of the spacer disks and fuel spacer grids (dry, radial densities) in any of the models. Table A.5.3-2 provides the shield regional densities for models of the various stages of the loading/unloading and transfer conditions in the TC.

When the transfer cask/24PT4-DSC annulus and 24PT4-DSC are filled with water, the wet axial densities are used for the homogenized regions.

**Table A.5.3-1
Materials Composition and Atom Number Densities (Dry)**

Material Name	Composition	Densities of Components Atoms/barn-cm
Stainless Steel	Cr	1.743e-2
	Fe	6.128e-2
	Ni	7.511e-3
Carbon Steel	Fe	8.465e-2
Concrete	H	7.767e-3
	O	4.317e-2
	Na	1.022e-3
	Al	2.343e-3
	Si	1.559e-2
	K	6.776e-4
	Ca	2.855e-3
	Fe	3.019e-4
Air	N	3.587e-5
	O	9.534e-6
Bottom Nozzle	¹⁰ B	1.401e-4
	C	6.570e-4
	Al	2.905e-3
	Cr	2.397e-3
	Mn	2.374e-4
	Fe	8.212e-3
	Ni	9.889e-4
	Zr	7.999e-3
	Sn	1.003e-4
In-Core	¹⁰ B	1.402e-4
	C	6.572e-4
	O	9.029e-3
	Al	2.906e-3
	Cr	7.497e-4
	Mn	7.416e-5
	Fe	2.567e-3
	Ni	3.089e-4
	Zr	2.942e-3
	Sn	3.687e-5
	²³⁵ U	2.221e-4
	²³⁸ U	4.273e-3

Table A.5.3-1
Materials Composition and Atom Number Densities (Dry)
(Concluded)

Material Name	Composition	Densities of Components Atoms/barn-cm
Plenum	¹⁰ B	1.403e-4
	C	6.577e-4
	Al	2.908e-3
	C	1.869e-3
	Mn	1.855e-4
	Fe	6.408e-3
	Ni	7.726e-4
	Zr	3.803e-3
	Sn	4.767e-5
Top Nozzle	¹⁰ B	1.402e-4
	C	6.572e-4
	Al	2.941e-3
	Ti	2.651e-5
	Cr	2.575e-3
	Mn	1.988e-4
	Fe	7.556e-3
	Ni	2.231e-3
	Zr	4.537e-5
	Mo	4.962e-5
	Sn	5.687e-7
BISCO NS3	H	4.498e-2
	¹⁰ B	3.054e-4
	C	9.595e-3
	O	3.704e-2
	Al	6.887e-3
	Si	1.243e-3
	Ca	1.454e-3
Fe	1.042e-4	
Lead	Pb	3.296e-2

**Table A.5.3-2
Materials Composition and Atom Densities During Decontamination
and Wet Welding Stage Calculation**

Material Name	Composition	Densities of Components Atoms/barn-cm
Water	H	6.393e-2
	O	3.203e-2
Bottom Nozzle	H	3.619e-2
	¹⁰ B	1.401e-4
	C	6.570e-4
	O	1.808e-2
	Al	2.925e-3
	Ti	1.475e-5
	Cr	2.720e-3
	Mn	2.374e-4
	Fe	1.208e-2
	Ni	1.770e-3
	Zr	7.999e-3
	Mo	2.761e-5
Sn	1.003e-4	
In-Core	H	3.844e-2
	¹⁰ B	1.402e-4
	C	6.572e-4
	O	2.823e-2
	Al	2.907e-3
	Ti	4.638e-7
	Cr	7.603e-4
	Mn	7.416e-5
	Fe	5.097e-3
	Ni	3.335e-4
	Zr	3.210e-3
	Mo	8.679e-7
	Sn	4.024e-5
	²³⁵ U	2.221e-4
²³⁸ U	4.273e-3	

**Table A.5.3-2
Materials Composition and Atom Densities During Decontamination
and Wet Welding Stage Calculation**

(Concluded)

Material Name	Composition	Densities of Components Atoms/barn-cm
Plenum	H	3.803e-2
	¹⁰ B	1.403e-4
	C	6.577e-4
	O	1.900e-2
	Al	2.908e-3
	Cr	1.869e-3
	Mn	1.855e-4
	Fe	8.307e-3
	Ni	7.726e-4
	Zr	4.162e-3
	Sn	5.216e-5
Top Nozzle	H	4.790e-2
	¹⁰ B	1.402e-4
	C	6.572e-4
	O	2.393e-2
	Al	2.941e-3
	Ti	2.651e-5
	Cr	2.575e-3
	Mn	1.988e-4
	Fe	1.184e-2
	Ni	2.231e-3
	Zr	4.537e-5
	Mo	4.962e-5
	Sn	5.687e-7

**Table A.5.3-3
Flux to Dose Rate Conversion Factors**

Neutron		Gamma	
E (MeV)	(mrem/hr)/(n/cm ² /s)	E (MeV)	(mrem/hr)/(γ/cm ² /s)
2.50E-08	3.67E-03	0.01	3.96E-03
1.00E-07	3.67E-03	0.03	5.82E-04
1.00E-06	4.46E-03	0.05	2.90E-04
1.00E-05	4.54E-03	0.07	2.58E-04
1.00E-04	4.18E-03	0.1	2.83E-04
0.001	3.76E-03	0.15	3.79E-04
0.01	3.56E-03	0.2	5.01E-04
0.1	2.17E-02	0.25	6.31E-04
0.5	9.26E-02	0.3	7.59E-04
1	1.32E-01	0.35	8.78E-04
2.5	1.25E-01	0.4	9.85E-04
5	1.56E-01	0.45	1.08E-03
7	1.47E-01	0.5	1.17E-03
10	1.47E-01	0.55	1.27E-03
14	2.08E-01	0.6	1.36E-03
20	2.27E-01	0.65	1.44E-03
		0.7	1.52E-03
		0.8	1.68E-03
		1	1.98E-03
		1.4	2.51E-03
		1.8	2.99E-03
		2.2	3.42E-03
		2.6	3.82E-03
		2.8	4.01E-03
		3.25	4.41E-03
		3.75	4.83E-03
		4.25	5.23E-03
		4.75	5.60E-03
		5	5.80E-03
		5.25	6.01E-03
		5.75	6.37E-03
		6.25	6.74E-03
		6.75	7.11E-03
		7.5	7.66E-03
		9	8.77E-03
		11	1.03E-02
		13	1.18E-02
		15	1.33E-02

A.5.4 Shielding Evaluation

A.5.4.1 Computer Program

The Monte Carlo N-Particle (MCNP) computer program [A5.8] determines the particle (neutron and/or photon) flux throughout three-dimensional geometric systems by using the Monte Carlo method. The flux is converted to a dose rate using the ANSI/ANS-6.1.1-1977 flux to dose conversion factors. Particles can be generated by either particle interaction with the transport medium or extraneous sources incident upon the system. MCNP is an industry standard code distributed by ORNL/RSIC.

MCNP was chosen for this application because of its ability to solve three-dimensional, deep penetration, radiation transport problems applicable to the Advanced NUHOMS[®] System.

A.5.4.1.1 Spatial Source Distribution

The fixed source components are:

- A neutron source due to the active fuel regions of the 24 fuel assemblies,
- A gamma source due to the active fuel regions of the 24 fuel assemblies,
- A gamma source due to the plenum regions of the 24 fuel assemblies,
- A gamma source due to the top nozzle regions of the 24 fuel assemblies, and
- A gamma source due to the bottom nozzle regions of the 24 fuel assemblies,

Axial peaking is accounted for in the active fuel region by inputting a relative flux factor at twenty axial locations. The flux factor data for axial peaking is taken from DeHart [A5.10] for (CE 14x14) PWR fuel. This burn-up profile is applicable for evaluations of a CE 16x16 fuel assembly with similar heavy metal loading, neutron spectrum, and total length. The peak flux factor used is 1.072 for neutrons and gamma-rays. The flux factor data for axial peaking used in this analysis is shown in Table A.5.4-1.

A.5.4.1.2 Cross-Section Data

The cross-section data used in this analysis is the standard ENDF/B-V continuous cross section data distributed with the MCNP code [A5.1]. Cross-sections are at a temperature of 300K. Because continuous cross-section data are utilized, cross-section processing is not required.

A.5.4.2 Flux-to-Dose Rate Conversion

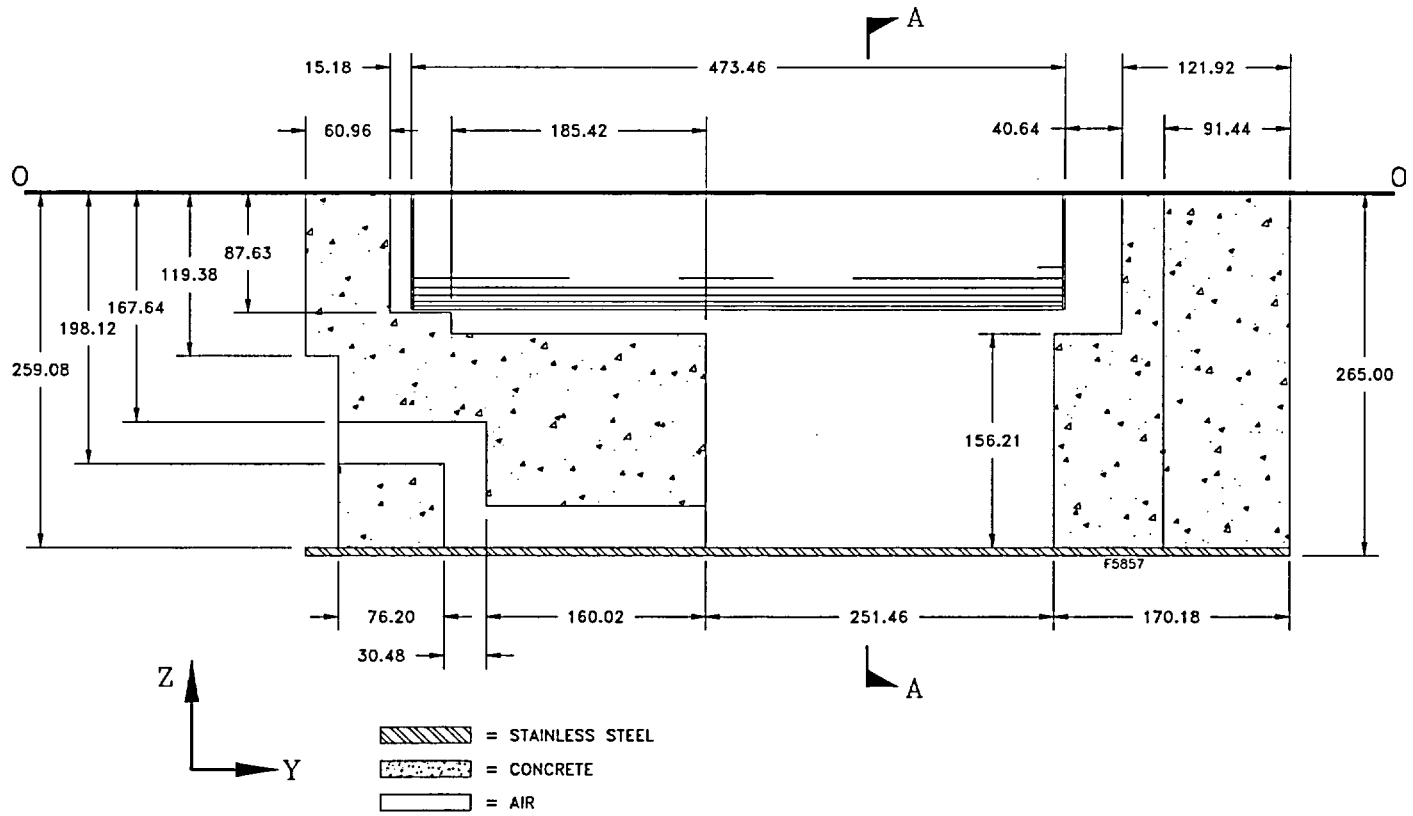
The flux distribution calculated by the MCNP code is converted to dose rates using the flux-to-dose rate conversion factors provided in ANSI/ANS-6.1.1-1977 [A5.9]. The gamma ray and neutron flux-to-dose rate conversion factors are shown in Table A.5.3-3.

A.5.4.2.1 Model Geometry

Figure A.5.4-1 through A.5.4-4 show the MCNP models for the AHSM and 24PT4-DSC. Section **Error! Reference source not found.** contains samples of the input listing of the MCNP model for the AHSM. Figure A.5.4-5 through Figure A.5.4-10 show the MCNP models of the Transfer Cask and 24PT4-DSC for the various loading/transfer configurations. Sample input listings of the MCNP model for the Transfer Cask is provided in Section **Error! Reference source not found.**

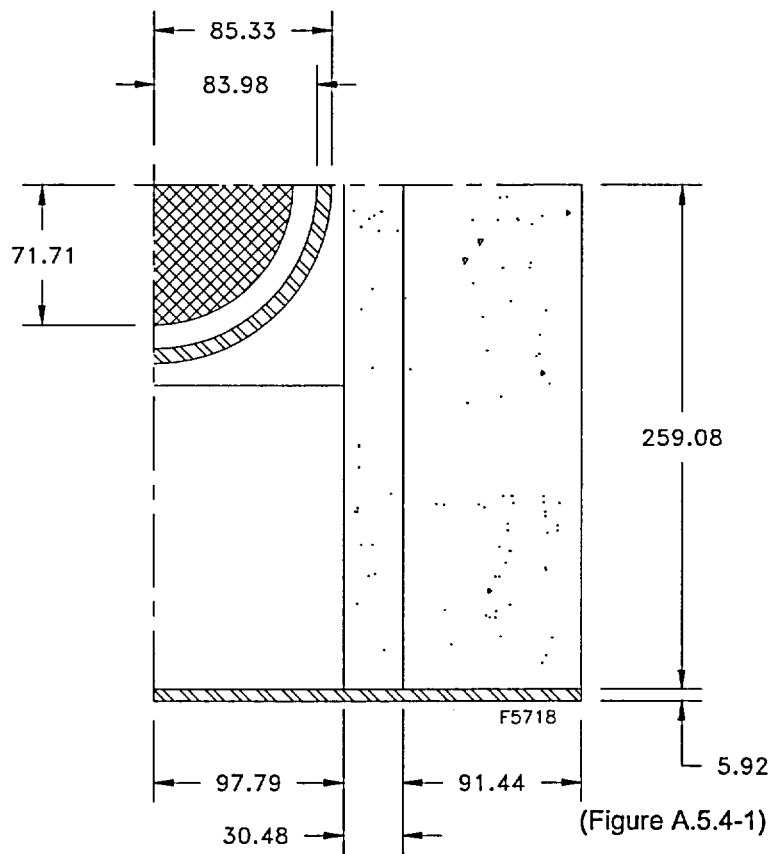
**Table A.5.4-1
Normalized Burn-Up Shape for CE 16×16 Fuel Assembly**

Zone Number	Zone Center in % of height	Zone Center mapped on the axis of the active fuel zone, cm	Flux Factor
1	2.5	9.50	0.655
2	7.5	28.50	0.911
3	12.5	47.50	1.009
4	17.5	66.50	1.041
5	22.5	85.50	1.069
6	27.5	104.50	1.072
7	32.5	123.50	1.072
8	37.5	142.50	1.071
9	42.5	161.50	1.070
10	47.5	180.50	1.069
11	52.5	199.50	1.069
12	57.5	218.51	1.068
13	62.5	237.51	1.068
14	67.5	256.51	1.069
15	72.5	275.51	1.068
16	77.5	294.51	1.066
17	82.5	313.51	1.041
18	87.5	332.51	0.994
19	92.5	351.51	0.879
20	97.5	370.51	0.639




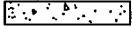
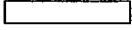

Note: All dimensions in centimeters.

**Figure A.5.4-1
AHSM Bottom MCNP Model, (x,z) Cut**



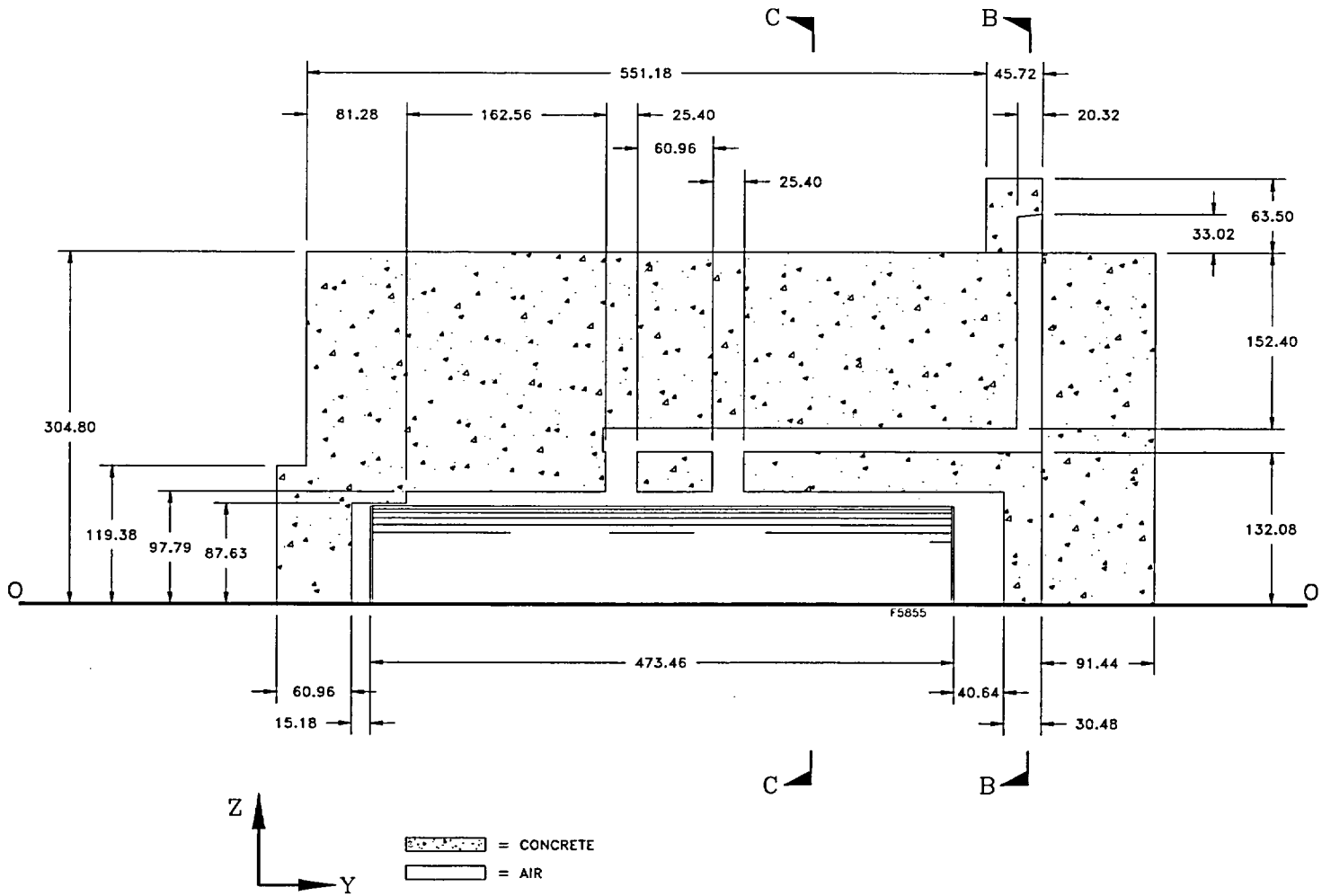
(Figure A.5.4-1)

SECTION A-A

-  = STAINLESS STEEL
-  = CONCRETE
-  = AIR
-  = FUEL (IN-CORE) REGION

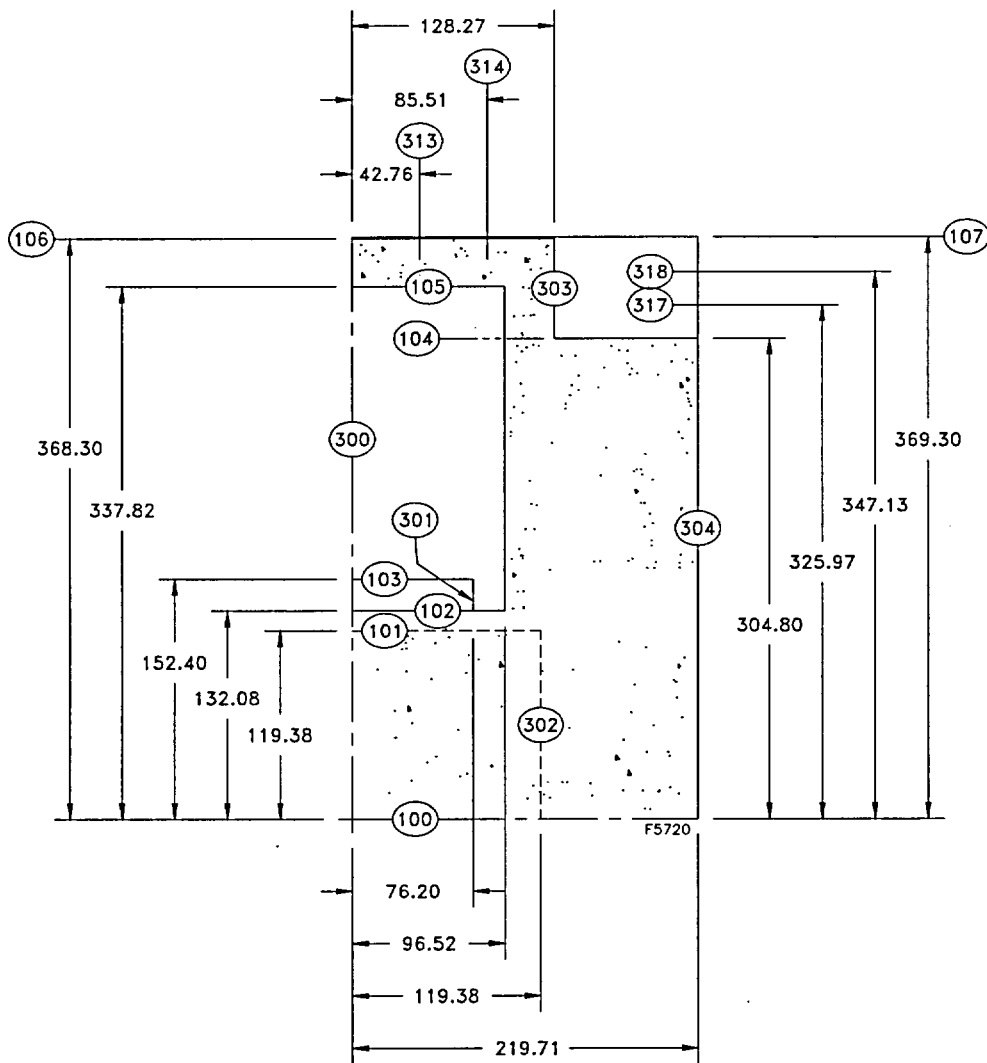
Note: All dimensions in centimeters.

**Figure A.5.4-2
AHSM Bottom MCNP Model, (y,z) Cut**

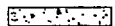
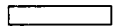


Note: All dimensions in centimeters.

Figure A.5.4-3
AHSM Top MCNP Model, (x,z) Cut

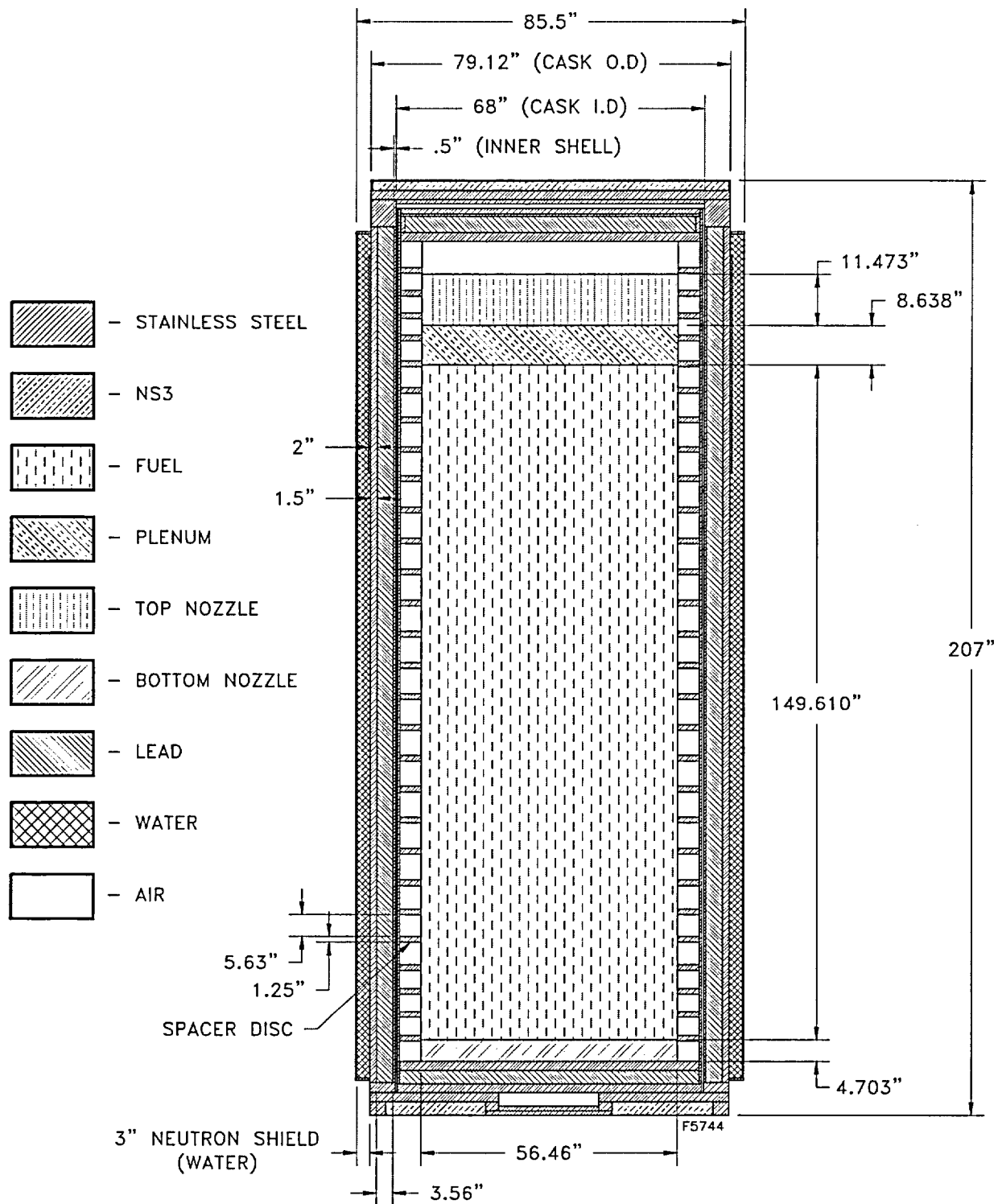


SECTION B-B

-  = CONCRETE
-  = AIR

Note: All dimensions in centimeters.

Figure A.5.4-4
AHSM Top MCNP Model, (y,z) Cut



Note: See Figure A.5.4-6 and Figure A.5.4-7 for details of the DSC top and bottom ends, respectively.

Figure A.5.4-5
OS197H MCNP Model

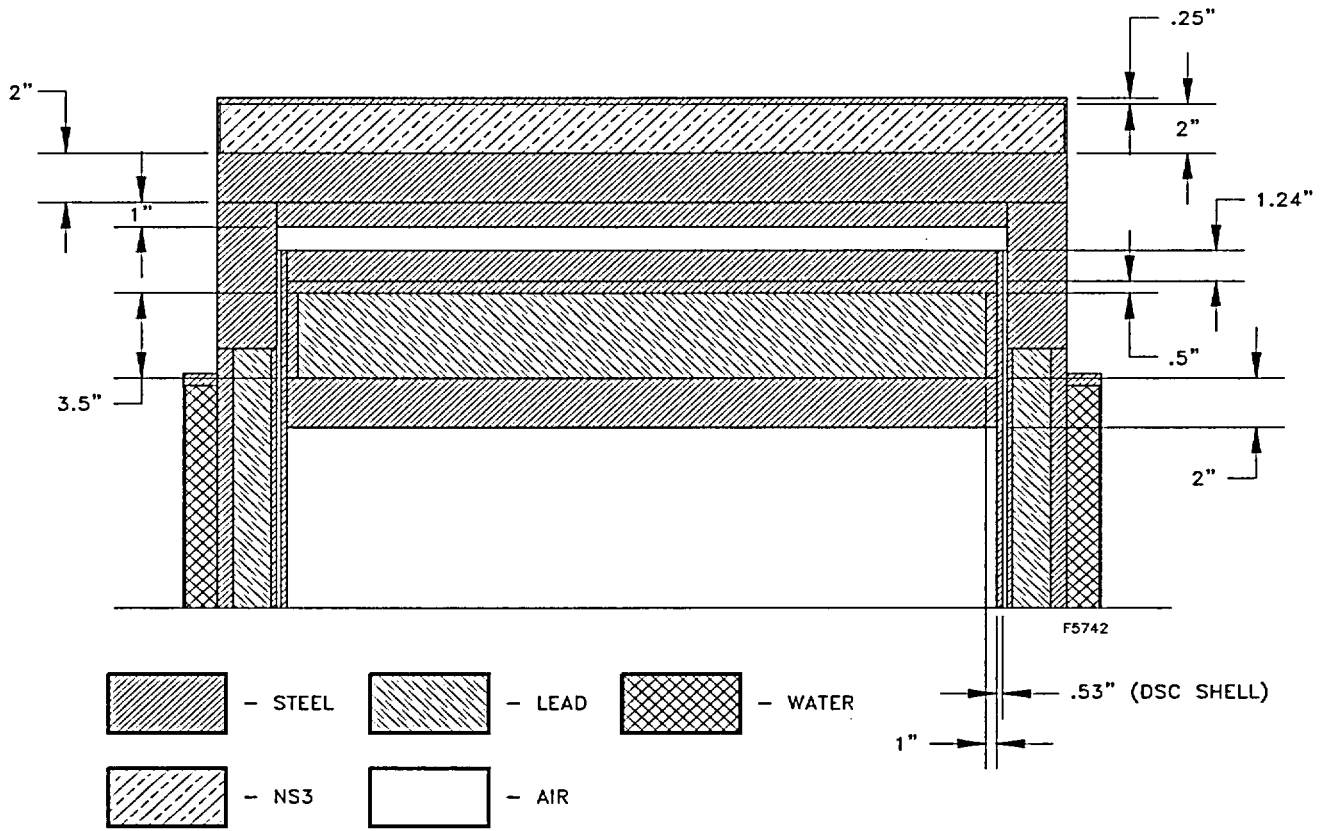


Figure A.5.4-6
OS197H Cask MCNP Model—Top Section

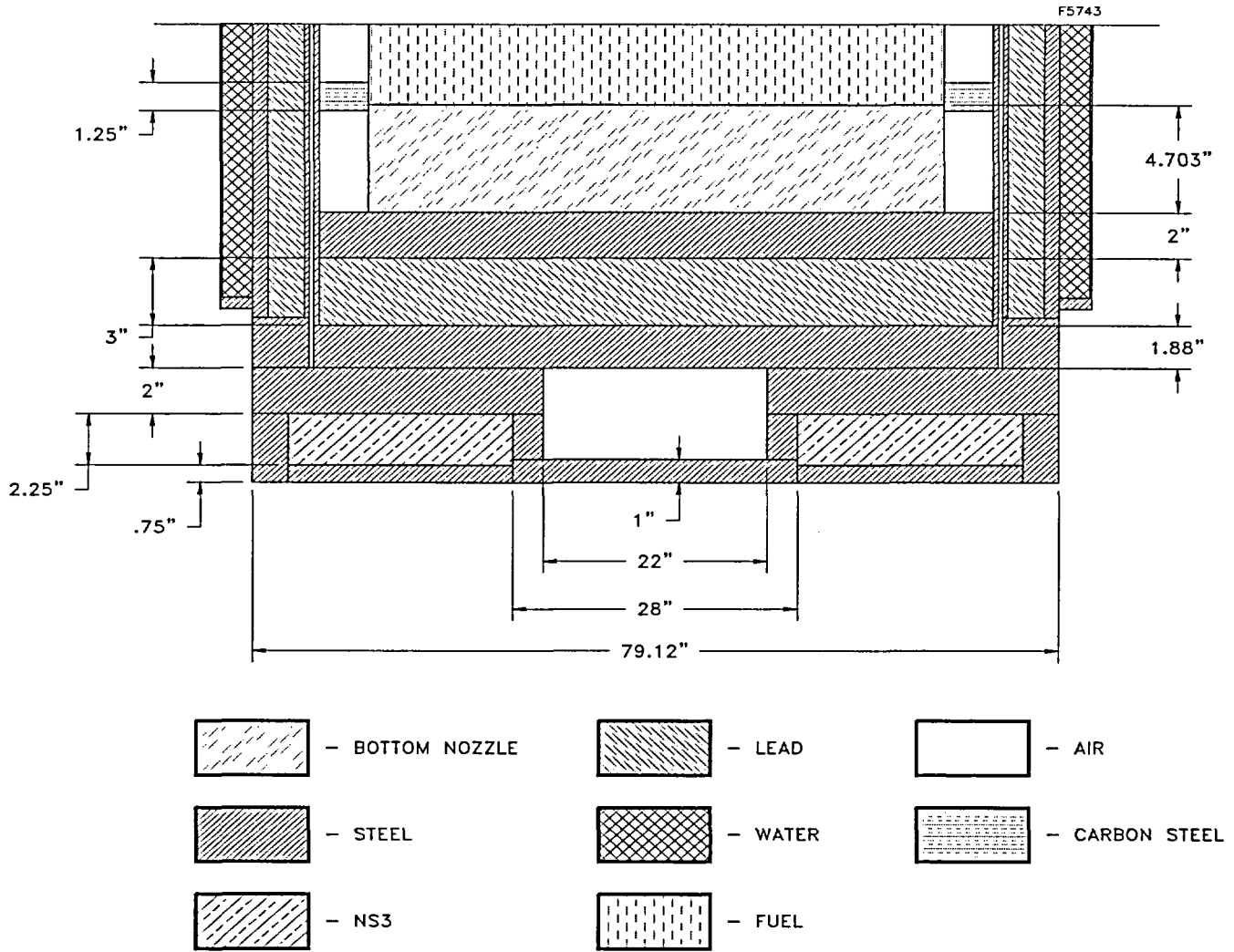
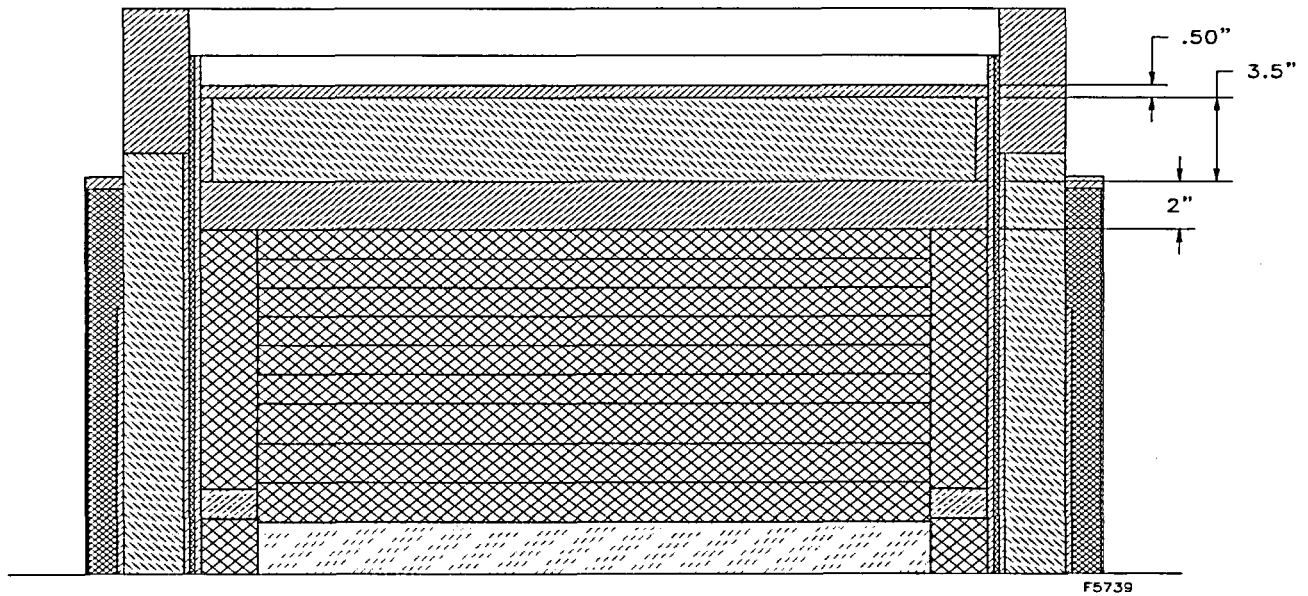


Figure A.5.4-7
OS197H Cask MCNP Model—Bottom Section








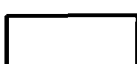
- | | | | |
|---|----------------|--|---------|
|  | - TOP NOZZLE |  | - LEAD |
|  | - STEEL |  | - WATER |
|  | - CARBON STEEL |  | - AIR |

Figure A.5.4-8
OS197H Cask MCNP Model (Top) during Decontamination

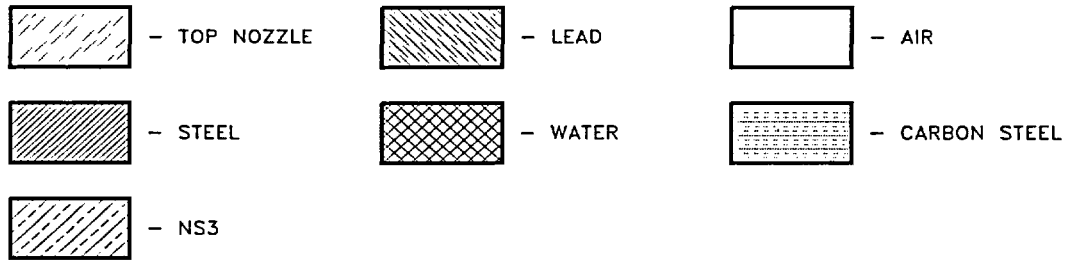
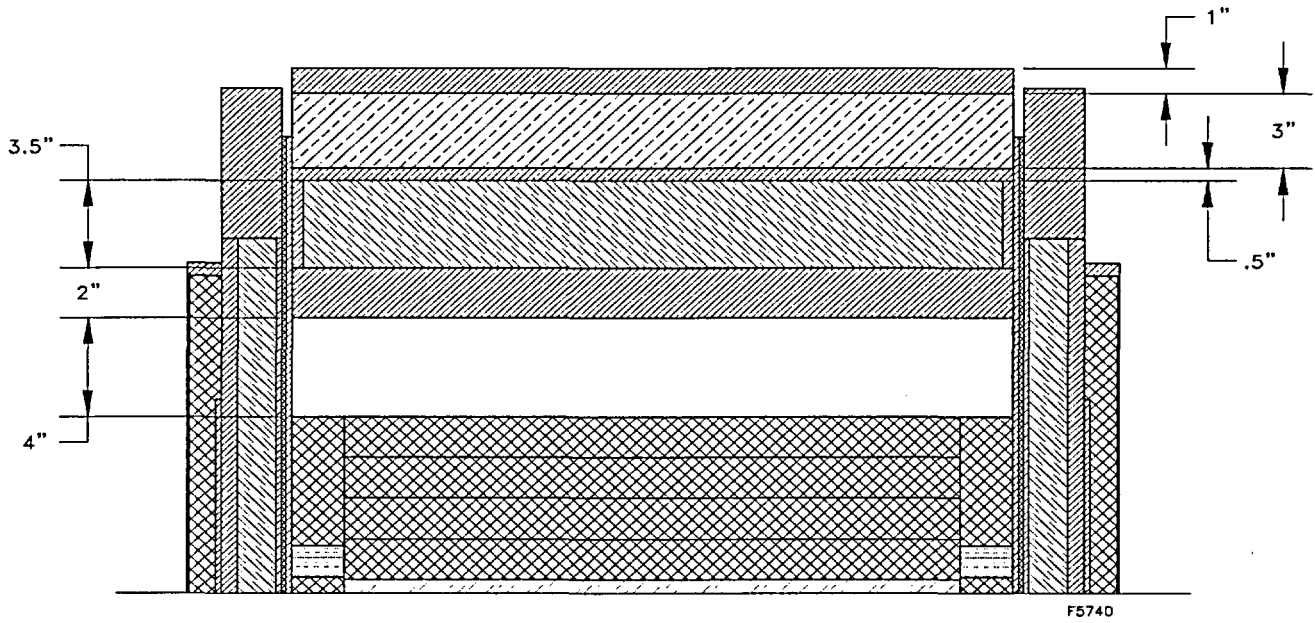


Figure A.5.4-9
OS197H Cask MCNP Model (Top) during Wet Welding

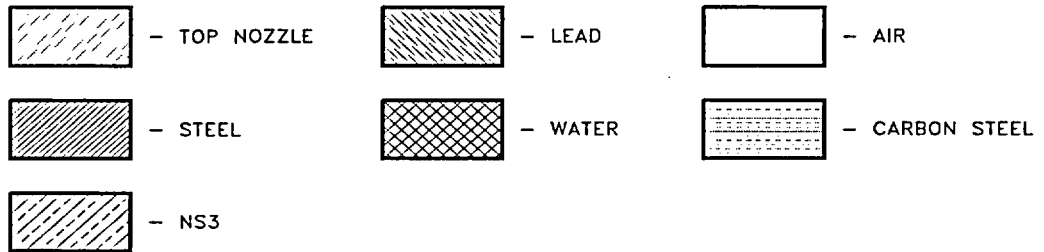
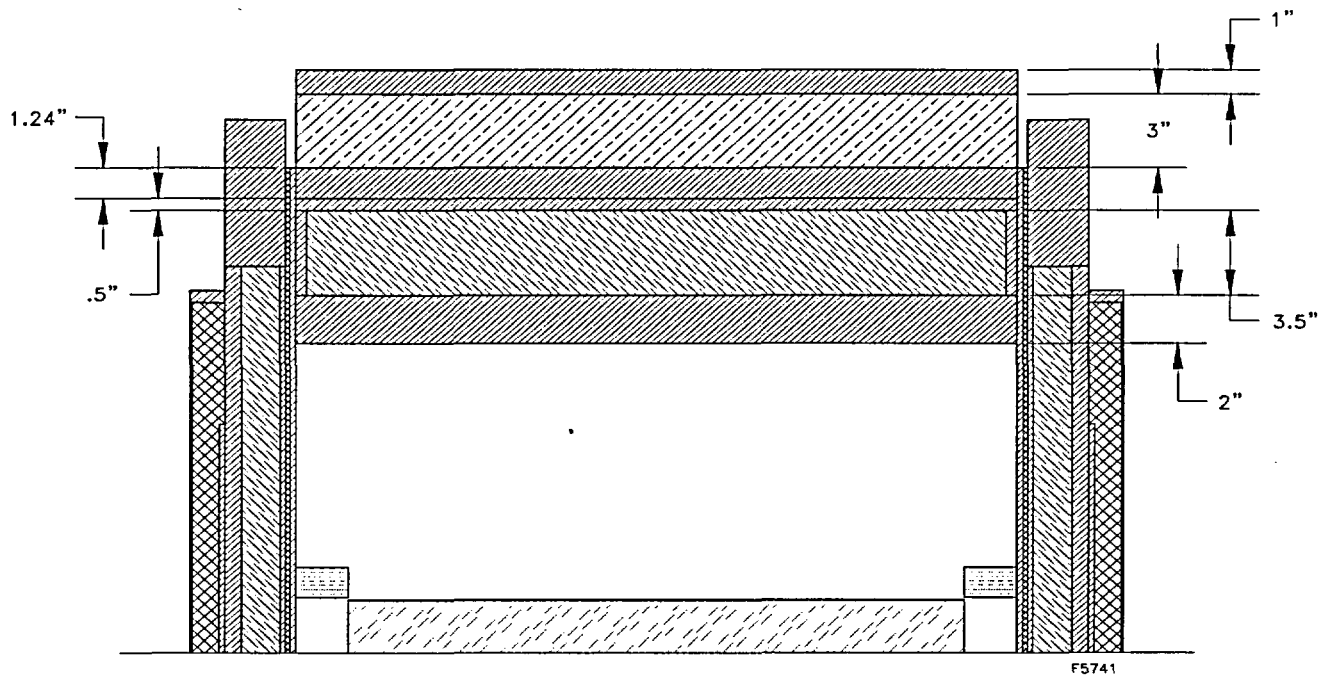


Figure A.5.4-10
OS197H Cask MCNP Model (Top) during Dry Welding

A.5.5 Supplemental Information

A.5.5.1 References:

- [A5.1] Oak Ridge National Laboratory, RSIC Computer Code Collection, "SCALE: A Modular Code System for Performing Standardized Computer Analysis for Licensing Evaluations for Workstations and Personal Computers," NUREG/CR-0200, Revision 6, ORNL/NUREG/CSD-2/V2/R6.
- [A5.2] Ludwig, S.B., and J.P. Renier, "Standard- and Extended-Burnup PWR and BWR Reactor Models for the ORIGEN2 Computer Code," ORNL/TM-11018, Oak Ridge National Laboratory, December 1989.
- [A5.3] Office of Civilian Radioactive Waste Management, "Characteristics of Potential Repository Wastes", DOE/RW-0184-R1, July 1992.
- [A5.4] CCC-254, Oak Ridge National Laboratory, RSIC Computer Code Collection, "ANISN-ORNL - One-Dimensional Discrete Ordinates Transport Code System with Anisotropic Scattering", QA040.220.0002, April 1991.
- [A5.5] "Certificate of Compliance for Dry Spent Fuel Storage Casks," 10 CFR Part 72, Certificate Number 1004, Amendment 2, September 5, 2000.
- [A5.6] Transnuclear West, "Final Safety Analysis Report for the Standardized NUHOMS[®] Horizontal Modular Storage System for Irradiated Nuclear Fuel," Revision 6, November 2001, (US NRC Docket No. 72-1004) File Number NUH003.0103.
- [A5.7] Oak Ridge National Laboratory, "CASK-81 22 Neutron, 18 Gamma-Ray, P₃, Cross Sections for Shipping Cask Analysis", Report DLC-23.
- [A5.8] Oak Ridge National Laboratory, RSICC Computer Code Collection, MCNP 4C2-Monte Carlo N-Particle Transport Code System", CCC-701, June 2001.
- [A5.9] American Nuclear Society, "American National Standard Neutron and Gamma-Ray Flux-to-Dose Rate Factors". ANSI/ANS-6.1.1-1977, La Grange Park, Illinois, March 1977.
- [A5.10] M. D. DeHart, "Sensitivity and Parametric Evaluations of Significant Aspects of Burn-up Credit for PWR Spent Fuel Packages", ORNL/TM-12973, May 1996.
- [A5.11] U.S. Nuclear Regulatory Commission, "Review of Technical Issues Related to Predicting Isotopic Compositions and Source Terms for High Burnup LWR Fuel," NUREG/CR-6701, Published January 2001, ORNL/TM-2000/277
- [A5.12] MD DeHart and OW Hermann, "An Extension of the Validation of SCALE (SAS2H) Isotopic Predictions for PWR Spent Fuel," ORNL/TM-13317, September 1996.

- [A5.13] OW Hermann, SM Bowman, MC Brady, CV Parks, "Validation of the SCALE System for PWR Spent Fuel Isotopic Composition Analyses," ORNL/TM-12667, March 1995.
- [A5.14] Japan Atomic Energy Research Institute, "Technical Development on Burn-up Credit for Spent LWR Fuels," JAERI-Tech 2000-071, September 21, 2000.
- [A5.15] U.S. Nuclear Regulatory Commission, "Nuclide Importance to Criticality Safety, Decay Heating, and Source Terms Related to Transport and Interim Storage of High Burnup LWR Fuel," NUREG/CR-6700, Published January 2001, ORNL/TM-2000/284.

A.5.5.2 Sample SAS2H Input Listing

A.5.5.3 Sample ANISN Model (Neutron Response Function for AHSM

A.5.5.4 Sample AHSM MCNP Analysis Input Files

A.5.5.5 Sample OS197H MCNP Analysis Input Files